Nanomaterials for sustainable remediation of chemical contaminants in water and soil

Raj Mukhopadhyay[a], Binoy Sarkar[b,*], Eakalak Khan[c], Daniel S. Alessi[d], Jayanta Kumar Biswas[e], K. M. Manjaiah[f], Miharu Eguchi[g], Kevin C.W. Wu[h], Yusuke Yamauchi[i,j], Yong Sik Ok[k,*]

[a] *Division of Irrigation and Drainage Engineering, ICAR-Central Soil Salinity Research Institute, Karnal – 132001, Haryana, India*

[b] *Lancaster Environment Centre, Lancaster University, Lancaster, LA1 4YQ, United Kingdom*

[c] *Department of Civil and Environmental Engineering and Construction, University of Nevada, Las Vegas, NV 89154, USA*

[d] *University of Alberta, Earth and Atmospheric Sciences, Edmonton, AB, T6G 2E3, Canada*

[e] *Department of Ecological Studies & International Centre for Ecological Engineering, University of Kalyani, Kalyani, Nadia- 741235, West Bengal, India*

[f] *ICAR-Indian Agricultural Research Institute, New Delhi – 110012, India*

[g] *Electronic Functional Materials Group, National Institute for Materials Science (NIMS), 1-1 Namiki, Tsukuba, Ibaraki 305-0044, Japan*

[h] *Department of Chemical Engineering, National Taiwan University, Taipei 10617, Taiwan*

[i] *Australian Institute for Bioengineering and Nanotechnology (AIBN) and School of Chemical Engineering, The University of Queensland, Brisbane, QLD 4072, Australia*

[j] *Yamauchi Materials Space-Tectonics Project and International Center for Materials Nanoarchitechtonics (WPI-MANA), National Institute for Materials Science (NIMS), 1-1 Namiki, Tsukuba, Ibaraki 305-0044, Japan*

[k] *Korea Biochar Research Center, APRU Sustainable Waste Management Program & Division of Environmental Science and Ecological Engineering, Korea University, Seoul 02841, Republic of Korea*

[*]Co-corresponding authors:

Dr. Binoy Sarkar, Lancaster University, e-mail: b.sarkar@lancaster.ac.uk

Prof. Yong Sik Ok, Korea University, e-mail: yongsikok@korea.ac.kr

Graphical abstract

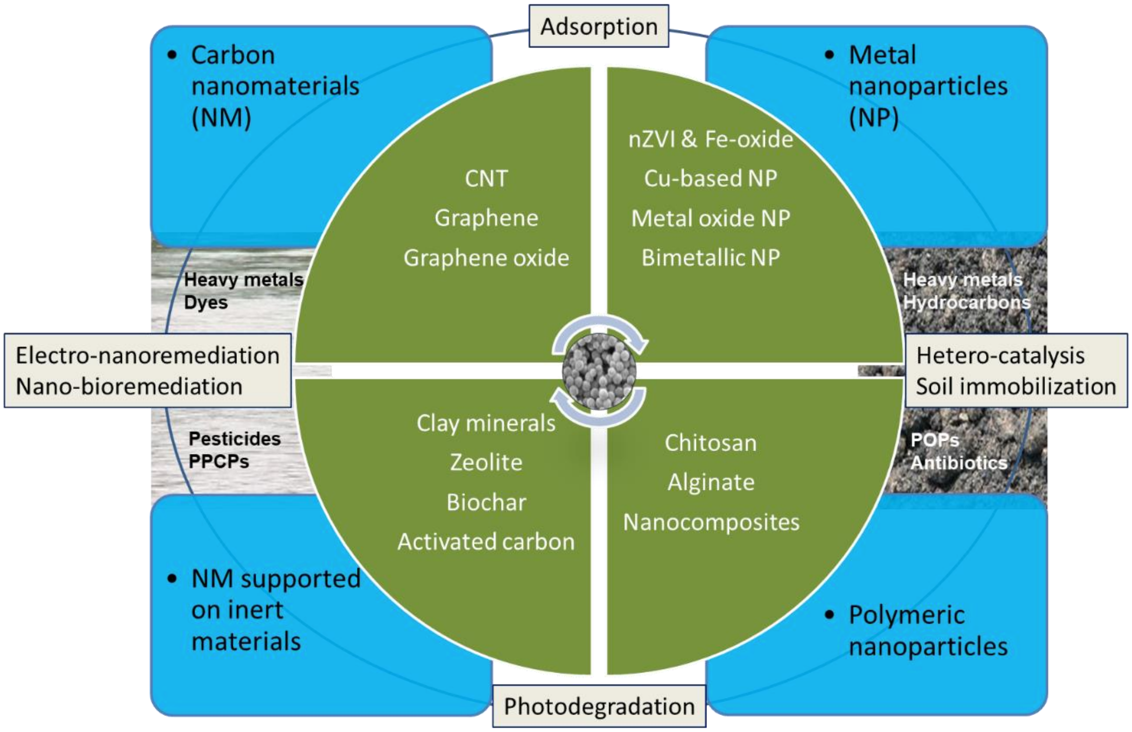

Abstract

Rapid growth in population, industry, urbanization and intensive agriculture have led to soil and water pollution by various contaminants. Nanoremediation has become one of the most successful emerging technologies for cleaning up soil and water contaminants due to the high reactivity of nanomaterials (NMs). Numerous publications are available on the use of NMs for removing contaminants, and the efficiencies are often improved by modifications of NMs with polymers, clay minerals, zeolites, activated carbon, and biochar. This paper critically reviews the current state-of-the-art NMs used for sustainable soil and water remediation, focusing on their applications in novel remedial approaches, such as adsorption/filtration, catalysis, photodegradation, electro-nanoremediation, and nano-bioremediation. Insights into process performances, modes of deployment, potential environmental risks and their management, and the consequent societal and economic implications of using NMs for soil and water remediation indicate that widespread acceptance of nanoremediation technologies requires not only a substantial advancement of the underpinning science and engineering aspects themselves, but also practical demonstrations of the effectiveness of already recognized approaches at real world *in-situ* conditions. New research involving green nanotechnology, nano-bioremediation, electro-nanoremediation, risk assessment of NMs, and outreach activities are needed to achieve successful applications of nanoremediation at regional and global scales.

Key Words: Environmental protection; Green and sustainable remediation; Sustainable development goals; Soil remediation; Soil pollution; Wastewater treatment

1. Introduction

One of the biggest problems faced currently by most countries in the world is the deterioration of environmental quality due to wastewater generation, groundwater contamination, and land degradation. Providing a clean environment to humankind is a major challenge to the global community. The challenges of contaminated environment are represented by the United Nation's Sustainable Development Goals (SDGs): 'Clean Water and Sanitation', 'Life on Land', and 'Life Below Water' (UN, 2016).

Continuous accumulation of toxic trace elements in soil and water environments accelerate their bioaccumulation. Human exposure to cadmium (Cd), lead (Pb), arsenic (As) and fluoride (F) via drinking water and the consumption of contaminated food can lead to severe health problems in the skin, lungs, kidneys and brain (Schaefer et al., 2020; Wang et al., 2019). Organic contaminants such as industrial dyes are difficult to treat due to their recalcitrance and sensitivity on physicochemical properties of the surrounding environment for degradation (Lellis et al., 2019). Likewise, the excessive application of pesticides in agriculture has contaminated soil and water resources globally (de Souza et al., 2020). Anthropogenic and natural activities including coal gasification, coal-tar pitches and open burning can produce large quantities of polycyclic aromatic hydrocarbons (PAHs) due to the incomplete combustion of hydrocarbons (Li et al., 2020). Pharmaceuticals and personal care products (PPCPs) are contaminants of emerging concern found in wastewater due to discharge from households, healthcare facilities, and the pharmaceutical manufacturing industry (Meyer et al., 2019).

There is a need to develop cost-effective and ecologically benign materials for cleaning up contaminated soil and water. Nanotechnology offers rapid, inexpensive and environmentally safe solutions, and has great potential to reduce contaminant levels to 'nearly zero' (Bardos et al., 2018). Nanoremediation of the environment can be defined as the process whereby suitable nanomaterials (NMs) are used for cleaning up environmental contaminants in the soil, water, and air. Nanoremediation technologies can eliminate the need for excavating and transporting contaminated soils because the cleanup process often takes place *in-situ* (Cai et al., 2019; Fajardo et al., 2020). Furthermore, several approaches can be applied to regenerate and reuse nanomaterials in contaminant treatment applications (e.g., magnetic separation of iron nanoparticles, recovery of metals from spent nanosorbents) (Mehta et al., 2015).

Nanoparticles (NPs) are particles with sizes of <100 nm in all dimensions (e.g., metal oxides), while NMs require only one dimension to be <100 nm (e.g., carbon nanotubes) (Khan et al., 2019). Nanocomposites are defined as multiphase materials consisting of at least one nanoscale phase that is dispersed in another phase to obtain a combination of the individual properties of its constituents (Bassyounia et al., 2019; Mukhopadhyay et al., 2020). Therefore, one of the constituent materials in nanocomposites should have a dimension <100 nm (Schaefer and Justice, 2007; Zhao et al., 2011). Nanoscale metal oxides, nano-scale zero valent iron (nZVI), bimetallic nanoparticles (BNPs), carbon nanotubes (CNTs), graphene oxides, silica-based NPs, polymers, clay minerals and zeolites have been shown to decontaminate soil and water (Awad et al., 2020; Mukhopadhyay et al., 2020; Sarkar et al., 2018; Zou et al., 2016). Applications of NMs supported on clay minerals, zeolites, activated carbon and biochar have also improved the reactivity and contaminant removal performances of NMs (Mandal et al., 2018). Reactive nanomaterials can chemically reduce and/or aid in the catalytic reactions to degrade, detoxify and transform specific pollutants (Kumar et al., 2020a). Expediting the cleanup of contaminants in water and soil using NMs holds the potential to improve environmental health for human civilization in meeting multiple SDGs.

Based on the functions of various NMs, they can be classified as adsorbents (for adsorption of contaminants), catalysts (for degradation/transformation of pollutants) and membranes (pressure-driven technique for wastewater and seawater treatment) (Anjum et al., 2019). However, most of the literature focuses on the remediation of aqueous systems, and most of these studies are at the bench scale. Cleanup of contaminated soils using NMs has received less attention. Multiple technological, societal and economic bottlenecks (e.g., high preparation and implementation costs of NMs, a lack of desired contaminant removal efficiency under *in-situ* conditions) have hindered the widespread application of nanotechnologies in environmental remediation.

No comprehensive critical review is currently available that discusses both water and soil remediation using various types of nanomaterials, their fates and concurrent effects on living organisms, feasibility in field-level applications, environmentally benign and inexpensive synthesis methods, and scientific, societal and economic bottlenecks hindering widespread application, which are addressed for the first time in this work. Specifically, focus has been made on toxic trace elements, pesticides/herbicides, dyes and selected aromatic compounds, which are most encountered in various industrial systems/discharges, wastewater, contaminated irrigation water and agricultural systems.

2. Nanomaterials for contaminants remediation in water

Nanomaterials can be grouped into: (i) metal-based or inorganic NMs, (ii) carbonaceous NMs, (iii) polymer-based NMs, and (iv) composite NMs (Guerra et al., 2018). Fig. 1 depicts a schematic representation of various types of NMs used for the removal of environmental contaminants. Metal based NMs (e.g., Fe-based NPs, Cu-based NPs, BNPs) are widely used in environmental remediation followed by carbonaceous NMs (e.g., CNTs, graphene and graphene oxides), while polymer (e.g., chitosan, alginate) and composite (e.g., clay-polymer nanocomposites, zeolite and biochar supported) NMs have received considerable research attention but limited practical applications (Guerra et al., 2018; Mukhopadhyay et al., 2020). Fe-based NPs have been successfully used in the field, in addition to a few examples of Cu-based NPs, BNPs, other metal oxide NPs (e.g., TiO_2, ZnO) and CNTs. The main motivations for using NMs for water and soil treatment are: their high selectivity, high adsorption capacity (due to high specific surface area and numerous adsorption sites), and easy regeneration after use.

2.1 Iron-based nanoparticles

Iron-based NPs include various oxidic NPs (either magnetic or non-magnetic) as well as nZVI, as discussed below:

2.1.1 Iron oxide NPs

Iron-based NPs (Fe NPs) such as iron oxides (e.g., hematite (α-Fe_2O_3), maghemite (γ-Fe_2O_3), and magnetite (Fe_3O_4)) and oxy-hydroxides (e.g., goethite (α-FeOOH) and lepidocrocite (γ-FeOOH)) were reported to be effective adsorbents of As and other heavy metals (Supplementary Information: Table S1) in water. For instance, a novel nano-adsorbent was prepared by using Fe_3O_4 magnetic core shelled by mesoporous silica (Vojoudi et al., 2017). The obtained material was then modified with bis(3-triethoxysilylpropyl) tetrasulfide and used to remove heavy metals from aqueous solution. The adsorbent removed 303, 256.4 and 270.3 mg/g of Hg(II), Pd(II) and Pb(II) ions, respectively (Vojoudi et al., 2017). The magnetic Fe_3O_4 NMs were found suitable for the remediation of aqueous Cu^{2+}, Ni^{2+}, Cd^{2+} and Zn^{2+}. The amount of Cu^{2+}, Ni^{2+} and Zn^{2+} adsorption by Fe_3O_4 were 11.5, 6.07, 9.68 and 11.1 mg/g, respectively, at pH 6.0 after 50 min of reaction time (initial metal concentration = 50 mg/L for each metal ion; adsorbent dose = 6 g/L) (Ebrahim et al., 2016). Following modification with 2-mercaptobenzothiazole, magnetic Fe_3O_4 NPs removed 98.6% Hg(II) from a solution that initially contained 50 ng/mL Hg(II) in just four minutes through a complexation mechanism, versus 43.7% removal by the unmodified NPs (Parham et al., 2012). Green-synthesized α-Fe_2O_3 NPs using banana peel extracts showed high As(V) adsorption capacity (2.72 mg/g) (Majumder et al., 2019). Similarly, Fe oxide NPs synthesized from green tea leaf extracts removed 13.7 mg/g As(V) from aqueous solution (Kamath et al., 2020). Fe NPs supported on inert materials such as clay minerals, zeolites and biochar can improve the speed and efficiency of contaminant remediation by enhancing the dispersion of NPs and preventing their passivation and/or degradation (Supplementary Information: Table S1; Section 2.9). Apart from adsorption, Fe oxide NPs such as Fe_2O_3 and Fe_3O_4 can degrade phenol, aniline, and dye compounds via photochemical oxidation reactions (Fig. 2) (Saharan et al., 2014).

2.1.2 Nano-scale zero valent iron (nZVI)

ZVI (Fe^0) applied to groundwater was shown to be a strong adsorbing and reducing agent of redox-sensitive contaminants (e.g., Cr(VI), As(III), chloroethylene compounds), and displayed a low toxicity to biota living in the surrounding environment (Chekli et al., 2016). Considering these advantages, researchers have used nZVI for decontaminating oxyanion (e.g., CrO_4^{2-}, TcO_4^-, AsO_3^{3-}/AsO_4^{3-}, and SeO_3^{2-}/SeO_4^{2-}) and oxycation (e.g., UO_2^{2+}, VO_4^{3-}) contaminants in water (Supplementary Information: Table S1).

In some cases, nZVI was further modified to prepare advanced nanoremediation agents. For example, bare nZVI (B-nZVI) was modified with hydroxyethyl cellulose (E-nZVI) and hydroxyl propylmethyl cellulose (P-nZVI) to remediate dye compounds in water (Wang et al., 2015b). The discoloration efficiency was 93.4, 96.3, and 98.6% by B-nZVI, E-nZVI, and P-nZVI, respectively, at 0.7 mg/L initial dye concentration (Wang et al., 2015b).

The colloidal forms of ZVI (µm and nm particle sizes) can be mixed into natural aquifers to readily degrade or adsorb various pesticides (e.g., alachlor), dyes (e.g., malachite green, reactive yellow) and other organic contaminants (e.g., trichloroethylene, pentachloroethylene) (Lin et al., 2018). The nZVI interacts with heavy metals and metalloids through precipitation (Cu(II), Pb(II), Cd(II), Co(II) and Zn(II)), co-precipitation (Ni(II), Cr(VI), Se(VI)), redox reactions (As(V), Pb(II), Hg(II), Cu(II), Ag(II) U), and adsorption (Cr(VI), Ni(II), Se (VI)) (Pasinszki & Krebsz, 2020). The catalytic activity of nZVI at field conditions can be compromised due to its poor stability and agglomeration behavior (Stefaniuk et al., 2016). However, peroxide free Fenton-type reactions can catalyze organic contaminant degradation to overcome these limitations of nZVI (Pasinszki & Krebsz, 2020). The agglomeration of nZVI at large scales in aquifers may be problematic as this can cause the clogging of pores and reduce inherent hydraulic conductivity. Hence, future research should be concentrated on the modification of nZVI to reduce its agglomeration behavior at field conditions.

2.2 Copper-based nanoparticles

Copper based nanoparticles (Cu NPs) have chemical, photocatalytic, optical and electro-thermal properties applicable to remediation. Specifically, copper oxides (CuO and Cu_2O), are well-known p-type semi-conductors with a high thermal stability and chemical reduction potential (Isherwood, 2017). Positive surface charge, optical properties at visible wavelength, and the high surface area of Cu NPs are the beneficial properties for degradation, reduction, and adsorption of inorganic and organic contaminants (Khalaj et al., 2018) (Supplementary Information: Table S2). For example, CuO NPs synthesized via a sol-gel procedure was used for Cd^{2+} and Ni^{2+} removal from aqueous solution, wherein high pH of the aqueous medium generated surface negative charge on the adsorbent, and stimulated metal adsorption by electrostatic attraction (Hassan et al., 2017). Zero valent Cu NPs (Cu^0) (dose=2 g/L, pH=7.0) degraded 2,4-dichlorophenol (7.5 mg/L) to the tune of 60% within 5 days of reaction (Chang et al., 2019). Nutrients removal (N, P) from activated sludge using Cu-based NPs were investigated where phosphate removal capacity reached 98%, and N removal reached ~73% at a 5 mg/L dosage of NPs (Chen et al., 2012). CuO NPs also degraded nitrobenzene in aqueous solution upon sonication for 25 min via a Fenton reaction (·OH radicals) (ElShafei et al., 2014). Furthermore, green synthesized Cu-based NPs using *Punica granatum* leaf extracts improved the functionality of nanoparticles for removing methylene blue (MB) from aqueous solution through electrostatic attraction, with an adsorption capacity of 166 mg/g MB (Vidovix et al., 2019). However, the increasing application of Cu-based NPs raised concerns of negative environmental impacts to living organisms (Chen et al., 2012). The phytotoxicity of Cu NPs on wheat (Perreault et al., 2014), the cytotoxicity of the NPs on human epithelial cells (Moschini et al., 2013), NP-caused growth inhibitions, the Cu uptake of *Arabidopsis thaliana* upon application of Cu NPs (Wang et al., 2016), and their toxic effects on aquatic organisms such as *Hydra magnipapillata* have been reported (Murugadas et al., 2016). Therefore, it is prudent to synthesize encapsulated or supported Cu NPs, which have low toxicity toward organisms while retaining a high contaminant removal capability.

2.3 Bimetallic nanoparticles (BNPs)

BNPs contain two metallic elements, exhibiting properties related to each metal and resulting from synergistic interactions between two metals. The assembly of BNPs can be as random alloys, alloys with an intermetallic compound, cluster-in-cluster or core-shell structures (Zaleska-Medynska et al., 2016). The shape and size of metallic NPs are strictly dependent on their mode of preparation that also influences the physicochemical properties of the final product (Zaleska-Medynska et al., 2016). Preparation methods for the production of BNPs include chemical reduction, green synthesis, microemulsion method, photodeposition, and radiolysis (Zaleska-Medynska et al., 2016).

BNPs can remediate multiple contaminants in aqueous systems (Scaria et al., 2020). A $Fe_{0.9}/Cu_{0.1}$ BNP removed As(V) (60.22 mg/g) from aqueous solution (initial As(V) concentration = 200 mg/L; adsorbent dose = 2.5 g/L) (Sepúlveda et al., 2018). Incorporation of relatively low amounts of Cu in the Fe/Cu BNP resulted in a non-uniform core-shell structure with agglomerate-type chains of magnetite that enhanced electron transfers among the metals (Fe/Cu) and the target metalloid (As); hence, the adsorption of As(V) increased (Sepúlveda et al., 2018). To decontaminate Se(IV) in groundwater, Fe-Mn binary oxide NPs were synthesized and stabilized with starch and carboxy methyl cellulose (CMC) (Xie et al., 2015). The starch-stabilized NPs were more effective than CMC stabilized NPs in adsorbing Se(IV), with maximum adsorption capacities of 109 and 95 mg Se/g for the starch- and CMC-stabilized NPs (Xie et al., 2015).

Ascorbic acid-stabilized Fe/Pd BNPs and silica-based Fe and Fe/Fe-oxide NPs were successfully tested for degrading trichloroethylene in water (Meeks et al., 2012). Due to high catalytic activity of BNPs, Fe/Ni-polystyrene cation exchange resin composites showed nearly 91% degradation and/or dechlorination of trichloroethylene (20 mg/L initial concentration) (Zhou et al., 2016).

Similarly, biochar-supported Ni/Fe BNPs also enhanced the reduction of 1,1,1-trichloroethane (1,1,1-TCA) in groundwater remediation (Li et al., 2017). The 1,1,1-TCA removal efficiency increased up to 99.3% when the BC to Ni/Fe mass ratio reached 1.0 (Li et al., 2017).

2.4 Other metal oxide nanoparticles

The oxides of Ti, Mg, and Zn have proven useful for removing contaminants from the environment although the application of metal oxide nanoparticles can influence mineral nutrition, oxidative stress and photosynthesis of plants (Rizwan et al., 2017). Some nanoparticles synthesized with the mediation of plants and/or plant products (e.g., Au NPs from *Cassia fistula*, FeO from *Rumex acetosa*) have been reported to be beneficial in environmental, agricultural and biomedical applications (Rai et al., 2018). TiO_2 NPs displayed a high photocatalytic degradation efficiency of 90.24% at a 20 mg/L initial concentration and pH 5.0 for imidacloprid in an aqueous system (Akbari Shorgoli & Shokri, 2017). The catalytic activity of flower-like nanostructured rutile (TiO_2) was used to rapidly degrade methyl orange (MO) and inactivate drug-resistant bacteria such as *Klebsiella pneumonia* (Kőrösi et al., 2016). Similarly, photodegradation of levofloxacin by ternary nano $Ag_2CO_3/CeO_2/AgBr$ photocatalysts under visible-light irradiation was investigated and a double Z-scheme photocatalytic mechanism was proposed, which involved an electron transfer process by the active participation of radicals such as h^+, O_2^- and $\cdot OH$ in the photodegradation (Wen et al., 2018). Naphthalene was effectively removed (148.3 mg/g) from wastewater using ZnO NPs modified with 1-butyl-3-methylimidazolium tetrafluoroborate, and the removal capacity of the modified adsorbent was 122% higher than the bare ZnO NPs (Kaur et al., 2017). In spite of their capacity to remove a wide range of contaminants, metal oxide NPs may cause ecotoxicological effects towards various organisms. Therefore, care should be taken in terms of dosage during their application.

2.5 Carbon nanotubes

Single and multi-walled CNTs (SWCNTs and MWCNTs) are widely used as adsorbents for wastewater purification. The rolling of a single graphene layer into a cylindrical shape creates a SWCNT, while the rolling of many concentric SWCNTs into a tubular shape creates an MWCNT (Gusain et al., 2020). The removal of contaminants through adsorption is more rapid for CNTs than other carbonaceous adsorbents (activated carbon, graphene, graphene oxides, and biochar) due to availability of reactive adsorption sites and short diffusion distance (Lee et al., 2018). The major surface functional groups (e.g., -COOH and -OH) of CNTs participate in the bulk adsorption of contaminants. Studies have been conducted to graft other functional groups (e.g., $-NH_2$ and -SH) onto the surface of CNTs to enhance the adsorption capacities (Supplementary Information: Table S3). The adsorption affinity of CNTs can be increased by functionalizing the surfaces of CNTs through various processes such as oxidation, nonmagnetic metal oxide coating and grafting of magnetic iron oxides (Sarkar et al., 2018). The mechanisms involved in the adsorption process of contaminants by CNTs are dependent on the surface properties of CNTs and the chemistry of the contaminant ions or compounds. The mechanisms may include chemisorption or physisorption, while the ionic radius and hydration energy of the contaminants are important factors that determine the adsorption mechanisms (Sarkar et al., 2018).

The most prominent application of CNTs in environmental remediation includes the removal of organic contaminants through membrane filtration due to the high stability and large specific surface area of CNTs (Jame & Zhou, 2016). An electrochemically activated CNT filter was able to generate $^{\cdot}OH^{-}$ radicals from H_2O_2 to remove phenol from aqueous solution to the tune of 87% within 4 h (Liu et al., 2015). CNTs also show catalytic activity to clean wastewater due to their cylindrical hollow tubes, high mechanical strength, and electrochemical properties. Ruthenium (Ru) precursor impregnated MWCNTs converted 100% aniline in wastewater within 45 min of reaction time (Garcia et al., 2006). However, the catalytic activity of CNTs is limited due to their hydrophobic nature, and the presence of impurities (Lee et al., 2018). Another prominent application of CNTs is in sensor-based approaches for contaminant detection. A selective sensor for Hg(II) was developed by adsorbing cold mercury vapor on SWCNTs in industrial wastewater (Safavi et al., 2010). The sensor was able to sense as low as 0.64 µg/mL Hg(II) in various types of wastewater samples (Safavi et al., 2010). Future research should be focused on the application of CNTs for real water decontamination using membrane filtration, catalysis, and sensing approaches while also concentrating on the ecotoxicity assessment of CNTs.

2.6 Graphene and graphene oxide

Graphene is a 2D structured material having a single atomic layer of sp^2 bonded carbon atoms, with each atom bonded to 3 others in a hexagonal lattice. Graphene shows high strength, durability and specific surface area (Meyer et al., 2007). Graphene oxide (GO) has a structure similar to that of graphene, while having more oxygen containing functional groups (Ma et al., 2017). The presence of hydrophobic moieties and π–π interactions in GO lead to high removal efficiencies for aromatic pollutants (Ersan et al., 2017). Oxygen-containing surface functional groups (-COOH, -OH and –C=O) may also be present in GO due to the incomplete reduction of GO. Another oxidized form of GO is exfoliated graphene oxide (EGO), which contains various surface functional groups such as hydroxyl, carboxyl, and epoxy groups (Ramesha et al., 2011). The advantages of graphene oxides for water treatment are their colloidal stability and high dispersibility in water, while graphene-based nanocomposites (modified with organic molecules and magnetic graphene nanocomposites) show higher specific surface areas and improved functionality than unmodified graphene (Perreault et al., 2015). In addition, reduced GO (rGO) shows high electron transport capacity and increased interaction with metal contaminants (Gollavelli et al., 2013; Lin et al., 2019). The adsorption of dyes such as MB, methyl violet, and rhodamine B onto EGO and reduced GO (rGO) sheets has been widely studied in water (Supplementary Information: Table S4). The elevated negative charge density assists in the effective adsorption of cationic dyes on EGO. In contrast, rGO, which has a high surface area, is effective in anionic dye adsorption due to van der Waals interactions (Ramesha et al., 2011). The prevalence of surface charges and different functional groups on EGO, GO, and rGO play important roles in the adsorption of polar contaminants such as phenolics and naphthol, charged heavy metals (Ahmad et al., 2020; Ersan et al., 2017), antibiotics such as sulfamethoxazole, sulfapyridine, and sulfathiazole (Çalışkan Salihi et al., 2020), and volatile organic compounds (Kumar et al., 2020b). The adsorption of phenolic compounds generally increases with increasing reduction degree in GO, whereas the adsorption of heavy metal ions shows the reverse trend (Wang & Chen, 2015). Likewise, Cd(II) and organic pollutants were co-adsorbed onto graphene *via* surface-bridging mechanisms (Wang & Chen, 2015). The adsorption affinity of four aromatics on GO increased in the following order: naphthalene (NAPH) < 1,2,4-trichlorobenzene (TCB) < 2,4,6-trichlorophenol (TCP) < 2-naphthol (Pei et al., 2013). The π–π interaction was the main mechanism involved during TCB, TCP and 2-naphthol adsorption onto graphene (Zhou et al., 2015), whereas H-bonding and O-containing surface functional groups were responsible for the adsorption of TCP and 2-naphthol onto GO (Pei et al., 2013). However, graphene-based NMs often suffer from low densities of reactive sites, including less oxygen-containing functional groups, while graphene-based nanocomposites show variable colloidal stability depending on modification type (Perreault et al., 2015). Future research should focus on the development of highly functionalized and stable graphene-based NMs for bulk removal of contaminants from aqueous solutions.

2.7 Polymer nanoparticles

The synthesis of polymer NPs follows two approaches: top-down and bottom-up (Krishnaswamy & Orsat, 2017). The top-down approach involves the dispersion of preformed polymers to produce polymer nanoparticles, while the bottom-up approach involves the polymerization of monomers to produce polymeric nanoparticles. Following the bottom-up approach, researchers synthesized hybrid polymer NPs from the ring-opening polymerization of pyromellitic acid dianhydride and phenylaminomethyl trimethoxysilane, followed by a sol-gel process to remove heavy metals such as Cu(II) and Pb(II) from water (Liu et al., 2010). These zwitterionic hybrid polymers adsorbed 0.28 and 1.56 mmol/g of Cu(II) and Pb(II), respectively, via electrostatic attraction when the initial metal concentrations were in the range of 0.001 to 0.1 mol/L, and the dose of adsorbent was 1 g/L (Liu et al., 2010). The development of a negative charge on the hybrid polymer NPs was mainly due to –COOH groups in the polymer hybrid which deprotonated to $–COO^-$ groups in aqueous system at pH > 4.0 and 5.0 during Cu(II) and Pb(II) adsorption, respectively, and was thus bound to positively charged metal ions on the NP surfaces (Liu et al., 2010).

MO was removed in an aqueous solution using polyamine nanoadsorbents. The MO adsorption capacity was increased by 32.04 and 30.28 mg/g, respectively, when the initial dye concentrations were increased from 10 to 100 mg/L at 65 °C and 25 °C, respectively. The MO adsorption was endothermic in nature, and the maximum MO adsorption capacity was 75.9 mg/g within 60 min of reaction time when pH of the medium was 6-10. Strong electrostatic attraction was the primary mechanism that caused maximum MO adsorption (Tanzifi et al., 2017). Chitosan, a biopolymer, is widely used to synthesize NPs for environmental remediation due to its low toxicity and high biodegradability. In a recent study, chitosan NPs were synthesized through ionotropic gelation for encapsulating enzymatic activity (Alarcón-Payán et al., 2017). The chitosan-NPs were loaded with versatile peroxidases and were successful in the biodegradation of phenolic compounds. The chitosan-based enzymatic NPs had a higher affinity constant toward phenolic compounds, were more thermostable than free enzymes, and their operational stability was further enhanced in a real-world wastewater situation when modified with different aldehydes (Alarcón-Payán et al., 2017). Similarly, chitosan NPs prepared through ionotropic gelation between chitosan and tripolyphosphates showed a 98% Congo red (CR) removal efficiency and adsorbed 5,107 mg CR/g of adsorbent in an aqueous solution (Alver et al., 2017). CR removal was dependent on the pH, ionic strength, encapsulation time and tripolyphosphate concentration. The mechanism involved was a strong electrostatic attraction between the protonated amino groups, with anionic CR at low pH (Alver et al., 2017). However, chitosan suffers from poor solubility in water (soluble in acid) and stability, which restrict its applicability in a wide range of contaminant removal applications (Saheed et al., 2020). Future research should be carried out in order to remove these barriers by using novel modifications.

2.8 Nanomaterials supported on inert materials and polymers

Environmental applications of NMs supported on inert materials (bulky, stable and non-toxic to organisms) such as activated carbon, BC, clay minerals, biodegradable polymers, and zeolites have recently attracted widespread attention (Mandal et al., 2018). Their availability, low-cost, and less toxic nature made these support materials popular in the field of soil and water remediation (Krasucka et al., 2021; Lazaratou et al., 2020). Pristine clay minerals, zeolites, and biochar often suffer from low contaminant adsorption and poor regeneration capacity, which can be improved by supporting NMs (e.g., nZVI) on the former materials leading to improved functionality and dispersion of the NMs (Mukhopadhyay et al., 2020; Premarathna et al., 2019; Alam et al., 2020) For example, granular activated carbon (GAC) was used to impregnate NPs (e.g., nZVI), and the supported material subsequently removed nitrobenzene from water (Mines et al., 2018). Reduction of nitrobenzene (with an initial concentration of 500 μM) was achieved at up to 56.6% by GAC-nZVI, which further improved to 63.6% following an additional modification step of the material with a covalent organic polymer (Mines et al., 2018). The π-π interaction between the aromatic groups of covalent organic polymer materials and nitrobenzene likely facilitated the removal of the contaminant (Mines et al., 2018).

Clay minerals were used extensively to support NMs for environmental remediation applications. For instance, a cationic surfactant cetyltrimethylammonium bromide (CTMAB) was used to improve the hydrophobic property of Fe-NPs supported on palygoskite clay, and the nanocomposite removed acid orange 7 (AO-7) by 98.4% (initial concentration of 20 mg/L) within 2 h of reaction from aqueous solution. At low pH, dissolved oxygen in the solution enabled hydrogen ions to produce H_2O_2 and $^{\bullet}OH$ radicals, which provided more oxidants to degrade AO-7 (Quan et al., 2018). Palygorskite-carbon nanocomposites were prepared through two methods: composite 1 involved a hydrothermal carbonization with starch on palygorskite, while composite 2 included a thermal activation (550°C for 3 h in a CO_2 environment) of composite 1 (Sarkar et al., 2015). Composite 2 adsorbed a large amount of anionic orange II dye (23.0 mg/g), whereas composite 1 efficiently adsorbed cationic MB (46.3 mg/g) (Sarkar et al., 2015). Similarly, a nanocomposite synthesized *in-situ* by embedding magnetite NPs into the palygorskite structure through the co-precipitation method had a maximum Pb(II) adsorption capacity of 26.6 mg/g (Rusmin et al., 2017).

nZVI can aggregate in aqueous solution when its concentration is high. Therefore, to avoid rapid aggregation and to improve its reactivity, zeolite supported nZVI (Z-nZVI) was prepared via the liquid phase reduction of Fe(III) salts (Suazo-Hernández et al., 2019). The maximum adsorption capacity of Z-nZVI was 11.52 mg As(III)/g, 48.63 mg Cd(II)/g, and 85.37 mg Pb(II)/g at pH 6, involving mechanisms such as electrostatic attraction, ion exchange, oxidation, reduction, co-precipitation, and complexation depending upon the ionic nature of heavy metal(loid)s (Li et al., 2018). nZVI supported on CTMAB-modified organobentonite was used as a reducing agent for organic contaminants such as 2-chlorophenol(2-CP), 2,4-dichlorophenol (2,4-DCP), 2,4,6-trichlorophenol (2,4,6-TCP) and pentachlorophenol (PCP) in an aqueous system; their removal efficiencies were 95.4, 96.8, 97.8, and 100%, respectively (Li et al., 2013).

Similar to clay minerals, biochar is another inert material used widely for supporting NMs (Liu et al., 2020). A novel GO-coated BC nanocomposite achieved a 30% enhancement in sulfamethazine sorption through π-π interactions between the antibiotic molecules and NPs (Huang et al., 2017). A ZVI-BC-chitosan nanocomposite was also shown suitable for removing heavy metals such as Pb(II) and As(V) and MB dye (Zhou et al., 2014). The novel nanocomposite removed Pb(II), As(V) and MB at 93, 95 and 68%, respectively (the initial concentrations of Pb(II), As(V) and MB were 40, 21 and 20 mg/L, respectively) (Zhou et al., 2014). The Cr(VI) removal in an aqueous system was also achieved by using nZVI assisted BC composites where the adsorbent showed 58.82 mg/g Cr(VI) removal *via* electrostatic attraction, complexation, metal reduction, and precipitation reactions (Zhu et al., 2018). The nZVI/biochar composite can play a dual role, firstly by converting the contaminant into a less toxic form by nZVI, and then adsorbing the contaminant *via* the active surface functional groups present on biochar, involving electron donor-acceptor reactions, chemisorption, and electrostatic attraction mechanisms (Fig. 3).

Attempts were made to stabilize CNTs on BC to remove heavy metals from wastewater (Inyang et al., 2015). Pb(II) was removed from wastewater using multi-walled CNTs dispersed on BC hickory chips (pyrolysis at 600°C in N_2 environment for 1 h), and the nanocomposite adsorbed 31.05 mg Pb(II)/g (initial concentration of 40 mg/L) (Inyang et al., 2015). The authors (Inyang et al., 2015) also found that bagasse BC modified with sodium dodecylbenzenesulfonate-CNTs (prepared using the same conditions above) was successful in fixing sulfapyridine by 56% (the initial concentration was 20 mg/L, solid: solution = 2:1, reaction time 24 h) in wastewater.

Chitosan-based composite NMs were also successful in removing heavy metals. The efficiency of alginate-coated chitosan NPs (Alg-CS-NPs) in removing Ni(II) from industrial effluents was investigated (Esmaeili & Khoshnevisan, 2016), showing that nearly 95% of Ni(II) was removed from solution under the following conditions: pH = 3, initial Ni(II) concentration = 70 mg/L, adsorbent dose = 0.3 g, and contact time = 30 min (Esmaeili & Khoshnevisan, 2016). At pH 3.0, the formation of sparingly soluble hydroxides of metals occurred, which contributed to overall metal removal from solution. At a high initial Ni(II) concentration (70 mg/L), the competitive adsorption of Ni(II) on the outer surface of the NPs led to a high adsorption capacity, whereas a high biomass dose (0.3 g) provided an increased surface area for the Ni(II) biosorption process (Esmaeili & Khoshnevisan, 2016).

Like chitosan, entrapment of nZVI in Ca-alginate beads (polymer) showed promising results for NO_3^- removal from groundwater. Ca-alginate beads acted as a bridge to bind the nZVI particles. Between 50-73% NO_3-N was removed by the alginate-entrapped nZVI, which was statistically similar to bare nZVI within the 2 h reaction period (Bezbaruah et al., 2009). Like NO_3^-, TCE degradation was also achieved, up to 81-90%, due to encapsulation of nZVI within Ca-alginate beads. The encapsulation resulted in greater mobility of nZVI particles than the entrapment method, and the required amount of Ca-alginate was significantly lower than for the entrapment method (Bezbaruah et al., 2011).

Entrapped nZVI in the alginate polymer matrix showed enhanced removal capacity of 1,1,2-trichloroethane (TCA) during the treatment of hydraulic fracturing wastewater (Lei et al., 2018). Results suggested that nZVI entrapment in alginate with or without polyvinyl alcohol removed 1,1,2-TCA from water (62.6-72.3%) with lower Fe aggregation after 90 days. The nZVI provided a chemically reducing condition, while the polymers adsorbed 1,1,2-TCA during wastewater remediation. Sun et al. (2018) reported that alginate-polyvinyl entrapped nZVI, aged for 2-months, showed a high removal capacity for Cu(II) (84.2%) and Cr(VI) (70.8%), much higher than for freshly prepared beads. The corresponding removal efficiencies were 31.2 and 39.2% in case of Zn(II) and As(V), respectively. The aging effect of the adsorbent for removing heavy metals was dependent on electrostatic interaction and specific bond formation mechanisms (Sun et al., 2018).

2.9 Carbo-iron nanomaterials

Carbo-iron is a composite NM consisting of nZVI clusters on activated carbon colloids (ACC) with a particle size of 0.8 µm. The material is especially designed for the *in-situ* generation of reactive zones and contaminant source removal when applied in groundwater remediation processes (Bleyl et al., 2012; Mackenzie et al., 2012). The carbo-iron colloids (CIC) can overcome the limitations of nZVI during *in-situ* groundwater remediation. The ACC gets reduced by H_2 in order to form CIC. The ACC have sorption properties, while nZVI provides strong reactivity to degrade or immobilize the contaminants. For example, CIC produced 60% chlorine-free-C_2-hydrocarbons when degrading TCE (Mackenzie et al., 2012). Similarly, pentachloroethane (PCE) dechlorination in groundwater was achieved at field scale in Germany with NM transport lengths of several metres and fast PCE decomposition without forming toxic vinyl chloride (Mackenzie et al., 2016). However, the release of Carbo-iron NM (in g/L concentration) in the environment during groundwater treatment may have ecotoxicological effects on amphipod *Hyalella azteca* leading to inhibited weight, length, and feeding rate of the animal (Weil et al., 2016). However, the ecotoxicological data on *Daphnia magna* (Crustacea), *Scenedesmus vacuolatus* (Algae), *Chironomus riparius* (Insecta), and nitrifying soil microorganisms revealed no effect at 0.1 mg/L NM concentration in acute or chronic toxicity tests in groundwater contaminated with chlorohydrocarbons (Weil et al., 2019). The risks to organisms were minimized by around 50% after the first injection of Carbo-iron NM in heavily contaminated aquifer zones, which suggested more benefits of remediation than detriments due to toxicity effects (Weil et al., 2019).

2.10 Other nanomaterials

NPs such as $NiFe_2O_4$ and zinc aluminate were reported to degrade dyes in aqueous solution. For example, 77% degradation of MO (initial concentration of 10 mg/L) was achieved by $NiFe_2O_4$

NPs within 5 h of exposure to sunlight, compared to no significant degradation under dark conditions (Hirthna et al., 2018). The dye removal mechanism in this study followed an electron paramagnetic resonance type of photodegradation (Hirthna et al., 2018). Likewise, 98.28% photodegradation of MB (initial concentration 10 mg/L) was achieved in 150 min using bismuth doped zinc aluminate NPs (Kirankumar & Sumathi, 2017). Bismuth doping into zinc aluminate decreased the band gap energy significantly, which in turn increased the photocatalytic degradation of MB. A hybrid-nano Ag_3PO_4 composite was synthesized by a two-step solvothermal process using reduced graphene oxide (rGO), Ag_3PO_4 NPs and molybdenum dichalcogenides (MoS_2, 99%); the synthesized hybrid-nano Ag_3PO_4 composite was suitable for the degradation of 4-nitrophenol, with a greater photocatalytic activity and stability than pure Ag_3PO_4 NPs (Zhang et al., 2018a).

3. Nanomaterials for contaminants treatment in soil

Several studies have reported the immobilization of toxic metal(loids) in soils using NMs (Baragaño et al., 2020; Matos et al., 2017; Tafazoli et al., 2017). However, the fates of NMs after their application to soils for contaminant removal require proper understanding. Currently, available soil contaminant remediation strategies follow two main directions: (i) lowering the concentration of pollutants to well below a critical limit, and (ii) stabilization of pollutants within the soil to reduce their immediate risk to environmental receptors (Floris et al., 2017; Hou et al., 2020). There is a growing interest in NMs for soil remediation because of their large specific surface area, high chemical reactivity and selectivity, although their reactivity may vary with geochemical conditions. Reports are available on the use of NMs for the remediation of inorganic contaminants in soil (Supplementary Information: Table S5). Recently, nZVIs have attracted widespread research attention in detoxifying soil due to their effectiveness in reducing or inactivating various metallic species present in soils (Jiang et al., 2018). An nZVI/Cu treatment reduced Cr(VI) by 99% at pH 5.0 (Zhu et al., 2016), while the Cr(VI) reduction efficiency increased from 14.58 to 86.83% without maintaining pH of the soil (Singh et al., 2012b). In the presence of diethylenetriaminepentaacetic acid (DTPA), Cr release decreased up to 81% due to the application of 4% bentonite supported nZVI (prepared using green tea leaf extract and $FeSO_4.7H_2O$). The reduction in Cr release by the same material was 79% in the presence of $CaCl_2$ in the soil. The mechanisms involved precipitation and surface complexation reactions on the bentonite-nZVI (Soliemanzadeh & Fekri, 2017).

The bioavailability of single and multi-metal(loid)s (As, Cd, Cr, Pb, and Zn) in contaminated soils in the presence of nZVI was assessed under acidic and calcareous soils. The availability of heavy metals and metalloids such as As, Cr and Pb was reduced by 82% upon an application of 10% nZVI (w/w), whereas the corresponding values for Zn and Cd varied from 31 to 75% and 13 to 42% (Gil-Díaz et al., 2017b). Furthermore, the stability and effectiveness of nZVIs were confirmed in contaminated soils (Cd, Cr, and Zn) grown with barley plants. A 10% dose of nZVI enhanced the development of the barley plants and decreased the As uptake by decreasing the bioavailable As fraction (Gil-Díaz et al., 2016a; Gil-Díaz et al., 2016b). A nZVI/Ni BNPs prepared using $NaBH_4$ were applied to remediate Cr(VI) contaminated soils, and the reduction of Cr(VI) in the soil leachate reached as high as 99.84% at pH 5.0 (Zhu et al., 2017a).

Three commercial nZVI slurries from Toda (bare RNIP and RNIP-D; D denotes an organic dispersant) and from Nano Iron (25S) were used at different doses (1, 5 and 10%) to immobilize As and Hg in soils. A 5% application of nZVI showed a decreasing trend of exchangeable As (by >70%) in soil, whereas a 10% application of nZVI was necessary to achieve a reduction of exchangeable-Hg between 63 and 90% depending on the nZVI and soil types. Overall, the 5% nZVI application rate was more effective in the reduction of exchangeable As, whereas RNIP and RNIP-D were most effective at a 10% application rate for the reduction of exchangeable-Hg (Gil-Díaz et al., 2017a). A long-term soil heavy metal(loid) immobilization study (6-15 years) using nZVI concluded that nZVI remained “reactive” after 6-15 years, corresponding to an observation that available Cu and As were lower in the nZVI-treated soil than in the untreated soil and pH was considered the factor most responsible for both As and Cu immobilization (Tiberg et al., 2016). A similar type of investigation on the impact of pH (4-8) and time (48 and 192 h) on nZVI-mediated Pb, Cd, Zn and As immobilization in soils was conducted. The Zn and Cd concentrations in soils decreased by 29-34% and 38-44%, respectively, at pH 8, while the corresponding values for Pb and As were 98 and 96%, respectively (Vítková et al., 2017). The authors (Vítková et al., 2017) confirmed that Fe/Al oxides or hydroxides, organic matter and aluminosilicates played a major role in governing the solubility of metals and metalloids in soils, along with soil pH.

The immobilization and degradation of organic contaminants by NMs in soil is sporadically studied. The removal efficiency of hexachlorobenzene by nZVI was investigated in the presence of competing or coexisting anions present in the soil (Su et al., 2012). HCO_3^- had no effect on the decomposition of hexachlorobenzene, but Cl^- and SO_4^{2-} promoted rapid decomposition rates, while NO_3^- competed with the contaminant molecules (Su et al., 2012). *p,p′*-DDT degradation using nZVI-B (prepared using the sodium borohydride method) and nZVI-T (commercially purchased) in soil showed a low rate of DDT degradation (22.4 and 9.2%) due to the presence of organic matter and other soil constituents (El-Temsah et al., 2016). Han et al. (2016) reported degradation half-lives of 37.5, 73.7 and 24.1 h for DDT in flooded soil at 35°C by nZVI, nZVI coated with polyimide, and nZVI coated with sodium oleate, respectively. Similarly, the positive effect of Ni/Fe BNPs in reducing the phytotoxicity of polybrominated diphenyl ethers (PBDEs)-contaminated soil to Chinese cabbage was evaluated (Wu et al., 2016a). The germination rate, and shoot and root lengths of the Chinese cabbage in the Ni/Fe BNPs treated soil increased by nearly 15, 60, and 63%, respectively, compared to the control (Wu et al., 2016a).

Biochar supported nanoparticles have shown promise in heavy metal immobilization in soils, as they provide additional active sites for capturing metal ions (Zhu et al., 2017b). Biochar-supported nano iron phosphate particles were synthesized to remediate Cd(II) contaminated soil. The Cd(II) immobilization efficiency of the adsorbent was 81.3% after 28 days, and Cd(II) bioaccessibility (physiological-based extraction test) was reduced by 80.0%. Plant growth experiments proved that the composite inhibited the Cd(II) uptake to the below-ground and above-ground parts of cabbage mustard by 44.8% and 70.2%, respectively (Qiao et al., 2017). Application of BC–supported nano hydroxyapatite reduced Pb by 56.8% after 28 days of application in a Pb-contaminated soil (Yang et al., 2016b), and a column experiment showed significant mobility of BC–supported nano hydroxyapatite. The immobilization rate of Pb in the soil was 74.8% after nano hydroxyapatite-biochar remediation (Yang et al., 2016a).

Heavy metals such as Pb, Cu, and Zn were also immobilized by calcium phosphate nanoparticles (CPNs) in shooting range soils. Application of these NPs to the soil decreased Pb and Cu concentrations by more than 90%, and Zn by 50% (Arenas-Lago et al., 2016). Other examples include nano-hydroxyapatite, which reduced Pb(II) concentrations in Ryegrass by 2.86-21.1% and 13.19-20.3% in the roots and shoots, respectively, due to the secretion of tartaric acid in the root rhizosphere that enhanced Pb adsorption onto the NPs (Ding et al., 2017).

BNPs and carbonaceous NMs have also been used for soil remediation. For example, CMC-stabilized Pd/Fe^0 BNPs displayed a nearly 7-fold greater efficiency for γ- hexachlorocyclohexane degradation in soil as compared to Fe^0 NPs (nFe^0) alone (Singh et al., 2012a). Similarly, biochar-supported Ni/Fe BNPs debrominated decabromodiphenyl ether at 30.2 and 69.0% higher rates than pristine Ni/Fe and biochar in soil, respectively (Wu et al., 2016b). Similarly, GO was used to remediate Cd-contaminated soils; results suggested that GO could adsorb up to 103.3 mg/g Cd(II) when applied at a high dose (1 g/kg), and could be used for remediating highly contaminated sites (Xiong et al., 2018a).

4. Approaches for contaminant nanoremediation

Nanoremediation involves various technical approaches such as adsorption, photodegradation, heterogeneous catalysis, the involvement of microorganisms (nano-bioremediation), and deployment of electrical fields (electro-nanoremediation) for applying NMs to remove or immobilize contaminants in the environment. Hence, it is important to understand how the above approaches work while employing NMs for remediation.

4.1 Adsorption

Adsorption of contaminants occurs on the surface of an adsorbent at the solid-liquid interface (Fig. 4). The solid surface of the adsorbent interacts with the adsorbate/solute in the solution, and they are attracted to each other by solid-liquid intermolecular forces (Sadegh et al., 2017). In the case of bulk adsorbents, various bond (e.g., ionic, covalent and metallic) requirements of the constituent atoms in the adsorbent are filled by other atoms in the material. Since the bonds of atoms at the surface of the adsorbents are not fully satisfied, they adsorb the adsorbate to achieve a charge/bond balance. However, the nature of adsorption is highly dependent on the nature of the adsorbate species present in the liquid solution. Adsorption processes mainly include van der Waal's forces, electrostatic attraction, and chemisorption (covalent bonding) (Gupta et al., 2016; Sadegh et al., 2017; Sadegh et al., 2016). In addition, adsorption also involves a mass transfer process in which a solute mass is transferred to the surface of a solid and bound by chemisorption or physical adsorption. High specific surface area of an adsorbent can considerably control the degree of adsorbate deposition onto the adsorbent (Sadegh et al., 2017).

4.2 Photodegradation

Photocatalysis has been one of the most successful processes to remove contaminants from the environment due to its low cost and environmental compatibility (Al-Mamun et al., 2019; Raizada et al., 2019). Photocatalysis is a photoreaction that can be enhanced in the presence of a catalyst (Fig. 5). During photocatalytic activity, electron-hole pairs are generated depending upon the type of catalyst. These electron-hole pairs also generate the superoxide radicals that degrade contaminants. TiO_2 NPs were used as catalysts for practical applications. A novel nano-TiO_2 photocatalyst doped with neodymium (Nd^{3+}) was employed to remove Cr(VI) by catalytic reduction, obtaining a >99% efficiency in Cr(VI) reduction. Here, Nd^{3+} ions deposited on the TiO_2 surfaces facilitated the creation of sites for electron accumulation, and hence achieved a high Cr(VI) reduction rate (Rengaraj et al., 2007). However, TiO_2 promotes photodegradation primarily under UV-light, while other catalysts such as CeO_2 show rapid photodegradation rates under visible light (Qi et al., 2014). An $Ag_2CO_3/CeO_2/AgBr$ nano-photocatalyst was designed by the *in-situ* loading of Ag_2CO_3 onto CeO_2 spindles via the corrosion process, and the material showed visible light degradation of levofloxacin (Wen et al., 2018). Various carbon-based nanomaterials such as graphene composites containing NPs (e.g., TiO_2 NPs) showed enhanced photocatalytic activity. Under UV irradiation, the energy of photons was greater than the band gap of carbon materials, which generated valence band holes (h^+) and band electrons (e^-). The holes produced superoxide radicals that degraded the organic contaminants, while electrons from superoxide radicals reduced heavy metal contaminants (Raizada et al., 2019).

Likewise, the rGO/MS_2 (M= M_0, W) hybrid-nano Ag_3PO_4 composite was more suitable for a photocatalytic degradation of 4-nitrophenol than was pure Ag_3PO_4 (Zhang et al., 2018a). The Ag_3PO_4@MS_2/rGO composite photo-catalyst displayed a >98% degradation efficiency for 4-nitrophenol after four cycles of use. The MS_2/rGO hybrid strongly enhanced the photocatalytic stability of Ag_3PO_4 due to the reduction of Ag_3PO_4 to Ag^0 by photo-generated electrons (Zhang et al., 2018a). Khairy and Zakaria (2014) reported photocatalytic degradation of MO by Cu-doped TiO_2 NPs under both UV and visible light. Doping of metals (e.g., Cu) did not change the structure of the crystal, but a significant change was observed in the particle size and photodegradation rate. Cu-doped TiO_2 NPs had a higher MO degradation efficiency under UV irradiation (73%) than visible light irradiation (50%). The doping of metals in the pure oxide matrix served as electron-holes separation centers, which enhanced the degradation of MO (Khairy & Zakaria, 2014). Therefore, the introduction of doping metal ions can improve the catalytic activity of TiO_2 NPs under visible light illumination.

4.3 Heterogeneous catalysis

In heterogeneous catalysis, the phase of the catalyst must be different from the phase of the reactant. In general, heterogeneous catalysis involves a solid phase catalyst and a liquid phase reactant. The catalysts are employed to enhance the reaction or adsorption rates. However, mass, heat transfer and thermodynamic parameters also affect the reaction rate (Sievers et al., 2016). The most important parameter affecting the reaction rate of the catalyst is its surface area. Heterogeneous catalysts can be used with NPs to improve the degradation of organic contaminants due to the advanced oxidation capacity of the catalysts. Several oxidants such as persulfate (PS), peroxymonosulfate (PMS) and hydrogen peroxide (HP) have been successfully used for removing contaminants. nZVI coupled with common oxidants such as NaClO, $KMnO_4$ and H_2O_2 resulted in high removal efficiencies of As(V), Cd(II), and Hg(II) within only 10-30 min (Guo et al., 2016). nZVI with PS showed a high removal capacity of 1,4-dioxane and As(III) from contaminated water, where the As(III) removal capacity of PS/nZVI was 115.27 mg/g, and the 1,4-dioxane degradation rate was 0.0347 h/mg/min (Kang et al., 2018). Similarly, PS/nZVI removed nearly 97% of trichloroethene (TCE) in the presence of ethylenediaminetetraacetic acid (Dong et al., 2017).

Bimetallic nZVI NPs were used for dual Fenton oxidation and reductive dechlorination of 2,4-dichlorophenol. A nZVI-Fe/Pd heterogeneous catalyst composite showed an approximate 16% reductive dechlorination efficiency, and a 28% Fenton oxidation efficiency for 2,4-dichlorophenol (Li et al., 2015). A combined application of nZVI and bisulfite (S(IV)) revealed that an increased Fe^0 concentration in the Fe^0/S(IV)/O_2 system improved sulfamethoxazole removal from aqueous media due to an accelerated activation of S(IV) and Fe^0 corrosion (Du et al., 2018).

4.4 Electro-nanoremediation

Pre-magnetization by the application of a weak magnetic field was suitable for promoting the corrosion of Fe^0, which might enhance the removal rates of contaminants by nZVI in soil and water systems (Pan et al., 2017). In view of this principle, electrolysis was applied to micro-sized Fe^0 (mFe^0) for *p*-nitrophenol (PNP) removal (Xiong et al., 2018b). The results suggested that the rate constants of PNP removal by electrodialysed-mFe^0 (Ele-mFe^0) were 1.72-144.50 fold higher than those of pristine mFe^0 under various conditions because the electrolysis aggravated the corrosion of mFe^0 by releasing Fe(II) ions (Xiong et al., 2018b). Similarly, a combined system of nZVI and electro-kinetic remediation was used to study the transport and degradation of molinate in soils. Molinate was degraded by nZVI in soils at slower rates than in an aqueous system due to the heterogeneous nature of the soil (Gomes et al., 2014). The molinate degradation occurred via the oxidative pathway, which involved oxygen and the formation of hydrogen peroxide and hydroxyl radicals (Gomes et al., 2014). nZVI was employed along with electrokinetic treatment for the degradation of chlorinated ethenes (CEs) in the presence of *Dehalococcoides* spp. and *Desulfitobacterium* spp. (Czinnerová et al., 2020). The combined treatment resulted in a rapid 75% decrease of cis-1,2-dichloroethene (cDCE) concentration in the contaminated area, and produced methane, ethane, and ethene as the end products. The treated aquifer showed increased activity of organohalide-respiring bacteria, and cDCE-oxidizing methanotrophs and ethenotrophs proliferated near the anode under low oxygen conditions. The nZVI treatment resulted in mild negative effect on indigenous bacteria, but the microbiome was restored within 15 days (Czinnerová et al., 2020). Application of nZVI with a direct current (DC) electric field led to a greater increase of CE remediation efficiency than nZVI alone in a study in the Czech Republic (Černíková et al., 2020). This method was environmentally sound for improving CE reduction efficiency by improving the longevity, migration and reactivity of the nZVI, and reduced the cost of treatment by five times compared to bare nZVI (Černík et al., 2019; Černíková et al., 2020). Only a limited number of studies have been conducted on the electro-nanoremediation of contaminants assisted by NMs, but the potential of this method must be explored in the future for practical applications.

4.5 Nano-bioremediation

Biological technology offers cost-effectiveness and a low generation rate of toxic substances, but a relatively slower rate of remediation (Hou et al., 2020). Nano-bioremediation may be defined as the remediation of a contaminant using NPs and biological technology together for accelerating the removal/degradation rate of contaminants (Cecchin et al., 2017). The focus of the nano-bioremediation technique is to reduce the concentration of contaminants to a level where it becomes prone to biodegradation, and further reduce the contaminants to a safe limit through biodegradation. TCE was dechlorinated using a long-lasting emulsified colloidal substrate (LECS) that contained nZVI and microorganisms such as *Dehalococcoides* spp. and *Desulfitobacterium* spp. (Sheu et al., 2016). The supplement of LECS in TCE-polluted groundwater effectively stimulated the TCE dechlorination rate under anaerobic conditions (Sheu et al., 2016). Moreover, the population of *Dehalococcoides* sp. increased from 2×10^3 to 1.2×10^7 cells/L, and *Desulfitobacterium* sp. increased from 1×10^3 to 7.4×10^6 cells/L after 60 days. Similarly, TCE removal efficiency was promoted when nZVI was integrated with *Dehalococcoides* sp. BAV1 compared to systems with nZVI and *Dehalococcoides* sp. alone, and the optimum dose of nZVI for maintaining microbial activity was found to be 0.05 g/L (Shanbhogue et al., 2017).

Integration of anaerobic bacteria such as organohalide respiring bacteria, sulfate reducing bacteria (SRB) and iron reducing bacteria (IRB) with nZVI also showed promising results in removing inorganic and organic pollutants (Dong et al., 2019). Here, nZVI provided reducing conditions, where the generated hydrogen acted as an electron donor for hydrogenotrophic bacteria, resulting in the degradation of halogenated compounds. Xu et al. (2014) reported that ZVI was able to reduce higher congeners of PBDEs to lower congeners, and subsequently degradation was promoted by *Dehalococcoides* sp. CBDB1. Thus, complete degradation of PBDEs was achieved by the integration of nZVI with *Dehalococcoides* sp. CBDB1.

The combination of nZVI and SRB has also improved heavy metal removal from contaminated systems. Yi et al. (2009) reported that 98.1% of U(VI) was removed by a nZVI+SRB integrated system within 4 h of reaction, while the removal rate of the individual system of ZVI and SRB was 17.4 and 67.3%, respectively. Under anaerobic conditions, SRB transformed sulfate into sulfides (e.g., H_2S, S^{2-} and HS^-) via the metabolism of organic matter. Then sulfide could bind with heavy metals to form stable complexes with SRB metabolites (Kumar et al., 2015).

Similarly, Vogel et al. (2018) investigated the microbial degradation of PCE in the presence of *Sulfospirillum multivorans, Desulfitobacterium spp*. and *Dehalococcoides mccartyi* together with Carbo-iron NM. The study suggested that embedded nZVI decreased the redox potential of the groundwater due to their reaction with oxygen, leading to nZVI-corrosion-induced formation of H_2 within 190 days after the injection, the latter promoting sulphate-reducing conditions.

A similar approach to test the effectiveness of a hybrid system using nano scale zinc oxide (n-ZnO) and lindane-degrading yeast *Candida* VITJzN04 for lindane degradation was evaluated (Salam & Das, 2015). The half-life of the lindane was lower (9 h) with an embedded bio-nano hybrid as compared to yeast *Candida* VITJzN04 (28 h); the enhanced lindane degradation by the bio-nano hybrid was attributed to the increased porosity and permeability of the yeast cell membranes (Salam & Das, 2015). SiO_2 NPs coated with a zwitterionic lipid derivative were used in the bioremediation of benzo[a]pyrene (Wang et al., 2015a). The authors used *Pseudomonas* *aeruginosa*, a gram-negative bacterium, and 1,2-dimyristoyl-*sn*-glycero-3-phosphocholine as a source of lipids, which adsorbed and sequestered benzo[a]pyrene and maintained the colloidal stability of NPs for their transport to the contaminant source (Wang et al., 2015a). Another study using CMC-stabilized Pd/Fe^0 ($CMC-Pd/nFe^0$) BNPs, and the microorganism *Sphingomonas* sp. Strain NM05 targeted the degradation of hexachlorocyclohexane (γ-HCH) in soil and found that the γ-HCH degradation efficiency was ∼1.7–2.1 times greater in the integrated system than the control system (Singh et al., 2013). Dechlorination of the PCB Aroclor 1248 was performed using Pd/nFe BNPs and *Burkholderia xenovorans* LB400 under anoxic conditions. Toxic equivalent values of polychlorinated biphenyls (PCBs) decreased from 33.8×10^{-5} μg/g to 9.5×10^{-5} μg/g after the nano-bioremediation treatment (Le et al., 2015). Apart from organic contaminants, attempts have been made to immobilize heavy metals in soil through nano-bioremediation. *Citrobacter freundii* Y9, a Se reducing organism, secreted biogenic nano-Se^0, which converted 46-57 and 39-49% of elemental mercury (Hg^0) in soils to its insoluble mercuric selenide (Hg-Se) form under oxygen-rich and oxygen-free conditions, respectively. Furthermore, an addition of sodium dodecyl sulfonate enhanced soil Hg^0 remediation due to the increased release of intracellular nano-Se^0 from the bacterial cells (Wang et al., 2017).

5. Practical applications

Studies on *in-situ* remediation using NMs are important, but available literature is limited. Most field studies are confined to nZVI applications for contaminants removal from groundwater. Therefore, we discuss *in-situ* remediation applications focusing on various practical modes of nanoremediation along with a few examples of real field scale studies as well as issues that need to be resolved for the large-scale field application of NMs for environmental remediation.

5.1 Field-scale application of nZVI for groundwater remediation

Nanoremediation using nZVI requires specific conditions to be met for achieving the most effective outcome. Appropriate site characteristics in terms of location, geological conditions, soil hydrogeological conditions (e.g., porosity, hydraulic gradient, groundwater velocity), and soil physico-chemical composition (e.g., pH, type and concentration of contaminants, dissolved oxygen level, concentration of other ions, redox potential) need to be determined before the injection of nZVI for contaminant remediation. The above would ascertain effective infiltration of nZVI in the contaminated zone, and help to ensure the efficient degradation or adsorption of specific contaminants at *in-situ* conditions (Karn et al., 2009). At the field-level, most of the applications of nZVI are concentrated on the degradation of chlorinated solvents. However, field studies were also found successful for treatment of halogenated organic compounds, PAHs, heavy metals (Ni, Cr(VI)), diesel fuel, PCBs, and pesticides (Bardos et al., 2018). In a case study, three types of non-pumping reactive wells (slanting, horizontal and vertical) were mixed with zero valent micro- (dose 0-4 g/L) and nano-sized iron (Fe^0) (dose 0-2 g/L) for nitrate removal in groundwater (Hosseini et al., 2018). Removal was primarily dependent on the contact time of the reactant with nitrate and the zone captured by the tube wells. Slanted non-pumping reactive wells showed higher NO_3^- reduction rate (57%) compared to the vertical (38%) and horizontal (41%) configurations (Hosseini et al., 2018). Earlier, nZVI was used to remove TCE from a groundwater aquifer (80 m^3) with 1300 L total water capacity (Elliott & Zhang, 2001). Here, approximately 1.7 kg of nZVI equivalent, yielding a 0.75-1.5 g/L loading, was used to completely dechlorinate TCE over a period of 2 days. Similarly, Gavaskar et al. (2005) reported the field application of nZVI (at 2 g/L loading) for TCE removal in 68000 L water in 7300 m^3 of aquifer volume. Furthermore, complete reduction of TCE in groundwater was observed using emulsified nZVI (at 140 g/L loading) in an aquifer of 40 m^3 with a 8500 L water capacity (Quinn et al., 2005). Chlorinated hydrocarbons including TCE in the groundwater were also successfully removed using nZVI (at 30 g/L loading) in 75000 L of water in a 15000 m^3 aquifer (Varadhi et al., 2005).

5.2 Permeable reactive barriers and direct injection

Permeable reactive barriers (PRB) consist of a permeable matrix that supports and anchors a reactive material to retain contaminants when a plume passes through the matrix. The main challenge of PRB systems is the costliness of the reactive barrier materials in removing target contaminants at desired levels (Tasharrofi et al., 2020). A nZVI-zeolite composite was evaluated to overcome the cost limitation of reactive materials in a PRB system to remediate aqueous Cd(II) (Tasharrofi et al., 2020). The zeolite was able to disperse nZVI well, and prevented its agglomeration. The nZVI-zeolite composite adsorbed 20.6 g/kg Cd(II) within 90 min (initial Cd(II) concentration 50 mg/L), and discharged very low levels of Cd(II) back into the environment, making the material suitable for application in PRBs (Tasharrofi et al., 2020). Under a pilot scale application in the Czech Republic, nZVI was injected to successfully remove chlorinated hydrocarbons on a short-term basis before the installation of a complete PRB remediation system. The nZVI injection prevented the migration of contaminants to adjacent areas outside the PRB (Bone et al., 2020). Direct injection can be used for both contaminant source and pathway treatments. A known quantity of nZVI is applied to a known depth of an aquifer either by gravity or by introducing pressure. The injection processes may include: (a) direct push or a stationary injection point to emplace a nZVI slurry in the treatment zone, (b) hydraulic fracturing using air or water to create preferential flow, (c) liquid atomization (i.e., pulses of pressure during injection), and (d) injection through a carrier (e.g., surfactant) for delivery of nZVI in the vadose zone (Ding et al., 2013). Apart from trialling PRB and direct injection technologies under field conditions, future research should concentrate on the development of inexpensive and efficient modes of *in-situ* nanoremediation.

5.3 Issues with field application of nanomaterials for remediation

Field scale applications of various NMs in addition to nZVI are urgently needed for environmental remediation including soil contaminants treatment. However, the following issues should be considered to enhance the practical utility of nanoremediation.

(1) One of the key concerns of NMs application is the lack of dose optimization. High application rates of NMs in water may be useful for removing a target contaminant, but it can be a serious concern when applied to soil. The large quantity of NMs required for remediating contaminated soils at the field scale is unmanageable using conventional production facilities. In addition, high concentrations of NPs (e.g., nZVI) may cause toxicity to microorganisms (Dong et al., 2019).

(2) Standard protocols to apply NMs for environmental remediation are still lacking. Therefore, appropriate application procedures for different NMs need to be documented and updated for field scale applications.

(3) Regeneration of applied NMs in soil needs further investigation. It is difficult to separate NMs from soil once they are added or injected because soil itself is a highly heterogeneous medium. Adsorbed contaminants may desorb from the nanoadsorbents after some period.

(4) Various NMs such as CNTs and GO, and NPs such as BNPs, polymer NPs, and Cu- and Fe-based NPs are quite expensive but have enormous potential for both organic and inorganic contaminant remediation at the field scale. Green synthesis techniques (as applied for nZVI) should also be considered for these NMs to minimize environmental toxicity.

(5) The impact and fate of applied NMs on aquatic and soil organisms should be studied thoroughly before application to test their ecological and environmental safety (Besha et al., 2020).

(6) Optimum operational factors (e.g., competing ions, pH, time, organic matter, temperature) of various NMs for remediating various contaminants requires standardization at the field level due to the heterogeneous nature of field sites.

6. Environmental risk of nanomaterials

The potentially vast applications of NMs for remediating contaminated soil and water have earned widespread research attention; studies have specifically vied to understand the mechanisms of NM interactions with environmental components, microbial communities and target contaminants (Biswas & Sarkar, 2019; Rai & Biswas, 2018). The deposition of NMs in the environment through soil and wastewater treatment processes has been reported to cause toxicity to microorganisms such as bacteria including plant growth promoting rhizobacteria (Lewis et al., 2019). nZVI is the most widely used NPs for the remediation of various contaminants in the environment. The fate of NPs, particularly in soils, depends on several key parameters, such as soil texture, pH and organic matter contents. nZVI might have toxic effects on microbial communities (Lefevre et al., 2016). For example, nZVI disrupted microbial cells by producing reactive oxygen species that caused cytotoxicity and changed the population and functional composition of the microbial community (Lefevre et al., 2016). Similarly, nZVI particles at high concentrations showed a strain dependent antibacterial effect on *Escherichia coli* leading to cell inactivation via oxidative stress (Chaithawiwat et al., 2016a). Gram negative bacteria were more susceptible to nZVI toxicity than Gram positive bacteria (Chaithawiwat et al., 2016a). Chaithawiwat et al. (2016b) reported that the *rpoS* gene was mainly responsible for resisting nZVI toxicity at cellular level. Unlike *E. coli*, *Pseudomonas putida* F1 exhibited high tolerance to nZVI at a 0.1 g/L dose by virtue of the rigid cell membrane of the bacterium (Kotchaplai et al., 2017).

Since nZVI is an efficient As(V) removal agent in aqueous systems, the effects of its excessive application on plants was studied using *Arabidopsis thaliana* grown hydroponically (Zhang et al., 2018b). Biosensors for inorganic phosphate (Pi) and Mg-ATP^{2-} were used to monitor *in vivo* Pi and Mg-ATP^{2-} levels in the cells. An excess nZVI exposure resulted in Pi starvation in plants, leading to adverse effects on plant growth (Zhang et al., 2018b). Additionally, earthworm species such as *Eisenia fetida* and *Lumbricus rubellus* were also affected by the application of nZVI in soil at a high dose (500 mg/kg). However, aging or oxidation of nZVI may reduce its toxicity level (El-Temsah & Joner, 2012). For example, Fajardo et al. (2015) reported that aged nZVI had no adverse effects on soil physico-chemical properties and *Caenorhabditis elegans* in a Zn-contaminated soil, although the Fe content in the soil was increased. However, in contrast to the Zn-contaminated soil, the growth of *C. elegans* was decreased in a nZVI-treated Pb-polluted soil (Fajardo et al., 2015).

Based on ecotoxicity tests performed by Hjorth et al. (2017), most nZVI products would receive no environmental hazard classification according to European regulations, except for the ball-milled nZVI particles; none of the other nZVI particles showed toxicity below a 100 mg/L concentration. An injection of nZVI to Cr(VI)-contaminated water rapidly decreased total Cr(VI) in the groundwater, whereas an ecotoxicological test on *Vibrio fischeri* with nZVI did not indicate any negative changes on the toxicity of the groundwater (based on the cultivable psychrophilic bacteria population and phospholipid fatty acid analysis) (Němeček et al., 2014).

It is not clear whether NPs of metal oxides or metal salts are toxic to aquatic organisms. Microarray results suggested that exposure of *Daphnia magna* to CuO and ZnO NPs and their metallic salts had no significant differences between the species' transcribed gene fragments (Adam et al., 2015). It was elucidated that the toxicity of ZnO and CuO NPs to *D. magna* was solely caused by toxic metal ions (Adam et al., 2015). Ti-based NPs also showed deleterious effects on microorganisms in soil (Li et al., 2016); hence, they should be replaced with less toxic metal oxide NPs such as Zn, Fe and Cu, where possible.

Toxicity of the NPs in water, particularly Fe NPs (e.g., nZVI), also depends on the mixing and dispersing agents present. There may be residual NPs in water even after pollutant removal is complete (Peeters et al., 2016). The dispersion of Fe NPs with tetramethylammonium hydroxide (TMAH) resulted in a slower settling of the iron aggregates. In Milli-Q and forest spring waters treated with Fe NPs and dispersed by TMAH, the nano iron remained in solution for a day after the treatment, which represented a residual effect and may pose a threat to aquatic ecosystems (Peeters et al., 2016). Likewise, during the use of nano-TiO_2 in aqueous systems, a combination of humic acid and HCO_3^- increased the release of Ti in water. Olabarrieta et al. (2018) reported that the nano-TiO_2 rejection rate was generally above 95% in a low-pressure membrane filtration pilot plant, and 2.3 g of the NPs could be released when treating 31 m^3 of tap water with 2 mg/L nano-TiO_2.

CNTs can be toxic toward bacteria at the cellular level. SWCNTs with varying functional groups altered the gene and protein expressions of *E. coli* at even a low SWCNT concentration (10 μg/mL) causing cell perturbation (Anh Le et al., 2019). In contrast, CNT toxicity to bacteria could be eliminated by entrapping CNTs using polymeric gels such as alginate and poly vinyl alcohol (Le et al., 2016).

One of the key concerns in the treatment and remediation of chemical contaminants with NMs is the introduction of little-known man-made materials to the environment/nature. This stigma needs to be overcome to gain public acceptance of nanoremediation technologies. Risk assessments of engineered NMs have been conducted for at least two decades, and the perception of risk has begun to change to some extent. For example, Ag-based NPs, which are mainly used for antimicrobial activity and were thought to be very harmful to the environment, were found to pose a small overall risk to terrestrial environments because (1) only a small fraction of Ag NPs ultimately enter into the soil, (2) the nano-properties and activities of Ag NPs are diminishable quickly when present in the soil, and (3) only minor bioaccumulation of Ag occurs in edible plant parts (Wang et al., 2018). Moreover, researchers have advocated the application of NM-based fertilizers and pesticides (e.g., Fe-, Cu-, Mg-, Mn-, Si-based NMs) directly to soil and/or on the plant bodies because these NMs pose negligible environmental risks but support crop production (Adisa et al., 2019; Kopittke et al., 2019). Nevertheless, NMs of various types may be associated with different risks, which should be researched thoroughly before their application for environmental remediation.

7. Risk management applications of nanoremediation

Risk management includes three strategies: (i) contaminant removal at the source, (ii) plume control or pathway treatment, and (iii) limiting the use of resources. Risk management can be achieved by eliminating contaminants at their source point and destroying the linkage between contaminant sources, pathways (migration of contaminants), and receptors (Nathanail & Bardos, 2004). However, complete mass removal of contaminants at the source is quite difficult due to residues and the presence of non-aqueous phase liquids (NAPL) (e.g., chlorinated solvents), contributing to low concentrations of contaminants that are still in excess of regulatory groundwater threshold values (Gavaskar et al., 2005). nZVI is capable of managing source and pathway treatments under *in-situ* conditions in the host geologic material as well as in groundwater. The application of nZVI in geologic media through direct injection can cause the *in-situ* degradation of organic contaminants, and adsorption and transformation of inorganic contaminants due to pH and redox potential changes (Pasinszki & Krebsz, 2020; Stefaniuk et al., 2016). In groundwater, nZVI application by direct injection into the *in-situ* source zone, or via groundwater funneling to an *in-situ* treatment zone (e.g., PRB), and using integrated approaches (e.g., nano-bioremediation, electro-nanoremediation) are effective risk management applications of nanoremediation (Bardos et al., 2015). Bioengineering approaches such as using biomarkers (a tool of biological monitoring) to track nZVI during contaminant treatment may effectively minimize the risk of release of contaminant-loaded NMs into the environment (Patil et al., 2016). Permeable iron barriers in shallow aquifers capable of collecting nZVI after use could also be useful for minimizing the further release of NMs into the system (Patil et al., 2016). However, risk management studies involving other NMs under field conditions are currently scarce, and warrant future research.

8. Societal and economic implications

Sustainable remediation involves the elimination or control of a contamination risk in a safe and timely manner, while optimizing the environmental, social, and economic values of the work (Nathanail et al., 2017). Sustainable remediation may comprise of one or multiple remediation technologies including *in-situ* and *ex-situ* treatments, and a combination of physical, chemical, thermal and biological processes (Nathanail et al., 2017). The International Standard for Organization (ISO) has taken the policy, legislations, and practices for risk management around the world through committee draft ISO/CD 18504, and published international standard ISO/DIS 18504. To make the concept widely popular and comprehensive to end users (practitioners, regulators, and stakeholders in land quality), clear definitions of the approaches, standard methodologies, and demonstrations of specific remediation strategies are the need of the hour. The approaches should meet the three pillars of sustainable remediation: (a) inexpensive, (b) eco-friendly, and (c) acceptable to society.

8.1 Societal implications

While *in-situ* nanoremediation has become environmentally and socially sustainable (Corsi et al., 2018), exposures of human beings to NMs through drinking of water, inhalation of polluted air, and contact with skin, potentially leading to health problems involving the lungs, liver, respiratory system, and brain. To overcome these barriers, monitoring and interventions must be performed. To promote this technology without causing harm to humans, the following steps must be considered (Corsi et al., 2018):

(1) Nanoremediation techniques (success stories) requires documentation in a simple and comprehensive manner.

(2) Development of standard protocols is needed to evaluate the ecosafety and economic sustainability of NMs.

(3) Manufacturers need to inform the consumers via proper labeling of products of the level of risks, potential ecotoxicity, health impact and risk management of nanoproducts.

(4) Science-Policy-Interfacing in needed through conversations among scientists, Government/non-Governmental officials and extension workers about the benefits and potential hazards of NMs, and the hazard mitigation strategies.

(5) High quality and thoroughly validated information (including levels of risks) are needed for a policy framework to encourage *in-situ* uses of NMs for treating contaminated soil and water.

8.2 Economic implications

The costs of remediation technologies encompass capital costs, reagent costs, maintenance, overhead costs and operational costs. The use of nZVIs for remediating organic pollutants such as TCE, chloramphenicol, lindane, and heavy metals such as Pb, Zn, As, Cr, Cd, and Pb, is less expensive than existing advanced technologies such as membrane and ozonation (Adeleye et al., 2016). Current technologies such as adsorption and precipitation for heavy metal remediation generate substantial solid waste production that can be mitigated by the effective application of nanoremediation technologies (metal oxides and nZVI). For As and NO_3^- remediation, using nZVI appears to be less expensive than carbon-based nanotechnologies (Adeleye et al., 2016). Although a laboratory scale experiment requires substantially lower amounts of nZVIs, costs for a field scale application are still high. nZVI production costs are approximately $0.05-0.10/g, whereas micro and bulk Fe^0 cost less than $0.001/g to produce (Adeleye et al., 2016). TiO_2 NPs are currently available at prices ranging from roughly $0.03/g to $1.21/g (Lu et al., 2011).

Photocatalysts can potentially be regenerated, as they are hardly degraded during oxidized radical production (Kim et al., 2012), and have potential to further decrease the overall costs associated with using photocatalytic metal oxide NPs for water treatment. Similarly, for carbon-based NMs, the cost of nanotechnology varies widely depending upon the material type, functionalization, purity level (wt. %), and grade. Currently, prices range between \$2.50 - 1000/g for graphene and derivatives, \$0.10 - 25/g for MWCNTs and \$25 - 300/g for SWCNTs. Aqueous Pb(II) removal using SWCNTs via adsorption may cost an average of \$2.2/g-Pb (Adeleye et al., 2016). However, carbon-based NMs are extremely expensive from a remediation point of view. The best way to reduce the cost is to further develop regeneration and recycling strategies for nanomaterials. Improved marketability of nanoremediation technology can potentially be achieved via: (1) encouraging NM synthesis from inexpensive renewable sources such as leaf extracts, agro-wastes, microorganisms, and natural clay minerals, and (2) identifying factors that govern the acceptability of the technology among various stakeholders, and taking regional and need-based adoption strategies.

9. Conclusions and future outlooks

The NMs discussed in this article exhibit high potential for the remediation of contaminated soil and water. Inorganic and organic modification of NPs along with supporting agents such as clay minerals, biochar, biodegradable polymers, and minimal amounts of zeolite improves the contaminant removal capacity of the NMs. The high degradation capacities and photodegradation efficiencies of NMs, and their possible uses as mediums to target multiple contaminants hold great promise. The practical field application of NMs is, however, still limited to nZVI for soil and groundwater remediation. NMs may pose positive or negative impacts on living organisms, the environment, society and economy, which should be evaluated in a case-specific context. Appropriate documentation of NM risks, field scale validation of remediation results, science-policy interface consultations, and suitable market development initiatives are ways to increase the popularity and acceptability of nanoremediation technologies.

We put forward the following research challenges for a wider acceptability of nanoremediation technologies:

(1) Future research on both the fundamental and practical aspects of nano-bioremediation is recommended. The operational conditions of nano-bioremediation such as pH, dosage, temperature, and solution composition should be optimized to work in real, field contaminated systems.

(2) Molecular mechanisms of biological degradation and removal in nano-bioremediation techniques need further investigation.

(3) Since soil is a complex and heterogeneous system, efficient soil remediation techniques must be developed. The influence of the application of NMs on soil geochemistry, microbiology, and ultimately toxicity in soil systems should be further studied.

(4) Most extant research on nanoremediation is confined to laboratory studies and modeling. Transferring these studies to *in situ* conditions is a challenge. Systematic experimentation of the impact of NMs on soil environments is needed in order to develop standard protocols and doses for the application of NMs at the field level.

(5) Supporting NMs on inert materials such as activated carbon (e.g., Carbo-iron), clay minerals, polymers, zeolite, and biochar is believed to improve contaminant remediation performance while simultaneously reducing unwanted risks of NMs to terrestrial and aquatic organisms. This requires future research attention for field validation and uptake by industry.

(6) Ecotoxicological and risk assessment studies of NMs are still limited to specific bacteria and their strains. Studies on the effect of NMs on diverse living organisms, including humans, and evaluation of toxicity transmission along the food chain are the need of the hour.

Acknowledgements

This work was carried out with support from Lancaster Environment Centre Project, and Cooperative Research Program for Agriculture Science and Technology Development (Project No. PJ01475801), Rural Development Administration, Republic of Korea, National Research Foundation of Korea (NRF) (NRF-2015R1A2A2A11001432), and NRF Germany-Korea Partnership Program (GEnKO Program) (2018–2020). This work was also supported in part by the Queensland node of the Australian National Fabrication Facility (ANFF), a company established under the National Collaborative Research Infrastructure Strategy to provide nano and microfabrication facilities for Australia's researchers.

Conflicts of interest

There is no conflict of interest to declare.

Contributions

RM, BS and YSO conceptualized the work. RM and BS prepared the first draft, and revised the manuscript. All authors provided input on sections in later drafts and edited the manuscript.

References

Adam, N., Vergauwen, L., Blust, R., Knapen, D. 2015. Gene transcription patterns and energy reserves in Daphnia magna show no nanoparticle specific toxicity when exposed to ZnO and CuO nanoparticles. *Environmental Research*, **138**, 82-92.

Adeleye, A.S., Conway, J.R., Garner, K., Huang, Y., Su, Y., Keller, A.A. 2016. Engineered nanomaterials for water treatment and remediation: Costs, benefits, and applicability. *Chemical Engineering Journal*, **286**, 640-662.

Adisa, I.O., Pullagurala, V.L.R., Peralta-Videa, J.R., Dimkpa, C.O., Elmer, W.H., Gardea-Torresdey, J.L., White, J.C. 2019. Recent advances in nano-enabled fertilizers and pesticides: a critical review of mechanisms of action. *Environmental Science: Nano*, **6**(7), 2002-2030.

Ahmad, S.Z.N., Wan Salleh, W.N., Ismail, A.F., Yusof, N., Mohd Yusop, M.Z., Aziz, F. 2020. Adsorptive removal of heavy metal ions using graphene-based nanomaterials: toxicity, roles of functional groups and mechanisms. *Chemosphere*, **248**, 126008.

Akbari Shorgoli, A., Shokri, M. 2017. Photocatalytic degradation of imidacloprid pesticide in aqueous solution by TiO_2 nanoparticles immobilized on the glass plate. *Chemical Engineering Communications*, **204**(9), 1061-1069.

Alam, M.S., Bishop, B., Chen, N., Safari, S., Warter, V., Byrne, J.M., Warchola, T., Kappler, A., Konhauser, K.O., Alessi, D.S. 2020. Reusable magnetite nanoparticles - biochar composites for the efficient removal of chromate from water. *Scientific Reports*, **10**, 19007.

Al-Mamun, M.R., Kader, S., Islam, M.S., Khan, M.Z.H. 2019. Photocatalytic activity improvement and application of UV-TiO2 photocatalysis in textile wastewater treatment: A review. *Journal of Environmental Chemical Engineering*, **7**(5), 103248.

Alarcón-Payán, D.A., Koyani, R.D., Vazquez-Duhalt, R. 2017. Chitosan-based biocatalytic nanoparticles for pollutant removal from wastewater. *Enzyme and Microbial Technology*, **100**, 71-78.

Alver, E., Bulut, M., Metin, A.Ü., Çiftçi, H. 2017. One step effective removal of Congo Red in chitosan nanoparticles by encapsulation. *Spectrochimica Acta Part A: Molecular and Biomolecular Spectroscopy*, **171**, 132-138.

Anh Le, T.T., Thuptimdang, P., McEvoy, J., Khan, E. 2019. Phage shock protein and gene responses of *Escherichia coli* exposed to carbon nanotubes. *Chemosphere*, **224**, 461-469.

Anjum, M., Miandad, R., Waqas, M., Gehany, F., Barakat, M.A. 2019. Remediation of wastewater using various nano-materials. *Arabian Journal of Chemistry*, **12**(8), 4897-4919.

Arenas-Lago, D., Rodríguez-Seijo, A., Lago-Vila, M., Couce, L.A., Vega, F.A. 2016. Using $Ca_3(PO_4)_2$ nanoparticles to reduce metal mobility in shooting range soils. *Science of The Total Environment*, **571**, 1136-1146.

Awad, A.M., Jalab, R., Benamor, A., Nasser, M.S., Ba-Abbad, M.M., El-Naas, M., Mohammad, A.W. 2020. Adsorption of organic pollutants by nanomaterial-based adsorbents: An overview. *Journal of Molecular Liquids*, **301**, 112335.

Baragaño, D., Forján, R., Welte, L., Gallego, J.L.R. 2020. Nanoremediation of As and metals polluted soils by means of graphene oxide nanoparticles. *Scientific Reports*, **10**(1), 1896.

Bardos, P., Bone, B., Daly, P., Jones, S., Elliott, D., Lowry, G., Merly, C., Bartke, S., Braun, J., Harries, N., Hartog, N., Hofmann, T., Wagner, S., Nathanail, P. 2015. A Risk/Benefit Appraisal for the Application of Nano-Scale Zero Valent Iron (nZVI) for the Remediation of Contaminated Sites. NanoRem; http://www.nanorem.eu/Displaynews.aspx?ID=525.

Bardos, P., Merly, C., Kvapil, P., Koschitzky, H.-P. 2018. Status of nanoremediation and its potential for future deployment: Risk-benefit and benchmarking appraisals. *Remediation Journal*, **28**(3), 43-56.

Bassyounia, M., Abdel-Aziz, M.H., Zorombab, M.S., Abdel-Hamide, S.M.S., Drioli, E. 2019. A review of polymeric nanocomposite membranes for water purification. *Journal of Industrial and Engineering Chemistry*, **73**, 19-46.

Besha, A.T., Liu, Y., Bekele, D.N., Dong, Z., Naidu, R., Gebremariam, G.N. 2020. Sustainability and environmental ethics for the application of engineered nanoparticles. *Environmental Science & Policy*, **103**, 85-98.

Bezbaruah, A.N., Krajangpan, S., Chisholm, B.J., Khan, E., Elorza Bermudez, J.J. 2009. Entrapment of iron nanoparticles in calcium alginate beads for groundwater remediation applications. *Journal of Hazardous Materials*, **166**(2), 1339-1343.

Bezbaruah, A.N., Shanbhogue, S.S., Simsek, S., Khan, E. 2011. Encapsulation of iron nanoparticles in alginate biopolymer for trichloroethylene remediation. *Journal of Nanoparticle Research*, **13**(12), 6673-6681.

Biswas, J.K., Sarkar, D. 2019. Nanopollution in the aquatic environment and ecotoxicity: no nano issue! *Current Pollution Reports*, **5**(1), 4-7.

Bleyl, S., Kopinke, F.-D., Mackenzie, K. 2012. Carbo-Iron®—Synthesis and stabilization of Fe(0)-doped colloidal activated carbon for in situ groundwater treatment. *Chemical Engineering Journal*, **191**, 588-595.

Bone, B., Bardos, P., Edgar, S., Kvapil, P. 2020. Chapter 14 - The sustainability of nanoremediation—two initial case studies from Europe. in: *Sustainable Remediation of Contaminated Soil and Groundwater*, (Ed.) D. Hou, Butterworth-Heinemann, pp. 367-404.

Cai, C., Zhao, M., Yu, Z., Rong, H., Zhang, C. 2019. Utilization of nanomaterials for in-situ remediation of heavy metal(loid) contaminated sediments: A review. *Science of The Total Environment*, **662**, 205-217.

Çalışkan Salihi, E., Wang, J., Kabacaoğlu, G., Kırkulak, S., Šiller, L. 2020. Graphene oxide as a new generation adsorbent for the removal of antibiotics from waters. *Separation Science and Technology*, 1-9.

Cecchin, I., Reddy, K.R., Thomé, A., Tessaro, E.F., Schnaid, F. 2017. Nanobioremediation: Integration of nanoparticles and bioremediation for sustainable remediation of chlorinated organic contaminants in soils. *International Biodeterioration & Biodegradation*, **119**, 419-428.

Černík, M., Nosek, J., Filip, J., Hrabal, J., Elliott, D.W., Zbořil, R. 2019. Electric-field enhanced reactivity and migration of iron nanoparticles with implications for groundwater treatment technologies: Proof of concept. *Water Research*, **154**, 361-369.

Černíková, M., Nosek, J., Černík, M. 2020. Combination of nZVI and DC for the in-situ remediation of chlorinated ethenes: An environmental and economic case study. *Chemosphere*, **245**, 125576.

Chaithawiwat, K., Vangnai, A., McEvoy, J.M., Pruess, B., Krajangpan, S., Khan, E. 2016a. Impact of nanoscale zero valent iron on bacteria is growth phase dependent. *Chemosphere*, **144**, 352-359.

Chaithawiwat, K., Vangnai, A., McEvoy, J.M., Pruess, B., Krajangpan, S., Khan, E. 2016b. Role of oxidative stress in inactivation of *Escherichia coli* BW25113 by nanoscale zero-valent iron. *Science of The Total Environment*, **565**, 857-862.

Chang, P.-H., Chou, T.-H., Sahu, R.S., Shih, Y.-h. 2019. Chemical reduction-aided zerovalent copper nanoparticles for 2,4-dichlorophenol removal. *Applied Nanoscience*, **9**(3), 387-395.

Chekli, L., Bayatsarmadi, B., Sekine, R., Sarkar, B., Shen, A.M., Scheckel, K.G., Skinner, W., Naidu, R., Shon, H.K., Lombi, E., Donner, E. 2016. Analytical characterisation of nanoscale zero-valent iron: A methodological review. *Analytica Chimica Acta*, **903**, 13-35.

Chen, Y., Wang, D., Zhu, X., Zheng, X., Feng, L. 2012. Long-term effects of copper nanoparticles on wastewater biological nutrient removal and N_2O generation in the activated sludge process. *Environmental Science & Technology*, **46**(22), 12452-12458.

Chong, M.N., Jin, B., Chow, C.W.K., Saint, C. 2010. Recent developments in photocatalytic water treatment technology: A review. *Water Research*, **44**(10), 2997-3027.

Corsi, I., Winther-Nielsen, M., Sethi, R., Punta, C., Della Torre, C., Libralato, G., Lofrano, G., Sabatini, L., Aiello, M., Fiordi, L., Cinuzzi, F., Caneschi, A., Pellegrini, D., Buttino, I. 2018. Ecofriendly nanotechnologies and nanomaterials for environmental applications: Key issue and consensus recommendations for sustainable and ecosafe nanoremediation. *Ecotoxicology and Environmental Safety*, **154**, 237-244.

Czinnerová, M., Vološčuková, O., Marková, K., Ševců, A., Černík, M., Nosek, J. 2020. Combining nanoscale zero-valent iron with electrokinetic treatment for remediation of chlorinated ethenes and promoting biodegradation: A long-term field study. *Water Research*, **175**, 115692.

de Souza, R.M., Seibert, D., Quesada, H.B., de Jesus Bassetti, F., Fagundes-Klen, M.R., Bergamasco, R. 2020. Occurrence, impacts and general aspects of pesticides in surface water: A review. *Process Safety and Environmental Protection*, **135**, 22-37.

Ding, L., Li, J., Liu, W., Zuo, Q., Liang, S.-X. 2017. Influence of nano-hydroxyapatite on the metal bioavailability, plant metal accumulation and root exudates of Ryegrass for phytoremediation in lead-polluted soil. *International Journal of Environmental Research and Public Health*, **14**(5), 532.

Ding, Y., Liu, B., Shen, X., Zhong, L., Li, X. 2013. Foam-assisted delivery of nanoscale zero valent iron in porous media. *Journal of Environmental Engineering*, **139**(9), 1206-1212.

Dong, H., He, Q., Zeng, G., Tang, L., Zhang, L., Xie, Y., Zeng, Y., Zhao, F. 2017. Degradation of trichloroethene by nanoscale zero-valent iron (nZVI) and nZVI activated persulfate in the absence and presence of EDTA. *Chemical Engineering Journal*, **316**, 410-418.

Dong, H., Li, L., Lu, Y., Cheng, Y., Wang, Y., Ning, Q., Wang, B., Zhang, L., Zeng, G. 2019. Integration of nanoscale zero-valent iron and functional anaerobic bacteria for groundwater remediation: A review. *Environment International*, **124**, 265-277.

Du, J., Guo, W., Wang, H., Yin, R., Zheng, H., Feng, X., Che, D., Ren, N. 2018. Hydroxyl radical dominated degradation of aquatic sulfamethoxazole by Fe^0/bisulfite/O_2: Kinetics, mechanisms, and pathways. *Water Research*, **138**, 323-332.

Ebrahim, S.E., Sulaymon, A.H., Saad Alhares, H. 2016. Competitive removal of Cu^{2+}, Cd^{2+}, Zn^{2+}, and Ni^{2+} ions onto iron oxide nanoparticles from wastewater. *Desalination and Water Treatment*, **57**(44), 20915-20929.

El-Temsah, Y.S., Joner, E.J. 2012. Ecotoxicological effects on earthworms of fresh and aged nano-sized zero-valent iron (nZVI) in soil. *Chemosphere*, **89**(1), 76-82.

El-Temsah, Y.S., Sevcu, A., Bobcikova, K., Cernik, M., Joner, E.J. 2016. DDT degradation efficiency and ecotoxicological effects of two types of nano-sized zero-valent iron (nZVI) in water and soil. *Chemosphere*, **144**, 2221-2228.

Elliott, D.W., Zhang, W.-x. 2001. Field Assessment of Nanoscale Bimetallic Particles for Groundwater Treatment. *Environmental Science & Technology*, **35**(24), 4922-4926.

ElShafei, G.M.S., Yehia, F.Z., Dimitry, O.I.H., Badawi, A.M., Eshaq, G. 2014. Ultrasonic assisted-Fenton-like degradation of nitrobenzene at neutral pH using nanosized oxides of Fe and Cu. *Ultrasonics Sonochemistry*, **21**(4), 1358-1365.

Ersan, G., Apul, O.G., Perreault, F., Karanfil, T. 2017. Adsorption of organic contaminants by graphene nanosheets: A review. *Water Research*, **126**, 385-398.

Esmaeili, A., Khoshnevisan, N. 2016. Optimization of process parameters for removal of heavy metals by biomass of Cu and Co-doped alginate-coated chitosan nanoparticles. *Bioresource Technology*, **218**, 650-658.

Fajardo, C., Gil-Díaz, M., Costa, G., Alonso, J., Guerrero, A.M., Nande, M., Lobo, M.C., Martín, M. 2015. Residual impact of aged nZVI on heavy metal-polluted soils. *Science of The Total Environment*, **535**, 79-84.

Fajardo, C., Sánchez-Fortún, S., Costa, G., Nande, M., Botías, P., García-Cantalejo, J., Mengs, G., Martín, M. 2020. Evaluation of nanoremediation strategy in a Pb, Zn and Cd contaminated soil. *Science of The Total Environment*, **706**, 136041.

Floris, B., Galloni, P., Sabuzi, F., Conte, V. 2017. Metal systems as tools for soil remediation. *Inorganica Chimica Acta*, **455**, 429-445.

Garcia, J., Gomes, H.T., Serp, P., Kalck, P., Figueiredo, J.L., Faria, J.L. 2006. Carbon nanotube supported ruthenium catalysts for the treatment of high strength wastewater with aniline using wet air oxidation. *Carbon*, **44**(12), 2384-2391.

Gavaskar, A., Tatar, L., Condit, W. 2005. Cost and performance report nanoscale zero-valent iron technologies for source remediation. Naval Facilities Engineering Service Center. N47408-01-D-8207.

Gil-Díaz, M., Alonso, J., Rodríguez-Valdés, E., Gallego, J.R., Lobo, M.C. 2017a. Comparing different commercial zero valent iron nanoparticles to immobilize As and Hg in brownfield soil. *Science of The Total Environment*, **584-585**, 1324-1332.

Gil-Díaz, M., Diez-Pascual, S., González, A., Alonso, J., Rodríguez-Valdés, E., Gallego, J.R., Lobo, M.C. 2016a. A nanoremediation strategy for the recovery of an As-polluted soil. *Chemosphere*, **149**, 137-145.

Gil-Díaz, M., González, A., Alonso, J., Lobo, M.C. 2016b. Evaluation of the stability of a nanoremediation strategy using barley plants. *Journal of Environmental Management*, **165**, 150-158.

Gil-Díaz, M., Pinilla, P., Alonso, J., Lobo, M.C. 2017b. Viability of a nanoremediation process in single or multi-metal(loid) contaminated soils. *Journal of Hazardous Materials*, **321**, 812-819.

Gollavelli, G., Chang, C.-C., Ling, Y.-C. 2013. Facile synthesis of smart magnetic graphene for safe drinking water: heavy metal removal and disinfection control. *ACS Sustainable Chemistry & Engineering*, **1**(5), 462-472.

Gomes, H.I., Fan, G., Mateus, E.P., Dias-Ferreira, C., Ribeiro, A.B. 2014. Assessment of combined electro–nanoremediation of molinate contaminated soil. *Science of The Total Environment*, **493**, 178-184.

Guerra, F.D., Attia, M.F., Whitehead, D.C., Alexis, F. 2018. Nanotechnology for environmental remediation: materials and applications. *Molecules*, **23**(7), 1760.

Guo, X., Yang, Z., Dong, H., Guan, X., Ren, Q., Lv, X., Jin, X. 2016. Simple combination of oxidants with zero-valent-iron (ZVI) achieved very rapid and highly efficient removal of heavy metals from water. *Water Research*, **88**, 671-680.

Gupta, V.K., Moradi, O., Tyagi, I., Agarwal, S., Sadegh, H., Shahryari-Ghoshekandi, R., Makhlouf, A.S.H., Goodarzi, M., Garshasbi, A. 2016. Study on the removal of heavy metal ions from industry waste by carbon nanotubes: Effect of the surface modification: a review. *Critical Reviews in Environmental Science and Technology*, **46**(2), 93-118.

Gusain, R., Kumar, N., Ray, S.S. 2020. Recent advances in carbon nanomaterial-based adsorbents for water purification. *Coordination Chemistry Reviews*, **405**, 213111.

Han, Y., Shi, N., Wang, H., Pan, X., Fang, H., Yu, Y. 2016. Nanoscale zerovalent iron-mediated degradation of DDT in soil. *Environmental Science and Pollution Research*, **23**(7), 6253-6263.

Hassan, K.H., Jarullah, A.A., Saadi, S.K. 2017. Synthesis of copper oxide nanoparticle as an adsorbent for removal of Cd(II) and Ni(II) ions from binary system. *International Journal of Applied Environmental Sciences*, **12**, 1841-1861.

Hirthna, Sendhilnathan, S., Rajan, P.I., Adinaveen, T. 2018. Synthesis and characterization of $NiFe_2O_4$ nanoparticles for the enhancement of direct sunlight photocatalytic degradation of methyl orange. *Journal of Superconductivity and Novel Magnetism*, **31**(10), 3315-3322.

Hjorth, R., Coutris, C., Nguyen, N.H.A., Sevcu, A., Gallego-Urrea, J.A., Baun, A., Joner, E.J. 2017. Ecotoxicity testing and environmental risk assessment of iron nanomaterials for sub-surface remediation – Recommendations from the FP7 project NanoRem. *Chemosphere*, **182**, 525-531.

Hosseini, S.M., Tosco, T., Ataie-Ashtiani, B., Simmons, C.T. 2018. Non-pumping reactive wells filled with mixing nano and micro zero-valent iron for nitrate removal from groundwater: Vertical, horizontal, and slanted wells. *Journal of Contaminant Hydrology*, **210**, 50-64.

Hou, D., O'Connor, D., Igalavithana, A.D., Alessi, D.S., Luo, J., Tsang, D.C.W., Sparks, D.L., Yamauchi, Y., Rinklebe, J., Ok, Y.S. 2020. Metal contamination and bioremediation of agricultural soils for food safety and sustainability. *Nature Reviews Earth & Environment*, **1**, 366–381.

Huang, D., Wang, X., Zhang, C., Zeng, G., Peng, Z., Zhou, J., Cheng, M., Wang, R., Hu, Z., Qin, X. 2017. Sorptive removal of ionizable antibiotic sulfamethazine from aqueous solution by graphene oxide-coated biochar nanocomposites: Influencing factors and mechanism. *Chemosphere*, **186**, 414-421.

Inyang, M., Gao, B., Zimmerman, A., Zhou, Y., Cao, X. 2015. Sorption and cosorption of lead and sulfapyridine on carbon nanotube-modified biochars. *Environmental Science and Pollution Research*, **22**(3), 1868-1876.

Isherwood, P.J.M. 2017. Copper zinc oxide: Investigation into a p-type mixed metal oxide system. *Vacuum*, **139**, 173-177.

Jame, S.A., Zhou, Z. 2016. Electrochemical carbon nanotube filters for water and wastewater treatment. *Nanotechnology Reviews*, **5**(1), 41-50.

Jiang, D., Zeng, G., Huang, D., Chen, M., Zhang, C., Huang, C., Wan, J. 2018. Remediation of contaminated soils by enhanced nanoscale zero valent iron. *Environmental Research*, **163**, 217-227.

Kamath, V., Chandra, P., Jeppu, G.P. 2020. Comparative study of using five different leaf extracts in the green synthesis of iron oxide nanoparticles for removal of arsenic from water. *International Journal of Phytoremediation*, **22**(12), 1278-1294.

Kang, Y.-G., Yoon, H., Lee, W., Kim, E.-j., Chang, Y.-S. 2018. Comparative study of peroxide oxidants activated by nZVI: Removal of 1,4-Dioxane and arsenic(III) in contaminated waters. *Chemical Engineering Journal*, **334**, 2511-2519.

Karn, B., Kuiken, T., Otto, M. 2009. Nanotechnology and *in situ* remediation: a review of the benefits and potential risks. *Environmental Health Perspectives*, **117**(12), 1813-1831.

Kaur, Y., Bhatia, Y., Chaudhary, S., Chaudhary, G.R. 2017. Comparative performance of bare and functionalize ZnO nanoadsorbents for pesticide removal from aqueous solution. *Journal of Molecular Liquids*, **234**, 94-103.

Khairy, M., Zakaria, W. 2014. Effect of metal-doping of TiO_2 nanoparticles on their photocatalytic activities toward removal of organic dyes. *Egyptian Journal of Petroleum*, **23**(4), 419-426.

Khalaj, M., Kamali, M., Khodaparast, Z., Jahanshahi, A. 2018. Copper-based nanomaterials for environmental decontamination – An overview on technical and toxicological aspects. *Ecotoxicology and Environmental Safety*, **148**, 813-824.

Khan, I., Saeed, K., Khan, I. 2019. Nanoparticles: Properties, applications and toxicities. *Arabian Journal of Chemistry*, **12**(7), 908-931.

Kim, Y.-M., Murugesan, K., Chang, Y.-Y., Kim, E.-J., Chang, Y.-S. 2012. Degradation of polybrominated diphenyl ethers by a sequential treatment with nanoscale zero valent iron and aerobic biodegradation. *Journal of Chemical Technology & Biotechnology*, **87**(2), 216-224.

Kirankumar, V.S., Sumathi, S. 2017. Catalytic activity of bismuth doped zinc aluminate nanoparticles towards environmental remediation. *Materials Research Bulletin*, **93**, 74-82.

Kopittke, P.M., Lombi, E., Wang, P., Schjoerring, J.K., Husted, S. 2019. Nanomaterials as fertilizers for improving plant mineral nutrition and environmental outcomes. *Environmental Science: Nano*, **6**(12), 3513-3524.

Kőrösi, L., Prato, M., Scarpellini, A., Kovács, J., Dömötör, D., Kovács, T., Papp, S. 2016. H_2O_2-assisted photocatalysis on flower-like rutile TiO2 nanostructures: Rapid dye degradation and inactivation of bacteria. *Applied Surface Science*, **365**, 171-179.

Kotchaplai, P., Khan, E., Vangnai, A.S. 2017. Membrane alterations in *Pseudomonas putida* F1 exposed to nanoscale zerovalent iron: effects of short-term and repetitive nZVI exposure. *Environmental Science & Technology*, **51**(14), 7804-7813.

Krasucka, P., Pan, B., Sik Ok, Y., Mohan, D., Sarkar, B., Oleszczuk, P. 2021. Engineered biochar – A sustainable solution for the removal of antibiotics from water. *Chemical Engineering Journal*, **405**, 126926.

Krishnaswamy, K., Orsat, V. 2017. Chapter 2 - Sustainable Delivery Systems Through Green Nanotechnology. in: *Nano- and Microscale Drug Delivery Systems*, (Ed.) A.M. Grumezescu, Elsevier, pp. 17-32.

Kumar, A., Sharma, G., Naushad, M., Al-Muhtaseb, A.a.H., García-Peñas, A., Mola, G.T., Si, C., Stadler, F.J. 2020a. Bio-inspired and biomaterials-based hybrid photocatalysts for environmental detoxification: A review. *Chemical Engineering Journal*, **382**, 122937.

Kumar, N., Chaurand, P., Rose, J., Diels, L., Bastiaens, L. 2015. Synergistic effects of sulfate reducing bacteria and zero valent iron on zinc removal and stability in aquifer sediment. *Chemical Engineering Journal*, **260**, 83-89.

Kumar, V., Lee, Y.-S., Shin, J.-W., Kim, K.-H., Kukkar, D., Fai Tsang, Y. 2020b. Potential applications of graphene-based nanomaterials as adsorbent for removal of volatile organic compounds. *Environment International*, **135**, 105356.

Lazaratou, C.V., Vayenas, D.V., Papoulis, D. 2020. The role of clays, clay minerals and clay-based materials for nitrate removal from water systems: A review. *Applied Clay Science*, **185**, 105377.

Le, T.T., Nguyen, K.-H., Jeon, J.-R., Francis, A.J., Chang, Y.-S. 2015. Nano/bio treatment of polychlorinated biphenyls with evaluation of comparative toxicity. *Journal of Hazardous Materials*, **287**, 335-341.

Le, T.T.A., McEvoy, J., Khan, E. 2016. Mitigation of bactericidal effect of carbon nanotubes by cell entrapment. *Science of The Total Environment*, **565**, 787-794.

Lee, K.M., Wong, C.P.P., Tan, T.L., Lai, C.W. 2018. Functionalized carbon nanotubes for adsorptive removal of water pollutants. *Materials Science and Engineering: B*, **236-237**, 61-69.

Lefevre, E., Bossa, N., Wiesner, M.R., Gunsch, C.K. 2016. A review of the environmental implications of in situ remediation by nanoscale zero valent iron (nZVI): Behavior, transport and impacts on microbial communities. *Science of The Total Environment*, **565**, 889-901.

Lei, C., Sun, Y., Khan, E., Chen, S.S., Tsang, D.C.W., Graham, N.J.D., Ok, Y.S., Yang, X., Lin, D., Feng, Y., Li, X.-D. 2018. Removal of chlorinated organic solvents from hydraulic fracturing wastewater by bare and entrapped nanoscale zero-valent iron. *Chemosphere*, **196**, 9-17.

Lellis, B., Fávaro-Polonio, C.Z., Pamphile, J.A., Polonio, J.C. 2019. Effects of textile dyes on health and the environment and bioremediation potential of living organisms. *Biotechnology Research and Innovation*, **3**(2), 275-290.

Lewis, R.W., Bertsch, P.M., McNear, D.H. 2019. Nanotoxicity of engineered nanomaterials (ENMs) to environmentally relevant beneficial soil bacteria – a critical review. *Nanotoxicology*, **13**(3), 392-428.

Li, D., Li, B., Wang, Q., Hou, N., Li, C., Cheng, X. 2016. Toxicity of TiO_2 nanoparticle to denitrifying strain CFY1 and the impact on microbial community structures in activated sludge. *Chemosphere*, **144**, 1334-1341.

Li, F., Chen, J., Hu, X., He, F., Bean, E., Tsang, D.C.W., Ok, Y.S., Gao, B. 2020. Applications of carbonaceous adsorbents in the remediation of polycyclic aromatic hydrocarbon-contaminated sediments: A review. *Journal of Cleaner Production*, **255**, 120263.

Li, H., Qiu, Y.-f., Wang, X.-l., Yang, J., Yu, Y.-j., Chen, Y.-q., Liu, Y.-d. 2017. Biochar supported Ni/Fe bimetallic nanoparticles to remove 1,1,1-trichloroethane under various reaction conditions. *Chemosphere*, **169**, 534-541.

Li, R., Gao, Y., Jin, X., Chen, Z., Megharaj, M., Naidu, R. 2015. Fenton-like oxidation of 2,4-DCP in aqueous solution using iron-based nanoparticles as the heterogeneous catalyst. *Journal of Colloid and Interface Science*, **438**, 87-93.

Li, Y., Zhang, Y., Li, J., Sheng, G., Zheng, X. 2013. Enhanced reduction of chlorophenols by nanoscale zerovalent iron supported on organobentonite. *Chemosphere*, **92**(4), 368-374.

Li, Z., Wang, L., Meng, J., Liu, X., Xu, J., Wang, F., Brookes, P. 2018. Zeolite-supported nanoscale zero-valent iron: New findings on simultaneous adsorption of Cd(II), Pb(II), and As(III) in aqueous solution and soil. *Journal of Hazardous Materials*, **344**, 1-11.

Lin, K.-S., Mdlovu, N.V., Chen, C.-Y., Chiang, C.-L., Dehvari, K. 2018. Degradation of TCE, PCE, and 1,2–DCE DNAPLs in contaminated groundwater using polyethylenimine-modified zero-valent iron nanoparticles. *Journal of Cleaner Production*, **175**, 456-466.

Lin, Z., Weng, X., Ma, L., Sarkar, B., Chen, Z. 2019. Mechanistic insights into Pb(II) removal from aqueous solution by green reduced graphene oxide. *Journal of Colloid and Interface Science*, **550**, 1-9.

Liu, J., Jiang, J., Meng, Y., Aihemaiti, A., Xu, Y., Xiang, H., Gao, Y., Chen, X. 2020. Preparation, environmental application and prospect of biochar-supported metal nanoparticles: A review. *Journal of Hazardous Materials*, **388**, 122026.

Liu, J., Ma, Y., Xu, T., Shao, G. 2010. Preparation of zwitterionic hybrid polymer and its application for the removal of heavy metal ions from water. *Journal of Hazardous Materials*, **178**(1), 1021-1029.

Liu, Y., Xie, J., Ong, C.N., Vecitis, C.D., Zhou, Z. 2015. Electrochemical wastewater treatment with carbon nanotube filters coupled with in situ generated H_2O_2. *Environmental Science: Water Research & Technology*, **1**(6), 769-778.

Lu, S.-y., Wu, D., Wang, Q.-l., Yan, J., Buekens, A.G., Cen, K.-f. 2011. Photocatalytic decomposition on nano-TiO2: Destruction of chloroaromatic compounds. *Chemosphere*, **82**(9), 1215-1224.

Ma, J., Ping, D., Dong, X. 2017. Recent Developments of Graphene Oxide-Based Membranes: A Review. *Membranes*, **7**(3), 52.

Mackenzie, K., Bleyl, S., Georgi, A., Kopinke, F.-D. 2012. Carbo-Iron – An Fe/AC composite – As alternative to nano-iron for groundwater treatment. *Water Research*, **46**(12), 3817-3826.

Mackenzie, K., Bleyl, S., Kopinke, F.-D., Doose, H., Bruns, J. 2016. Carbo-Iron as improvement of the nanoiron technology: From laboratory design to the field test. *Science of The Total Environment*, **563-564**, 641-648.

Majumder, A., Ramrakhiani, L., Mukherjee, D., Mishra, U., Halder, A., Mandal, A.K., Ghosh, S. 2019. Green synthesis of iron oxide nanoparticles for arsenic remediation in water and sludge utilization. *Clean Technologies and Environmental Policy*, **21**(4), 795-813.

Mandal, S., Sarkar, B., Mukhopadhyay, R., Biswas, J.K., Manjaiah, K.M. 2018. Microparticle-Supported Nanocomposites for Safe Environmental Applications. in: *Nanomaterials: Ecotoxicity, Safety, and Public Perception*, (Eds.) M. Rai, J.K. Biswas, Springer International Publishing. Cham, pp. 305-317.

Matos, M.P.S.R., Correia, A.A.S., Rasteiro, M.G. 2017. Application of carbon nanotubes to immobilize heavy metals in contaminated soils. *Journal of Nanoparticle Research*, **19**(4), 126.

Meeks, N.D., Smuleac, V., Stevens, C., Bhattacharyya, D. 2012. Iron-based nanoparticles for toxic organic degradation: silica platform and green synthesis. *Industrial & Engineering Chemistry Research*, **51**(28), 9581-9590.

Mehta, D., Mazumdar, S., Singh, S.K. 2015. Magnetic adsorbents for the treatment of water/wastewater—A review. *Journal of Water Process Engineering*, **7**, 244-265.

Meyer, J.C., Geim, A.K., Katsnelson, M.I., Novoselov, K.S., Booth, T.J., Roth, S. 2007. The structure of suspended graphene sheets. *Nature*, **446**(7131), 60-63.

Meyer, M.F., Powers, S.M., Hampton, S.E. 2019. An evidence synthesis of pharmaceuticals and personal care products (PPCPs) in the environment: imbalances among compounds, sewage treatment techniques, and ecosystem types. *Environmental Science & Technology*, **53**(22), 12961-12973.

Mines, P.D., Uthuppu, B., Thirion, D., Jakobsen, M.H., Yavuz, C.T., Andersen, H.R., Hwang, Y. 2018. Granular activated carbon with grafted nanoporous polymer enhances nanoscale zero-valent iron impregnation and water contaminant removal. *Chemical Engineering Journal*, **339**, 22-31.

Moschini, E., Gualtieri, M., Colombo, M., Fascio, U., Camatini, M., Mantecca, P. 2013. The modality of cell–particle interactions drives the toxicity of nanosized CuO and TiO_2 in human alveolar epithelial cells. *Toxicology Letters*, **222**(2), 102-116.

Mukhopadhyay, R., Bhaduri, D., Sarkar, B., Rusmin, R., Hou, D., Khanam, R., Sarkar, S., Kumar Biswas, J., Vithanage, M., Bhatnagar, A., Ok, Y.S. 2020. Clay–polymer nanocomposites: Progress and challenges for use in sustainable water treatment. *Journal of Hazardous Materials*, **383**, 121125.

Murugadas, A., Zeeshan, M., Thamaraiselvi, K., Ghaskadbi, S., Akbarsha, M.A. 2016. Hydra as a model organism to decipher the toxic effects of copper oxide nanorod: Eco-toxicogenomics approach. *Scientific Reports*, **6**(1), 29663.

Nathanail, C.P., Bakker, L.M.M., Bardos, P., Furukawa, Y., Nardella, A., Smith, G., Smith, J.W.N., Goetsche, G. 2017. Towards an international standard: The ISO/DIS 18504 standard on sustainable remediation. *Remediation Journal*, **28**(1), 9-15.

Nathanail, C.P., Bardos, R.P. 2004. Risk Management. in: *Reclamation of Contaminated Land*, (Eds.) C.P. Nathanail, R.P. Bardos, John Wiley & Sons Ltd. Chichester, UK, pp. 109-124.

Němeček, J., Lhotský, O., Cajthaml, T. 2014. Nanoscale zero-valent iron application for in situ reduction of hexavalent chromium and its effects on indigenous microorganism populations. *Science of The Total Environment*, **485-486**, 739-747.

Olabarrieta, J., Monzón, O., Belaustegui, Y., Alvarez, J.-I., Zorita, S. 2018. Removal of TiO_2 nanoparticles from water by low pressure pilot plant filtration. *Science of The Total Environment*, **618**, 551-560.

Pan, Y., Zhou, M., Li, X., Xu, L., Tang, Z., Sheng, X., Li, B. 2017. Highly efficient persulfate oxidation process activated with pre-magnetization Fe0. *Chemical Engineering Journal*, **318**, 50-56.

Parham, H., Zargar, B., Shiralipour, R. 2012. Fast and efficient removal of mercury from water samples using magnetic iron oxide nanoparticles modified with 2-mercaptobenzothiazole. *Journal of Hazardous Materials*, **205-206**, 94-100.

Pasinszki, T., Krebsz, M. 2020. Synthesis and application of zero-valent iron nanoparticles in water treatment, environmental remediation, catalysis, and their biological effects. *Nanomaterials*, **10**(5), 917.

Patil, S.S., Shedbalkar, U.U., Truskewycz, A., Chopade, B.A., Ball, A.S. 2016. Nanoparticles for environmental clean-up: A review of potential risks and emerging solutions. *Environmental Technology & Innovation*, **5**, 10-21.

Peeters, K., Lespes, G., Zuliani, T., Ščančar, J., Milačič, R. 2016. The fate of iron nanoparticles in environmental waters treated with nanoscale zero-valent iron, FeONPs and Fe_3O_4 NPs. *Water Research*, **94**, 315-327.

Pei, Z., Li, L., Sun, L., Zhang, S., Shan, X.-q., Yang, S., Wen, B. 2013. Adsorption characteristics of 1,2,4-trichlorobenzene, 2,4,6-trichlorophenol, 2-naphthol and naphthalene on graphene and graphene oxide. *Carbon*, **51**, 156-163.

Perreault, F., Fonseca de Faria, A., Elimelech, M. 2015. Environmental applications of graphene-based nanomaterials. *Chemical Society Reviews*, **44**(16), 5861-5896.

Perreault, F., Popovic, R., Dewez, D. 2014. Different toxicity mechanisms between bare and polymer-coated copper oxide nanoparticles in Lemna gibba. *Environmental Pollution*, **185**, 219-227.

Premarathna, K.S.D., Rajapaksha, A.U., Sarkar, B., Kwon, E.E., Bhatnagar, A., Ok, Y.S., Vithanage, M. 2019. Biochar-based engineered composites for sorptive decontamination of water: A review. *Chemical Engineering Journal*, **372**, 536-550.

Qi, J., Zhao, K., Li, G., Gao, Y., Zhao, H., Yu, R., Tang, Z. 2014. Multi-shelled CeO_2 hollow microspheres as superior photocatalysts for water oxidation. *Nanoscale*, **6**(8), 4072-4077.

Qiao, Y., Wu, J., Xu, Y., Fang, Z., Zheng, L., Cheng, W., Tsang, E.P., Fang, J., Zhao, D. 2017. Remediation of cadmium in soil by biochar-supported iron phosphate nanoparticles. *Ecological Engineering*, **106**, 515-522.

Quan, G., Kong, L., Lan, Y., Yan, J., Gao, B. 2018. Removal of acid orange 7 by surfactant-modified iron nanoparticle supported on palygorskite: Reactivity and mechanism. *Applied Clay Science*, **152**, 173-182.

Quinn, J., Geiger, C., Clausen, C., Brooks, K., Coon, C., O'Hara, S., Krug, T., Major, D., Yoon, W.-S., Gavaskar, A., Holdsworth, T. 2005. Field demonstration of DNAPL dehalogenation using emulsified zero-valent iron. *Environmental Science & Technology*, **39**(5), 1309-1318.

Rai, M., Biswas, J.K. 2018. *Nanomaterials: Ecotoxicity, Safety and Public Perception*. Springer Nature, Switzerland.

Rai, P.K., Kumar, V., Lee, S., Raza, N., Kim, K.-H., Ok, Y.S., Tsang, D.C.W. 2018. Nanoparticle-plant interaction: Implications in energy, environment, and agriculture. *Environment International*, **119**, 1-19.

Raizada, P., Sudhaik, A., Singh, P. 2019. Photocatalytic water decontamination using graphene and ZnO coupled photocatalysts: A review. *Materials Science for Energy Technologies*, **2**(3), 509-525.

Ramesha, G.K., Vijaya Kumara, A., Muralidhara, H.B., Sampath, S. 2011. Graphene and graphene oxide as effective adsorbents toward anionic and cationic dyes. *Journal of Colloid and Interface Science*, **361**(1), 270-277.

Rengaraj, S., Venkataraj, S., Yeon, J.-W., Kim, Y., Li, X.Z., Pang, G.K.H. 2007. Preparation, characterization and application of Nd–TiO2 photocatalyst for the reduction of Cr(VI) under UV light illumination. *Applied Catalysis B: Environmental*, **77**(1), 157-165.

Rizwan, M., Ali, S., Qayyum, M.F., Ok, Y.S., Adrees, M., Ibrahim, M., Zia-ur-Rehman, M., Farid, M., Abbas, F. 2017. Effect of metal and metal oxide nanoparticles on growth and physiology of globally important food crops: A critical review. *Journal of Hazardous Materials*, **322**, 2-16.

Rusmin, R., Sarkar, B., Tsuzuki, T., Kawashima, N., Naidu, R. 2017. Removal of lead from aqueous solution using superparamagnetic palygorskite nanocomposite: Material characterization and regeneration studies. *Chemosphere*, **186**, 1006-1015.

Sadegh, H., Ali, G.A.M., Gupta, V.K., Makhlouf, A.S.H., Shahryari-ghoshekandi, R., Nadagouda, M.N., Sillanpää, M., Megiel, E. 2017. The role of nanomaterials as effective adsorbents and their applications in wastewater treatment. *Journal of Nanostructure in Chemistry*, **7**(1), 1-14.

Sadegh, H., Zare, K., Maazinejad, B., Shahryari-ghoshekandi, R., Tyagi, I., Agarwal, S., Gupta, V.K. 2016. Synthesis of MWCNT-COOH-Cysteamine composite and its application for dye removal. *Journal of Molecular Liquids*, **215**, 221-228.

Safavi, A., Maleki, N., Doroodmand, M.M. 2010. Fabrication of a selective mercury sensor based on the adsorption of cold vapor of mercury on carbon nanotubes: Determination of mercury in industrial wastewater. *Journal of Hazardous Materials*, **173**(1), 622-629.

Saharan, P., Chaudhary, G.R., Mehta, S.K., Umar, A. 2014. Removal of water contaminants by iron oxide nanomaterials. *Journal of Nanoscience and Nanotechnology*, **14**(1), 627-643.

Saheed, I.O., Da, O.W., Suah, F.B.M. 2021. Chitosan modifications for adsorption of pollutants - a review. *Journal of Hazardous Materials*, **408**, 124889.

Salam, J.A., Das, N. 2015. Degradation of lindane by a novel embedded bio-nano hybrid system in aqueous environment. *Applied Microbiology and Biotechnology*, **99**(5), 2351-2360.

Sarkar, B., Liu, E., McClure, S., Sundaramurthy, J., Srinivasan, M., Naidu, R. 2015. Biomass derived palygorskite–carbon nanocomposites: Synthesis, characterisation and affinity to dye compounds. *Applied Clay Science*, **114**, 617-626.

Sarkar, B., Mandal, S., Tsang, Y.F., Kumar, P., Kim, K.-H., Ok, Y.S. 2018. Designer carbon nanotubes for contaminant removal in water and wastewater: A critical review. *Science of The Total Environment*, **612**, 561-581.

Scaria, J., Nidheesh, P.V., Kumar, M.S. 2020. Synthesis and applications of various bimetallic nanomaterials in water and wastewater treatment. *Journal of Environmental Management*, **259**, 110011.

Schaefer, D.W., Justice, R.S. 2007. How nano are nanocomposites? *Macromolecules*, **40**(24), 8501-8517.

Schaefer, H.R., Dennis, S., Fitzpatrick, S. 2020. Cadmium: Mitigation strategies to reduce dietary exposure. *Journal of Food Science*, **85**(2), 260-267.

Sepúlveda, P., Rubio, M.A., Baltazar, S.E., Rojas-Nunez, J., Sánchez Llamazares, J.L., Garcia, A.G., Arancibia-Miranda, N. 2018. As(V) removal capacity of FeCu bimetallic nanoparticles in aqueous solutions: The influence of Cu content and morphologic changes in bimetallic nanoparticles. *Journal of Colloid and Interface Science*, **524**, 177-187.

Shanbhogue, S.S., Bezbaruah, A., Simsek, S., Khan, E. 2017. Trichloroethene removal by separately encapsulated and co-encapsulated bacterial degraders and nanoscale zero-valent iron. *International Biodeterioration & Biodegradation*, **125**, 269-276.

Sheu, Y.T., Lien, P.J., Chen, K.F., Ou, J.H., Kao, C.M. 2016. Application of NZVI-contained emulsified substrate to bioremediate PCE-contaminated groundwater – A pilot-scale study. *Chemical Engineering Journal*, **304**, 714-727.

Sievers, C., Noda, Y., Qi, L., Albuquerque, E.M., Rioux, R.M., Scott, S.L. 2016. Phenomena affecting catalytic reactions at solid–liquid interfaces. *ACS Catalysis*, **6**(12), 8286-8307.

Singh, R., Manickam, N., Mudiam, M.K.R., Murthy, R.C., Misra, V. 2013. An integrated (nano-bio) technique for degradation of γ-HCH contaminated soil. *Journal of Hazardous Materials*, **258-259**, 35-41.

Singh, R., Misra, V., Mudiam, M.K.R., Chauhan, L.K.S., Singh, R.P. 2012a. Degradation of γ-HCH spiked soil using stabilized Pd/Fe^0 bimetallic nanoparticles: Pathways, kinetics and effect of reaction conditions. *Journal of Hazardous Materials*, **237-238**, 355-364.

Singh, R., Misra, V., Singh, R.P. 2012b. Removal of Cr(VI) by nanoscale zero-valent iron (nZVI) from soil contaminated with tannery wastes. *Bulletin of Environmental Contamination and Toxicology*, **88**(2), 210-214.

Soliemanzadeh, A., Fekri, M. 2017. The application of green tea extract to prepare bentonite-supported nanoscale zero-valent iron and its performance on removal of Cr(VI): Effect of relative parameters and soil experiments. *Microporous and Mesoporous Materials*, **239**, 60-69.

Stefaniuk, M., Oleszczuk, P., Ok, Y.S. 2016. Review on nano zerovalent iron (nZVI): From synthesis to environmental applications. *Chemical Engineering Journal*, **287**, 618-632.

Su, Y.-f., Hsu, C.-Y., Shih, Y.-h. 2012. Effects of various ions on the dechlorination kinetics of hexachlorobenzene by nanoscale zero-valent iron. *Chemosphere*, **88**(11), 1346-1352.

Suazo-Hernández, J., Sepúlveda, P., Manquián-Cerda, K., Ramírez-Tagle, R., Rubio, M.A., Bolan, N., Sarkar, B., Arancibia-Miranda, N. 2019. Synthesis and characterization of zeolite-based composites functionalized with nanoscale zero-valent iron for removing arsenic in the presence of selenium from water. *Journal of Hazardous Materials*, **373**, 810-819.

Sun, Y., Lei, C., Khan, E., Chen, S.S., Tsang, D.C.W., Ok, Y.S., Lin, D., Feng, Y., Li, X.-d. 2018. Aging effects on chemical transformation and metal(loid) removal by entrapped nanoscale zero-valent iron for hydraulic fracturing wastewater treatment. *Science of The Total Environment*, **615**, 498-507.

Tafazoli, M., Hojjati, S.M., Biparva, P., Kooch, Y., Lamersdorf, N. 2017. Reduction of soil heavy metal bioavailability by nanoparticles and cellulosic wastes improved the biomass of tree seedlings. *Journal of Plant Nutrition and Soil Science*, **180**(6), 683–693.

Tanzifi, M., Hosseini, S.H., Kiadehi, A.D., Olazar, M., Karimipour, K., Rezaiemehr, R., Ali, I. 2017. Artificial neural network optimization for methyl orange adsorption onto polyaniline nano-adsorbent: Kinetic, isotherm and thermodynamic studies. *Journal of Molecular Liquids*, **244**, 189-200.

Tasharrofi, S., Rouzitalab, Z., Maklavany, D.M., Esmaeili, A., Rabieezadeh, M., Askarieh, M., Rashidi, A., Taghdisian, H. 2020. Adsorption of cadmium using modified zeolite-supported nanoscale zero-valent iron composites as a reactive material for PRBs. *Science of The Total Environment*, **736**, 139570.

Tiberg, C., Kumpiene, J., Gustafsson, J.P., Marsz, A., Persson, I., Mench, M., Kleja, D.B. 2016. Immobilization of Cu and As in two contaminated soils with zero-valent iron – Long-term performance and mechanisms. *Applied Geochemistry*, **67**, 144-152.

Uddin, M.K. 2017. A review on the adsorption of heavy metals by clay minerals, with special focus on the past decade. *Chemical Engineering Journal*, **308**, 438-462.

UN. 2016. The Sustainable Development Goals Report 2016. United Nations.

Varadhi, S.N., Gill, H., Apoldo, L.J., Liao, K., Blackman, R.A., Wittman, W.K. 2005. Full-scale nanoiron injection for treatment of groundwater contaminated with chlorinated hydrocarbons. in: *Natural Gas Technologies Conference*. Orlando, FL.

Vidovix, T.B., Quesada, H.B., Januário, E.F.D., Bergamasco, R., Vieira, A.M.S. 2019. Green synthesis of copper oxide nanoparticles using Punica granatum leaf extract applied to the removal of methylene blue. *Materials Letters*, **257**, 126685.

Vítková, M., Rákosová, S., Michálková, Z., Komárek, M. 2017. Metal(loid)s behaviour in soils amended with nano zero-valent iron as a function of pH and time. *Journal of Environmental Management*, **186**, 268-276.

Vogel, M., Nijenhuis, I., Lloyd, J., Boothman, C., Pöritz, M., Mackenzie, K. 2018. Combined chemical and microbiological degradation of tetrachloroethene during the application of Carbo-Iron at a contaminated field site. *Science of The Total Environment*, **628-629**, 1027-1036.

Vojoudi, H., Badiei, A., Bahar, S., Mohammadi Ziarani, G., Faridbod, F., Ganjali, M.R. 2017. A new nano-sorbent for fast and efficient removal of heavy metals from aqueous solutions based on modification of magnetic mesoporous silica nanospheres. *Journal of Magnetism and Magnetic Materials*, **441**, 193-203.

Wang, H., Kim, B., Wunder, S.L. 2015a. Nanoparticle-supported lipid bilayers as an in situ remediation strategy for hydrophobic organic contaminants in soils. *Environmental Science & Technology*, **49**(1), 529-536.

Wang, J., Chen, B. 2015. Adsorption and coadsorption of organic pollutants and a heavy metal by graphene oxide and reduced graphene materials. *Chemical Engineering Journal*, **281**, 379-388.

Wang, M., Hossain, F., Sulaiman, R., Ren, X. 2019. Exposure to inorganic arsenic and lead and autism spectrum disorder in children: a systematic review and meta-analysis. *Chemical Research in Toxicology*, **32**(10), 1904-1919.

Wang, P., Lombi, E., Menzies, N.W., Zhao, F.-J., Kopittke, P.M. 2018. Engineered silver nanoparticles in terrestrial environments: a meta-analysis shows that the overall environmental risk is small. *Environmental Science: Nano*, **5**(11), 2531-2544.

Wang, X., Wang, P., Ma, J., Liu, H., Ning, P. 2015b. Synthesis, characterization, and reactivity of cellulose modified nano zero-valent iron for dye discoloration. *Applied Surface Science*, **345**, 57-66.

Wang, X., Zhang, D., Pan, X., Lee, D.-J., Al-Misned, F.A., Mortuza, M.G., Gadd, G.M. 2017. Aerobic and anaerobic biosynthesis of nano-selenium for remediation of mercury contaminated soil. *Chemosphere*, **170**, 266-273.

Wang, Z., Xu, L., Zhao, J., Wang, X., White, J.C., Xing, B. 2016. CuO Nanoparticle interaction with *Arabidopsis thaliana*: toxicity, parent-progeny transfer, and gene expression. *Environmental Science & Technology*, **50**(11), 6008-6016.

Weil, M., Mackenzie, K., Foit, K., Kühnel, D., Busch, W., Bundschuh, M., Schulz, R., Duis, K. 2019. Environmental risk or benefit? Comprehensive risk assessment of groundwater treated with nano Fe0-based Carbo-Iron®. *Science of The Total Environment*, **677**, 156-166.

Weil, M., Meißner, T., Springer, A., Bundschuh, M., Hübler, L., Schulz, R., Duis, K. 2016. Oxidized Carbo-Iron causes reduced reproduction and lower tolerance of juveniles in the amphipod Hyalella azteca. *Aquatic Toxicology*, **181**, 94-103.

Wen, X.-J., Niu, C.-G., Guo, H., Zhang, L., Liang, C., Zeng, G.-M. 2018. Photocatalytic degradation of levofloxacin by ternary Ag_2CO_3/CeO_2/AgBr photocatalyst under visible-light irradiation: degradation pathways, mineralization ability, and an accelerated interfacial charge transfer process study. *Journal of Catalysis*, **358**, 211-223.

Wu, J., Xie, Y., Fang, Z., Cheng, W., Tsang, P.E. 2016a. Effects of Ni/Fe bimetallic nanoparticles on phytotoxicity and translocation of polybrominated diphenyl ethers in contaminated soil. *Chemosphere*, **162**, 235-242.

Wu, J., Yi, Y., Li, Y., Fang, Z., Tsang, E.P. 2016b. Excellently reactive Ni/Fe bimetallic catalyst supported by biochar for the remediation of decabromodiphenyl contaminated soil: reactivity, mechanism, pathways and reducing secondary risks. *Journal of Hazardous Materials*, **320**, 341-349.

Xie, W., Liang, Q., Qian, T., Zhao, D. 2015. Immobilization of selenite in soil and groundwater using stabilized Fe–Mn binary oxide nanoparticles. *Water Research*, **70**, 485-494.

Xiong, T., Yuan, X., Wang, H., Leng, L., Li, H., Wu, Z., Jiang, L., Xu, R., Zeng, G. 2018a. Implication of graphene oxide in Cd-contaminated soil: A case study of bacterial communities. *Journal of Environmental Management*, **205**, 99-106.

Xiong, Z., Lai, B., Yang, P. 2018b. Enhancing the efficiency of zero valent iron by electrolysis: Performance and reaction mechanism. *Chemosphere*, **194**, 189-199.

Xu, G., Wang, J., Lu, M. 2014. Complete debromination of decabromodiphenyl ether using the integration of Dehalococcoides sp. strain CBDB1 and zero-valent iron. *Chemosphere*, **117**, 455-461.

Yang, Z., Fang, Z., Tsang, P.E., Fang, J., Zhao, D. 2016a. In situ remediation and phytotoxicity assessment of lead-contaminated soil by biochar-supported nHAP. *Journal of Environmental Management*, **182**, 247-251.

Yang, Z., Fang, Z., Zheng, L., Cheng, W., Tsang, P.E., Fang, J., Zhao, D. 2016b. Remediation of lead contaminated soil by biochar-supported nano-hydroxyapatite. *Ecotoxicology and Environmental Safety*, **132**, 224-230.

Yi, Z.-j., Lian, B., Yang, Y.-q., Zou, J.-l. 2009. Treatment of simulated wastewater from in situ leaching uranium mining by zerovalent iron and sulfate reducing bacteria. *Transactions of Nonferrous Metals Society of China*, **19**, s840-s844.

Zaleska-Medynska, A., Marchelek, M., Diak, M., Grabowska, E. 2016. Noble metal-based bimetallic nanoparticles: the effect of the structure on the optical, catalytic and photocatalytic properties. *Advances in Colloid and Interface Science*, **229**, 80-107.

Zhang, W., Li, G., Wang, W., Qin, Y., An, T., Xiao, X., Choi, W. 2018a. Enhanced photocatalytic mechanism of Ag_3PO_4 nano-sheets using MS2 (M = Mo, W)/rGO hybrids as co-catalysts for 4-nitrophenol degradation in water. *Applied Catalysis B: Environmental*, **232**, 11-18.

Zhang, W., Lo, I.M.C., Hu, L., Voon, C.P., Lim, B.L., Versaw, W.K. 2018b. Environmental risks of nano zerovalent iron for arsenate remediation: impacts on cytosolic levels of inorganic phosphate and MgATP2– in *Arabidopsis thaliana*. *Environmental Science & Technology*, **52**(7), 4385-4392.

Zhao, X., Lv, L., Pan, B., Zhang, W., Zhang, S., Zhang, Q. 2011. Polymer-supported nanocomposites for environmental application: A review. *Chemical Engineering Journal*, **170**(2), 381-394.

Zhou, Y., Apul, O.G., Karanfil, T. 2015. Adsorption of halogenated aliphatic contaminants by graphene nanomaterials. *Water Research*, **79**, 57-67.

Zhou, Y., Gao, B., Zimmerman, A.R., Chen, H., Zhang, M., Cao, X. 2014. Biochar-supported zerovalent iron for removal of various contaminants from aqueous solutions. *Bioresource Technology*, **152**, 538-542.

Zhou, Z., Ruan, W., Huang, H., Shen, C., Yuan, B., Huang, C.-H. 2016. Fabrication and characterization of Fe/Ni nanoparticles supported by polystyrene resin for trichloroethylene degradation. *Chemical Engineering Journal*, **283**, 730-739.

Zhu, F., Li, L., Ma, S., Shang, Z. 2016. Effect factors, kinetics and thermodynamics of remediation in the chromium contaminated soils by nanoscale zero valent Fe/Cu bimetallic particles. *Chemical Engineering Journal*, **302**, 663-669.

Zhu, F., Li, L., Ren, W., Deng, X., Liu, T. 2017a. Effect of pH, temperature, humic acid and coexisting anions on reduction of Cr(VI) in the soil leachate by nZVI/Ni bimetal material. *Environmental Pollution*, **227**, 444-450.

Zhu, S., Ho, S.-H., Huang, X., Wang, D., Yang, F., Wang, L., Wang, C., Cao, X., Ma, F. 2017b. Magnetic nanoscale zerovalent iron assisted biochar: interfacial chemical behaviors and heavy metals remediation performance. *ACS Sustainable Chemistry & Engineering*, **5**(11), 9673-9682.

Zhu, S., Huang, X., Wang, D., Wang, L., Ma, F. 2018. Enhanced hexavalent chromium removal performance and stabilization by magnetic iron nanoparticles assisted biochar in aqueous solution: Mechanisms and application potential. *Chemosphere*, **207**, 50-59.

Zou, Y., Wang, X., Khan, A., Wang, P., Liu, Y., Alsaedi, A., Hayat, T., Wang, X. 2016. Environmental remediation and application of nanoscale zero-valent iron and its composites for the removal of heavy metal ions: a review. *Environmental Science & Technology*, **50**(14), 7290-7304.

Figures

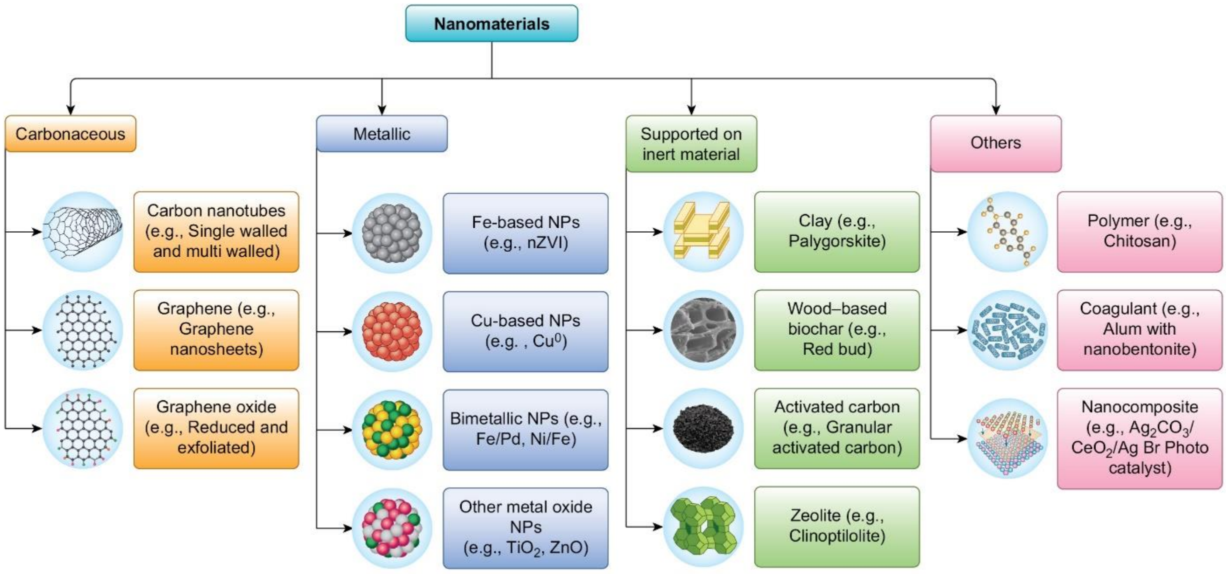

Fig. 1. Types of nanomaterials used for the removal of environmental contaminants.

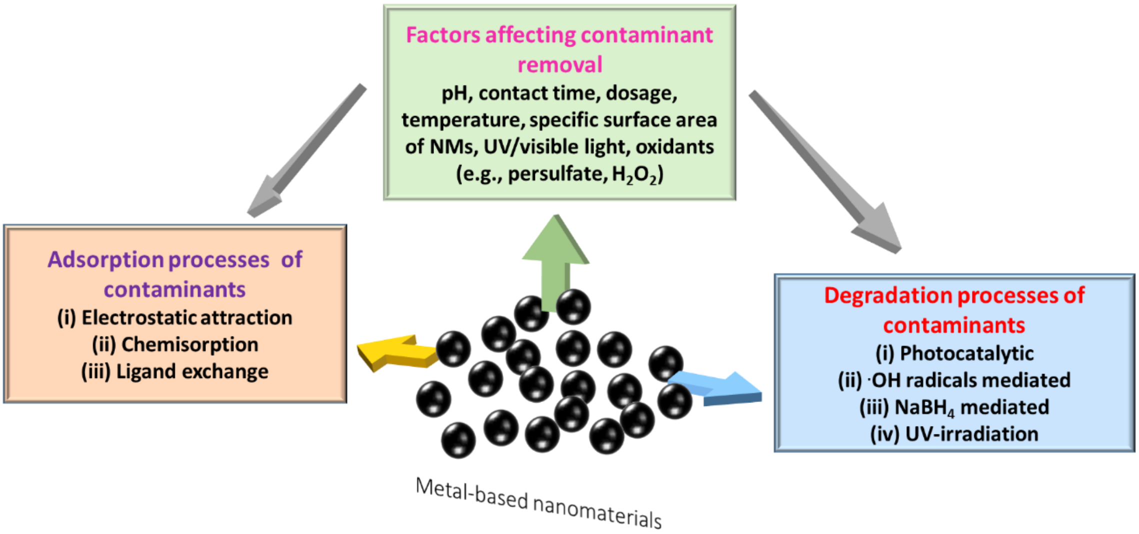

Fig. 2. Factors and processes affecting the adsorption and degradation of contaminants by metal-based NMs.

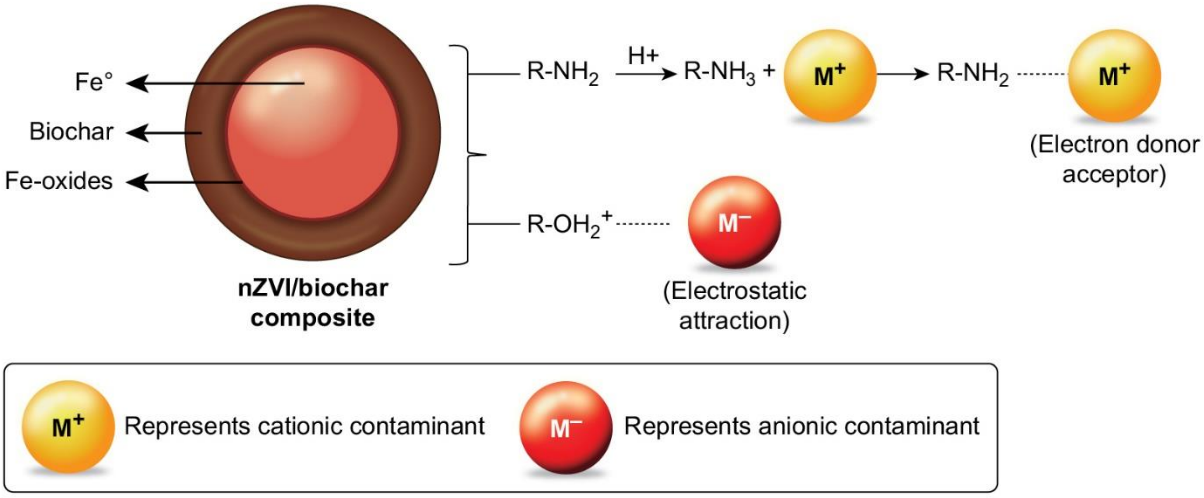

Fig. 3. Mechanisms of contaminants removal by nZVI/biochar composites (adapted from (Zhu et al., 2018))

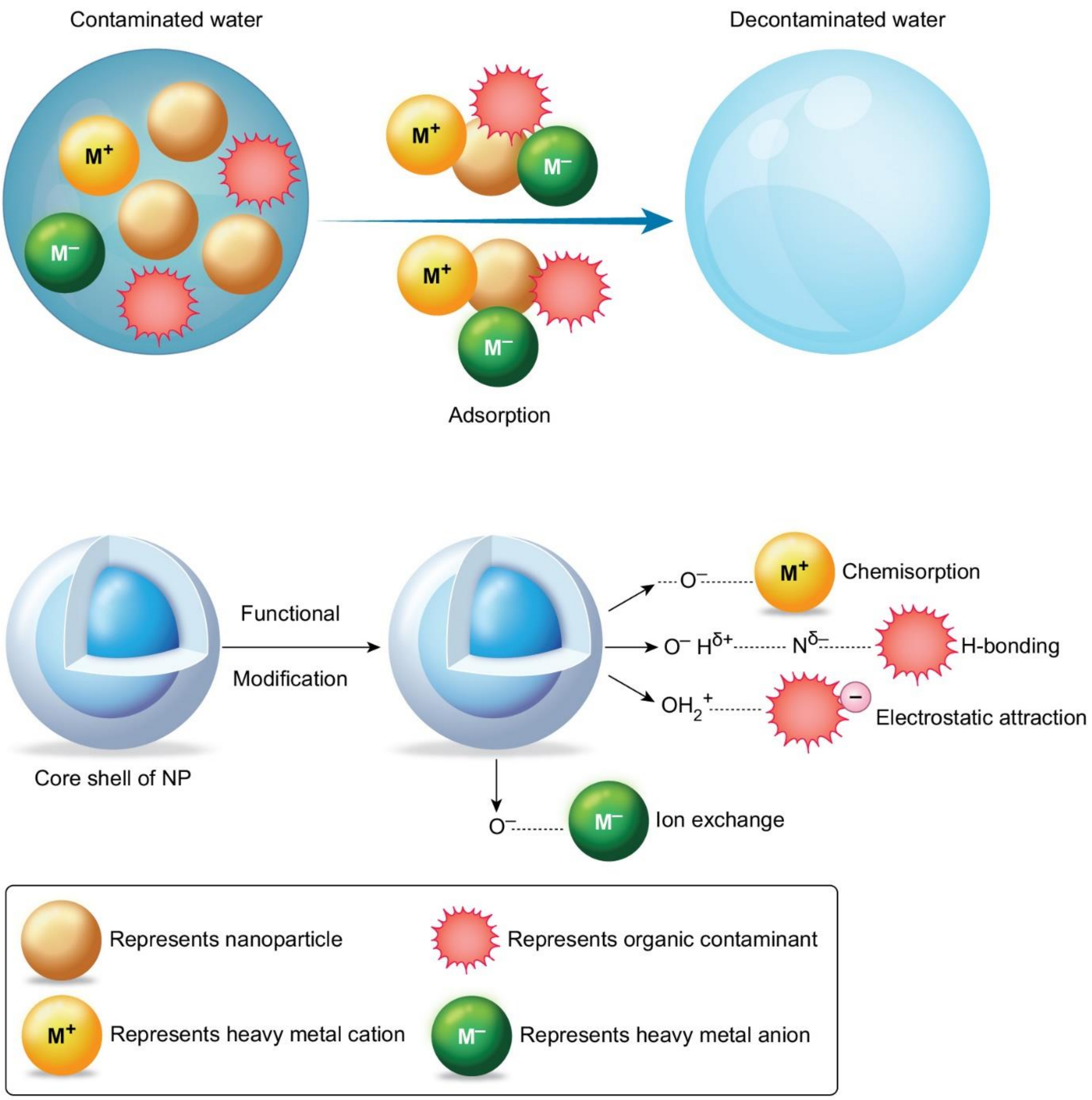

Fig. 4. Adsorption of contaminants onto nanoparticles, and mechanisms involved (adapted from (Mukhopadhyay et al., 2020; Uddin, 2017)).

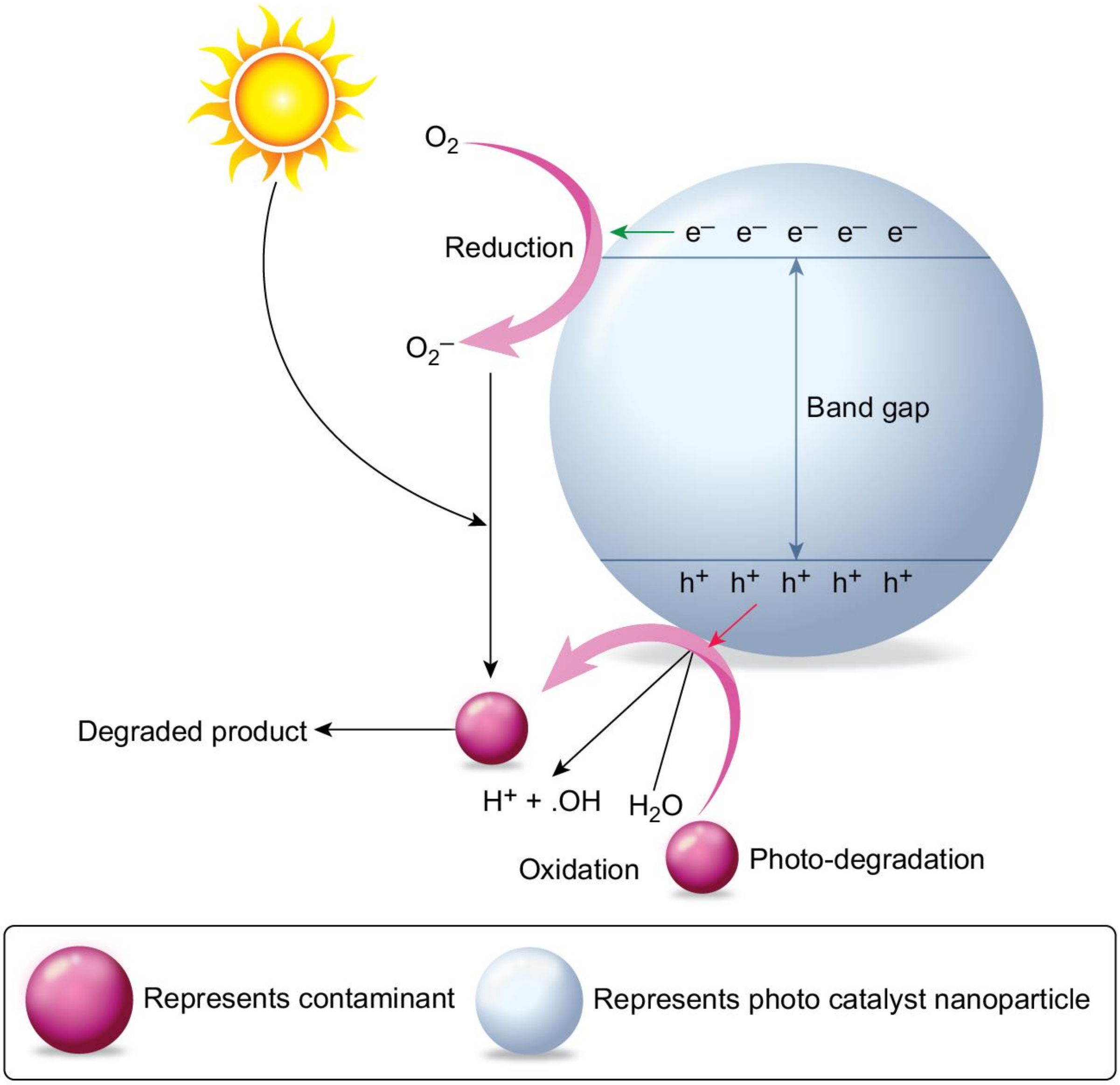

Fig. 5. Photodegradation of contaminants in the presence of a photocatalyst nanoparticle (adapted from (Chong et al., 2010)).

Supplementary Information for:

Nanomaterials for sustainable remediation of chemical contaminants in water and soil

Raj Mukhopadhyay[a], Binoy Sarkar[b,*], Eakalak Khan[c], Daniel S. Alessi[d], Jayanta Kumar Biswas[e], K. M. Manjaiah[f], Miharu Eguchi[g], Kevin C.W. Wu[h], Yusuke Yamauchi[i,j], Yong Sik Ok[k,*]

[a] *Division of Irrigation and Drainage Engineering, ICAR-Central Soil Salinity Research Institute, Karnal – 132001, Haryana, India*

[b] *Lancaster Environment Centre, Lancaster University, Lancaster, LA1 4YQ, United Kingdom*

[c] *Department of Civil and Environmental Engineering and Construction, University of Nevada, Las Vegas, NV 89154, USA*

[d] *University of Alberta, Earth and Atmospheric Sciences, Edmonton, AB, T6G 2E3, Canada*

[e] *Department of Ecological Studies & International Centre for Ecological Engineering, University of Kalyani, Kalyani, Nadia- 741235, West Bengal, India*

[f] *ICAR-Indian Agricultural Research Institute, New Delhi – 110012, India*

[g] *Electronic Functional Materials Group, National Institute for Materials Science (NIMS), 1-1 Namiki, Tsukuba, Ibaraki 305-0044, Japan*

[h] *Department of Chemical Engineering, National Taiwan University, Taipei 10617, Taiwan*

[i] *Australian Institute for Bioengineering and Nanotechnology (AIBN) and School of Chemical Engineering, The University of Queensland, Brisbane, QLD 4072, Australia*

[j] *Yamauchi Materials Space-Tectonics Project and International Center for Materials Nanoarchitechtonics (WPI-MANA), National Institute for Materials Science (NIMS), 1-1 Namiki, Tsukuba, Ibaraki 305-0044, Japan*

[k] *Korea Biochar Research Center, APRU Sustainable Waste Management Program & Division of Environmental Science and Ecological Engineering, Korea University, Seoul 02841, Republic of Korea*

[*]Co-corresponding authors:

Dr. Binoy Sarkar, Lancaster University, e-mail: b.sarkar@lancaster.ac.uk

Prof. Yong Sik Ok, Korea University, e-mail: yongsikok@korea.ac.kr

SI Tables

Table S1. Contaminant adsorption, degradation and removal efficiencies by Fe NPs in water systems.

Iron based nanoparticles	Contaminants	Amount removed /removal efficiency	Contact time	Mechanism(s)	References
nZVI	Co(II)	172 mg/g	10 min	Adsorption on negative charges developed upon hydroxylation of nZVI	Üzüm et al., 2008
Forager sponge-loaded superparamagnetic iron oxide NPs	As(III) and As(V)	As(III): 2.1 mmol/g As(V): 12.1 mmol/g	10 min	Adsorption via anion exchange and ligand exchange	Morillo et al., 2015
Ascorbic acid coated Fe_3O_4 NPs	As(III) and As(V)	As(III): 40.06 mg/g As(V): 16.56 mg/g	30 min	Adsorption on high surface area and separation using external magnetic field	Feng et al., 2012
Green nano-iron particles and chitosan composite	As(III) and As(V)	As(III): 98.79% As(V): 99.65%	30 min	Adsorption through ion exchange	Prasad et al., 2014
nZVI	PO_4^{3-}	96-100%	30 min	Adsorption through pH-induced positive charge formation	Almeelbi & Bezbaruah, 2012
nZVI	Cd(II) and Ni(II)	Cd(II): 65% Ni(II): 27%	2 h	Removal through pH rises and aging effect of nZVI	Calderon & Fullana, 2015
Sulfidized derivative of nZVI	Cd(II)	80%	1 h	Removal by complex formation between sulfidized nZVI-Cd	Stevenson et al., 2017
nZVI	Cr(VI)	3.33 mg/g	24 h	Reduction of Cr(VI) to Cr(III)	Vilardi et al., 2018
Polyethylenimine coated-nZVI	Cr(VI)	99.9%	10 min	Oxidation of nZVI to Fe_2O_3 and Fe_3O_4	Mdlovu et al., 2020
Iron oxide NPs	Cr(VI)	4.62 mg/g	2 h	Chemisorption	Mahanty et al., 2019
Sulfidated nZVI	Cr(VI)	100%	3 h	Surface reduction and precipitation	Zou et al., 2019
CNTs/nZVI composites	Se and Co	Se: 2.52 mg/g Co: 2.35 mg/g	24 h	Removal by chemisorption	Vilardi et al., 2018

nZVI	Yb and La (rare earth elements)	Yb: 410 mg/g La: 61 mg/g	30 min	Surface mediated precipitation	Crane & Sapsford, 2018
nZVI	Uranium (U(VI))	99%	<10 min	Removal via reduction, sorption and precipitation	Hua et al., 2018
Sodium hypochlorite (NaClO)-modified nZVI	PO_4^{3-}	94.8-98.2%	12 min	Rapid oxidation due to presence of NaClO as oxidant	Luo et al., 2020
Iron oxide NPs dispersed onto zeolite by Eucalyptus leaf extracts	NH_4^+ and PO_4^{3-}	NH_4^+: 3.47 mg/g PO_4^{3-}: 38.91 mg/g	15 min	Chemisorption	Xu et al., 2020
Starch modified nZVI	NO_3^-	91%	-	Force electromagnetism	Mofradnia et al., 2019
Zero valent (Fe/Ni) BNP	Profenofos	94.51%	-	Degradation by deprotonation at high pH	Mansouriieh et al., 2019
Potassium persulfate modified Fe_3O_4	Aldrin, eldrin and lindane	Aldrin: 24.7 mg/g Eldrin: 33.5 mg/g Lindane: 10.2 mg/g	10 min	Removal by chemisorption	Lan et al., 2014
nZVI-B (Sodium borohydride method) and nZVI-T (Commercially purchased)	DDT [1,1,1-trichloro2,2-bis(p-chlorophenyl) ethane]	nZVI-B: 92% nZVI-T: 78%	24 h	Degradation due to highly reactive functional surface sites	El-Temsah et al., 2016
Zeolite-supported Fe NPs	Methomyl	100%	4 h	Degradation via photocatalytic oxidation	Tomašević et al., 2010
nZVI	Alachlor	92-96%	72 h	Reductive degradation by nZVI	Bezbaruah et al., 2009
nZVI	Tributyltin and trimethyltin	Tributyltin: 96% Trimethyltin: 40%	7 days	High pH (8.0) followed by acidification with citric acid at pH 3.0	Peeters et al., 2015
Clinoptilolite/nZVI composite	MB and MO	MB: 96.6% MO: 90.2%	MB: 15 min MO: 30 min	Adsorption under wider dispersion of Fe nanoparticle chains in clinoptilolite matrix	Nairat et al., 2015
Fe-NPs	MO	100% degradation	6 h	Strong electrostatic attraction between anionic MO and Fe-NPs below point of zero charge of Fe-NPs	Xingu-Contreras et al., 2020

nZVI	Reactive yellow	59.9%	5 min	Removal via corrosion of nZVI and Fe(II) consumption	Mao et al., 2015
nZVI/H_2O_2 (Fenton like system)	MB	94.5%	1 h	·OH radical oxidation	Yang et al., 2019
Granular reinforced ZVI activated by persulfate	Acid orange 7	90.78%	2 h	Diffusion mediated reduction	Du et al., 2020
Biochar supported nZVI	Ciprofloxacin	70%	1 h	·OH radical oxidation	Mao et al., 2019
Wheat straw supported nZVI	Cu(II), chlorotetracycline	Cu(II): 376.4 mg/g Chlorotetracycline: 1280.8 mg/g	2 h	Chemisorption and redox reaction	Shao et al., 2020
Polyethylenimine (PEI) surface-modified zero-valent iron NPs (PEIenZVI)	Trichloroethylene, perchloroethylene, and 1,2-dichloroethene	99%	2 h	Removal through high surface area (53.4 m^2/g) particles	Lin et al., 2018
Sulfide-modified nZVI	Trichloroethylene	66%	1 h	Strong corrosion of Fe°	Wang et al., 2020
Sulfide-modified nZVI/graphene aerogel composite	Trichloroethylene	100%	50 min	Electron transfer from Fe core to trichloroethylene	Bin et al., 2020
Heat treated biochar impregnated nZVI	Trichloroethylene	88%	20 min	Chemisorption	Mortazavian et al., 2019

‘-‘ indicates unavailability of information on contact time.

Table S2. Cu NPs for contaminant adsorption/removal/degradation in water.

Copper based nanoparticles	Contaminants	Amount removed /removal efficiency	Contact time	Mechanism(s)	References
Chitosan encapsulated CuO	As(V)	28.1 mg/g	3.5 h	Adsorption by electrostatic attraction	Elwakeel & Guibal, 2015
CuO-Fe_3O_4	As(V)	118.11 mg/g	1 h	Removal through protonation and improved electrostatic gravity under acidic conditions	Sun et al., 2017
$CuFe_2O_4$	As	45.7 mg/g	5 h	Bonding with reactive surface sites	Masunga et al., 2019
Cu NPs intercalated into CNTs	As(III)	>90%	66.7 h	Adsorptive filtration and partial oxidation	Luan et al., 2019
CuO NPs	Cr(VI)	18.51 mg/g	3 h	Removal by chemisorption	Gupta et al., 2016
Alginate-coated chitosan/CuO	Ni(II)	94.48% removal	30 min	Removal through formation of less soluble hydrolyzed products such as NiOH and $Ni(OH)_2$ at pH 3.0	Esmaeili & Khoshnevisan, 2016
Nano structured CuO granules	Pb(II)	55.24 mg/g	5 h	Adsorption via strong electrostatic attraction under alkaline conditions	Ahmadi et al., 2012
Amine-functionalized copper ferrite chelated with La(III)	PO_4^{3-}	12.6 mg/g	40 min	Chemisorption	Gu et al., 2018
Cu NPs coated biochar (bamboo shoot shell)	Re(VII)	20.91 mg/g	5 h	Complexation	Hu et al., 2018
CuI-CuO NPs loaded activated carbon	Malachite green	136.67 mg/g	≥25 min	Adsorption via electrostatic attraction at low pH	Nekouei et al., 2015
3.025% Cu-embedded chitosan	Rhodamine B	99% degradation	1 h	Degradation through active •OH radicals	Senthil Kumar et al., 2015
CuO nano-needles on GO sheets	Coomassie brilliant blue (CBB), MB, Congo red (CR) and amido black 10B (AB)	>98% removal	13.33 h	Adsorption via strong electrostatic attraction and high surface area of CuO nano-needles on GO sheets	Rajesh et al., 2016
30% Cu_2O/TiO_2	Acid red B	>70% decolorization	1 h	Adsorptive decolorization via electrostatic attraction and large surface area of Cu_2O/TiO_2	Fei et al., 2015

Bio-engineered Cu NPs	Alizarin Yellow R	89.71%	36 h	Combination of van der Waals forces, electrostatic attraction and H-bonding	Usman et al., 2019
CuO/nanoTiO_2	MB	99% degradation	5 h	Degradation via electron scavenging effect of Cu^{2+} in seawater	Simamora et al., 2012
Cu-oxide NPs annealed at 600°C	MB	91% degradation	2.5 h	Generation of more electro-hole pairs and reduction in the electron-hole recombination rate	Nwanya et al., 2019
Cu_2O-zeolite	1,2-Dichloroethane	83.8% removal	2 h	Removal under UV irradiation at low relative humidity (15%)	Lin et al., 2014
Zero valent Cu	Dichloromethane	90% degradation	1 h	Degradation through hydrodechlorination with a high dose of zero valent Cu (2.5 g/L)	Huang et al., 2012
Zero valent Cu and reductant $NaBH_4$	Mono chloroaromatic	90% dechlorinated	12 h	Dechlorination through breaking of Ar-Cl bond by e^- produced by $NaBH_4$ and formation of Ar-H bond on zero valent Cu (Cu^0).	Raut et al., 2016
Nano CuO	Nitrobenzene	100% degradation	25 min	Degradation by •OH radicals	ElShafei et al., 2014
Cu-doped TiO_2	Phenol	52% degradation	3 h	Degradation through electron (e^-) scavenging effect of Cu^{2+} and prevention of recombination of electron hole pairs	Sohrabi & Akhlaghian, 2016
Chitosan embedded Cu NPs	4-nitroaniline	Rate of reduction: 7.51×10^{-3} /s	<4.5 min	Cu NP-assisted reduction by $NaBH_4$	Bakhsh et al., 2019
Graphene-wrapped zero-valent Cu NPs	Metronidazole	92%	2 h	·OH radical	Xu et al., 2019
Cu NPs	Ibuprofen	36.0 mg/g	1 h	Chemisorption	Husein et al., 2019
Bentonite supported green nZVI-Cu nanocomposite	Tetracycline	95%	1.5 h	·OH radical production due to galvanic corrosion of nZVI-Cu	Gopal et al., 2020

Table S3. Adsorption of different contaminants onto various carbon nanotubes in water.

Types of CNTs	Modification	Contaminants	Amount adsorbed /removal efficiency	Contact time	Mechanism(s)	References
MWCNTs	TiO_2-grafted	Pb(II)	137 mg/g	1 h	Electrostatic attraction	Zhao et al., 2010
MWCNTs	Nano iron oxide coated	Cr(III)	>90%	2 h	Cr (III) removal related to flow rate (inverse relation)	Gupta et al., 2011
MWCNTs	Iron oxide-coated	As(V) and As(III)	As(V): 0.19 mg/g As(III): 1.72 mg/g	30 min	Simple electrostatic Attraction	Addo Ntim & Mitra, 2011
MWCNTs	Al_2O_3	Cd(II)	27.2 mg/g	4 h	Sorption	Liang et al., 2015
MWCNTs	Oxidized	Cd(II)	22.4 mg/g	30 min	Precipitation	Vuković et al., 2010
MWCNTs	Iodide	Hg(II)	123.5 mg/g	2 h	Chemisorption	Gupta et al., 2014
SWCNTs	Thiol derived	Hg(II)	131.0 mg/g	1 h	Chemisorption	Bandaru et al., 2013
MWCNTs	-	Cr(III)	2.07 mmol/g	30 min	Electrostatic attraction	Manilo et al., 2017
Magnetic CNTs	N-doped	Cr(VI)	970.87 mg/g	10 min	Acid medium and reduction reaction between Fe^0 NPs and Cr(VI)	Huang et al., 2019
MWCNTs	Fe_3O_4	As(V)	39.1 mg/g	1 h	Inner sphere complex	Mishra & Ramaprabhu, 2010
Purified SWCNTs	-	Zn(II)	41.8 mg/g	1 h	-	Lu et al., 2006
MWCNTs	2-(5-Bromo-2-pyridylazo)-5-(diethylamino)phenol	U(VI)	83.4 mg/g	20 min	Trinuclear, $(UO_2)_3(OH)^{5+}$ formation	Khamirchi et al., 2018
CNTs	Oxidized	Co(II)	69.6 mg/g	20 min	Chemical interaction	Tofighy & Mohammadi, 2011
MWCNTs	Amidoamine	Hg(II)	45.05 mg/g	3 h	Chemisorption	Singha Deb et al., 2017
MWCNTs	Polypyrrole-coated and oxidized	Pb(II) and Cu(II)	Pb(II): 26.3 mg/g Cu(II): 24.4 mg/g	1 h	Deprotonation of NH_2 and nitrogen	Nyairo et al., 2018
MWCNTs	Chitin/magnetite	Cr(VI)	11.30 mg/g	45 min	Strong interaction with reactive functional groups	Salam, 2017

MWCNTs	Al_2O_3	Cd(II)	27.21 mg/g	1 h	Electrostatic attraction	Verma & Balomajumder, 2020
CNTs	Chitosan sponge	F^-	975.4 mg/g	20 min	Functional groups of chitosan and CNTs	Affonso et al., 2020
CNTs	Carbon graphite	Cu(II)	25%	-	Oxidation effect	Zghal et al., 2020
MWCNTs	Oxidation	Diuron	29.82 mg/g	1 h	Electrostatic attraction	Deng et al., 2012
MWCNTs	Oxidation	Methyl orange (MO)	306 mg/g	3.5 h	Electrostatic interaction	Mahmoodian et al., 2015
MWCNTs	Graphene oxide	Methylene blue (MB)	87.9 mg/g	2 h	Electrostatic interaction	Ai & Jiang, 2012
MWCNTs	-	Isoproturon	8.1 mg/g	-	Strong attraction between surface reactive sites and contaminant	Sotelo et al., 2012
SWCNTs	-	Atrazine	4.97 mg/g	-	Chemisorption	Jung et al., 2015
CNTs	Chitosan hydrogel scaffold	Food red 17 and Food blue 1	Food red 17: 1480 mg/g; Food blue 1: 1508 mg/g	50 min	Strong interaction with surface functionalized groups	Gonçalves et al., 2020
MWCNTs	COOH-carboxylate COOH-cysteamine	Amido black 10B	COOH-carboxylate: 90 mg/g COOH-cysteamine: 131 mg/g	18 min	Chemisorption and protonation due to pH of the medium	Sadegh et al., 2016
CNTs	Trimesoyl chloride and m-phenylenediamine grafting	Phenol	261.6 mg/g	50 min	Electrostatic attraction	Saleh et al., 2019
CNTs	Fe/Ni NPs supported	2,6 dichlorophenol	82.6% (dechlorination)	50 min	Bonding with reactive sites of Fe/Ni NPs	Liu et al., 2020
CNTs	Chitosan hydrogel scaffold	Phenol	404.2 mg/g	20 min	Chemisorption	Alves et al., 2019
Magnetic CNTs	Polyethyleneimine	Alizarin Red S	196.08 mg/g	40 min	Interaction with active sites and multiple interactions	Zhang et al., 2019

‘-‘indicates unavailability of information on contact time.

Table S4. Contaminant adsorption capacities of graphene oxide (GO) and GO composites in water.

Heavy metals	Adsorbents	Amount adsorbed /removal efficiency	Contact time	Mechanism(s)	References
Cu(II)	GO	46.6 mg/g	-	Electrostatic attraction and coordination between Cu(II) and carboxyl groups	Yang et al., 2010
Cd(II), Ni(II)	GO	Cd(II): 83.3 mg/g Ni(II): 62.3 mg/g	10 min	Lewis acid base interaction	Tan et al., 2015
Pb(II)	Few layered GO	842 mg/g	24 h	Surface complexation	Zhao et al., 2011
Sb(III)	Reduced GO (rGO)	8.1 mg/g	4 h	van der Waals force	Leng et al., 2012
Zn(II)	GO	245.7 mg/g	20 min	Ion exchange and electrostatic attraction	Wang et al., 2013
Eu(III)	GO nanosheets	175.4 mg/g	48 h	Mononuclear and binuclear complexes	Sun et al., 2012
Hg(II), Cu(II), Pb(II)	EDTA*-GO	Hg(II): 268.4 mg/g Cu(II): 301.2 mg/g Pb(II): 508.4 mg/g	Hg(II): 50 min Cu(II): 90 min Pb(II): 40 min	Electrostatic attraction	Cui et al., 2015
Co(II)	GO-NH_2	116.4 mg/g	5 min	Complexation with carboxyl and amino groups on GO surfaces	Fang et al., 2014
U(VI)	rGO/$CoFe_2O_4$/polyaniline	2430 mg/g	4 h	Strong electrostatic attraction	Dat et al., 2018
As(V)	GO/$CuFe_2O_4$ held onto Fe-Ni foam	125 mg/g	30 min	Ligand exchange	Wu et al., 2018
As(V)	GO/$MnFe_2O_4$	240 mg/g	20 min	Bonding with active sorption sites	Huong et al., 2016
Pb(II), Cr(III), Cu(II)	Magnetic GO	Pb(II): 200 mg/g Cr(III):24.3 mg/g Cu(II): 62.8 mg/g	Pb(II): 25 min Cr(III): 35 min Cu(II):25 min	Electrostatic attraction and precipitation	Ain et al., 2020

Hg(II)	Polyamine modified rGO in hydrothermal method	63.8 mg/g	10 min	Chemisorption	Yap et al., 2020
Hg(II)	Sulphur-doped carbon nitride/ graphene oxide	40 mg/g	2 h	Electrostatic attraction	Li et al., 2020
Pb(II)	rGO/Fe NPs	82.4%	10 min	Interaction with active functional groups	Xiao et al., 2019
Phenanthrene, biphenyls	GO	Phenanthrene: 174.6 mg/g Biphenyls: 59 mg/g	-	van der Waals force	Apul et al., 2013
TCP, TCB, 2-napthol, NAPH	GO	TCP: 3.5 mg/g TCB: 1.6 mg/g 2-napthol: 4.2 mg/g NAPH: 0.9 mg/g	24 h	π–π interaction	Pei et al., 2013
MB	Exfoliated GO (EGO)	17.3 mg/g	2 h	Electrostatic attraction/ van der Waals force	Ramesha et al., 2011
Methyl violet (MV) and Rhodamine B, (RhB)	EGO	MV: 2.5 mg/g RhB: 1.2 mg/g	MV: 2 h RhB: 25 min	Electrostatic attraction/ van der Waals force	Ramesha et al., 2011
MB	rGO/$ZnFe_2O_4$	9.7 mg/g	30 min	Bonding with reactive functional groups	Park et al., 2019
2,4-Dichlorophenol	Polysulfone-iron oxide/GO composite	96.5%	-	Oxygen-enriched functional groups and hydrophilicity	Modi & Bellare, 2020
Rhodamine-B	Polysulfone-GO	>90%	4 h	Chemisorption	Zambianchi et al., 2017
MB, RhB, MV	SiO_2-GO hybrid	MB: 300 mg/g RhB: 258 mg/g MV: 178 mg/g	3 min	Interfacial catalytic process	Czepa et al., 2020
MB	Sulfated-cellulose GO	421.90 mg/g	<1 h	Chemisorption	Wang et al., 2019
2, 4-Dichlorophenol	α-Fe_2O_3@Fe_3O_4 shell–core magnetic nanoparticles and GO	>60% degradation	2 h	Large surface area accompanied by pore size diameter	Pang et al., 2020

[*]EDTA: Ethylenediaminetetraacetic acid; ‘-‘ indicates unavailability of information on contact time.

Table S5. List of nanomaterials and their contaminant removal capacities in soil.

Contaminants	Nanomaterials	Removal capacity /degradation efficiency	Contact time	Mechanism(s)	References
Pb(II)	Nano-hydroxy apatite	Concentration decreased by 3-21% in roots and 13-20% in shoots of ryegrass	30 days (rye grass crop cycle)	Secretion of tartaric increased the Pb adsorption	Ding et al., 2017
Pb(II), Cu(II) and Zn(II)	Calcium phosphate nanoparticles (CPNs)	Pb: > 90% Cu: 50% Zn: 50%	10 days aging of CPNs and soil mixture	Insoluble complex formation between CPNs and heavy metals	Arenas-Lago et al., 2016
Pb(II)	nZVI/citric acid	87% in farmland soil	4 h	Organic acid and metal chelate formation	Wang et al., 2014
Cr(VI)	CMC-stabilized FeS NPs/biochar composite	11.9 to 0.63 mg/L in the leachate	180 days	Strong interaction with reactive surface sites	Lyu et al., 2018
Cr(VI)	nZVI/Cu	99%	10 min	Reduction of Cr(VI) to Cr(III) at low pH and generation of more electrons	Zhu et al., 2016
As	nZVI	40.4%	3 days	Bioaccessibility reduced through surface complexation	Zhang et al., 2010
As	Green iron oxide NPs	67.3%	120 days	Covalent bonding and high Fe content of soil due to application of Fe-oxide NPs	Su et al., 2020
Pb(II)	Biochar supported nZVI	54.68%	90 days	Co-precipitation and secondary Pb-Fe mineral formation under alkaline environment	Peng et al., 2019
Cr(VI)	CMC stabilized FeS NPs	Leachate Cr(VI) immobilized by >90%	42 h	Co-precipitation, adsorption and reduction	Wang et al., 2019
As	nZVI and n-goethite	nZVI: 89.5% n-goethite: 82.5% (decrease in As bioavailability)	-	Inner-sphere complexation	Baragaño et al., 2020

Cd(II)	nZVI/palm BC	Pronounced immobilization in soil	120 days (Rice life cycle)	Sorption and precipitation	Qiao et al., 2018
Sb(V)	nZVI	>90%	6-8 min	Chemisorption	Dorjee et al., 2014
Cd(II)	GO	103.3 mg/g	60 days	Adsorption via chelation to form stable Cd-complexes	Xiong et al., 2018
Decabromodiphenyl ether (BDE-209)	Ni/Fe BNPs	72%	72 h	Mass transfer and Generation of active H_2 species due to Fe corrosion in water	Xie et al., 2014
Decabromodiphenyl ether (BDE-209)	nZVI immobilized in mesoporous silica microspheres covered with FeOOH (SiO_2@FeOOH@Fe)	78%	120 h	Corrosion of Fe	Xie et al., 2016
Polychlorinated biphenyls (PCB)	nZVI	83%	5 days	Hydro-dechlorination by generation of H^+ in anode	Gomes et al., 2015
PAHs	Fe_3O_4/persulfate	75%	24 h	Generation of free radicals or reactive oxygen species	Dong et al., 2018
PAHs	nZVI/BC	40%	30 days	Active sites and functional groups of biochar	Oleszczuk & Kołtowski, 2017
Chlorpyriphos	Laccase immobilized iron oxide NPs	K_d: 112.3 L/kg	30 days	Hydrolysis of chlorpyriphos due to presence of Cu in laccase molecules	Das et al., 2020
Sulfamethazine	nZVI/corn stalk biochar	74%	12 h	Fenton like degradation	Deng et al., 2018
Ibuprofen	nZVI using grape vine leaf extract	66%	73 h	Low pH and faster reactivity	Machado et al., 2013

'-' indicates unavailability of information on contact time.

References

Addo Ntim, S., Mitra, S. 2011. Removal of trace arsenic to meet drinking water standards using iron oxide coated multiwall carbon nanotubes. *Journal of Chemical & Engineering Data*, **56**(5), 2077-2083.

Affonso, L.N., Marques, J.L., Lima, V.V.C., Gonçalves, J.O., Barbosa, S.C., Primel, E.G., Burgo, T.A.L., Dotto, G.L., Pinto, L.A.A., Cadaval, T.R.S. 2020. Removal of fluoride from fertilizer industry effluent using carbon nanotubes stabilized in chitosan sponge. *Journal of Hazardous Materials*, **388**, 122042.

Ahmadi, S.J., Sadjadi, S., Hosseinpour, M. 2012. Adsorption behavior of toxic metal ions on nano-structured CuO granules. *Separation Science and Technology*, **47**(7), 1063-1069.

Ai, L., Jiang, J. 2012. Removal of methylene blue from aqueous solution with self-assembled cylindrical graphene–carbon nanotube hybrid. *Chemical Engineering Journal*, **192**, 156-163.

Ain, Q.-U., Farooq, M.U., Jalees, M.I. 2020. Application of magnetic graphene oxide for water purification: heavy metals removal and disinfection. *Journal of Water Process Engineering*, **33**, 101044.

Almeelbi, T., Bezbaruah, A. 2012. Aqueous phosphate removal using nanoscale zero-valent iron. *Journal of Nanoparticle Research*, **14**(7), 900.

Alves, D.C.S., Gonçalves, J.O., Coseglio, B.B., Burgo, T.A.L., Dotto, G.L., Pinto, L.A.A., Cadaval, T.R.S. 2019. Adsorption of phenol onto chitosan hydrogel scaffold modified with carbon nanotubes. *Journal of Environmental Chemical Engineering*, **7**(6), 103460.

Apul, O.G., Wang, Q., Zhou, Y., Karanfil, T. 2013. Adsorption of aromatic organic contaminants by graphene nanosheets: Comparison with carbon nanotubes and activated carbon. *Water Research*, **47**(4), 1648-1654.

Arenas-Lago, D., Rodríguez-Seijo, A., Lago-Vila, M., Couce, L.A., Vega, F.A. 2016. Using $Ca_3(PO_4)_2$ nanoparticles to reduce metal mobility in shooting range soils. *Science of The Total Environment*, **571**, 1136-1146.

Bakhsh, E.M., Ali, F., Khan, S.B., Marwani, H.M., Danish, E.Y., Asiri, A.M. 2019. Copper nanoparticles embedded chitosan for efficient detection and reduction of nitroaniline. *International Journal of Biological Macromolecules*, **131**, 666-675.

Bandaru, N.M., Reta, N., Dalal, H., Ellis, A.V., Shapter, J., Voelcker, N.H. 2013. Enhanced adsorption of mercury ions on thiol derivatized single wall carbon nanotubes. *Journal of Hazardous Materials*, **261**, 534-541.

Baragaño, D., Alonso, J., Gallego, J.R., Lobo, M.C., Gil-Díaz, M. 2020. Zero valent iron and goethite nanoparticles as new promising remediation techniques for As-polluted soils. *Chemosphere*, **238**, 124624.

Bezbaruah, A.N., Thompson, J.M., Chisholm, B.J. 2009. Remediation of alachlor and atrazine contaminated water with zero-valent iron nanoparticles. *Journal of Environmental Science and Health, Part B*, **44**(6), 518-524.

Bin, Q., Lin, B., Zhu, K., Shen, Y., Man, Y., Wang, B., Lai, C., Chen, W. 2020. Superior trichloroethylene removal from water by sulfide-modified nanoscale zero-valent iron/graphene aerogel composite. *Journal of Environmental Sciences*, **88**, 90-102.

Calderon, B., Fullana, A. 2015. Heavy metal release due to aging effect during zero valent iron nanoparticles remediation. *Water Research*, **83**, 1-9.

Crane, R.A., Sapsford, D.J. 2018. Sorption and fractionation of rare earth element ions onto nanoscale zerovalent iron particles. *Chemical Engineering Journal*, **345**, 126-137.

Cui, L., Wang, Y., Gao, L., Hu, L., Yan, L., Wei, Q., Du, B. 2015. EDTA functionalized magnetic graphene oxide for removal of Pb(II), Hg(II) and Cu(II) in water treatment: Adsorption mechanism and separation property. *Chemical Engineering Journal*, **281**, 1-10.

Czepa, W., Pakulski, D., Witomska, S., Patroniak, V., Ciesielski, A., Samorì, P. 2020. Graphene oxide-mesoporous SiO_2 hybrid composite for fast and efficient removal of organic cationic contaminants. *Carbon*, **158**, 193-201.

Das, A., Jaswal, V., Yogalakshmi, K.N. 2020. Degradation of chlorpyrifos in soil using laccase immobilized iron oxide nanoparticles and their competent role in deterring the mobility of chlorpyrifos. *Chemosphere*, **246**, 125676.

Dat, T.Q., Ha, N.T., Thin, P.V., Tung, N.V., Hung, D.Q. 2018. Synthesis of RGO/CF/PANI Magnetic Composites for Effective Adsorption of Uranium. *IEEE Transactions on Magnetics*, **54**(6), 1-6.

Deng, J., Dong, H., Zhang, C., Jiang, Z., Cheng, Y., Hou, K., Zhang, L., Fan, C. 2018. Nanoscale zero-valent iron/biochar composite as an activator for Fenton-like removal of sulfamethazine. *Separation and Purification Technology*, **202**, 130-137.

Deng, J., Shao, Y., Gao, N., Deng, Y., Tan, C., Zhou, S., Hu, X. 2012. Multiwalled carbon nanotubes as adsorbents for removal of herbicide diuron from aqueous solution. *Chemical Engineering Journal*, **193–194**, 339-347.

Ding, L., Li, J., Liu, W., Zuo, Q., Liang, S.-X. 2017. Influence of nano-hydroxyapatite on the metal bioavailability, plant metal accumulation and root exudates of Ryegrass for phytoremediation in lead-polluted soil. *International journal of environmental research and public health*, **14**(5), 532.

Dong, C.-D., Tsai, M.-L., Chen, C.-W., Hung, C.-M. 2018. Remediation and cytotoxicity study of polycyclic aromatic hydrocarbon-contaminated marine sediments using synthesized iron oxide–carbon composite. *Environmental Science and Pollution Research*, **25**(6), 5243-5253.

Dorjee, P., Amarasiriwardena, D., Xing, B. 2014. Antimony adsorption by zero-valent iron nanoparticles (nZVI): Ion chromatography–inductively coupled plasma mass spectrometry (IC–ICP-MS) study. *Microchemical Journal*, **116**, 15-23.

Du, Y., Dai, M., Cao, J., Peng, C., Ali, I., Naz, I., Li, J. 2020. Efficient removal of acid orange 7 using a porous adsorbent-supported zero-valent iron as a synergistic catalyst in advanced oxidation process. *Chemosphere*, **244**, 125522.

ElShafei, G.M.S., Yehia, F.Z., Dimitry, O.I.H., Badawi, A.M., Eshaq, G. 2014. Ultrasonic assisted-Fenton-like degradation of nitrobenzene at neutral pH using nanosized oxides of Fe and Cu. *Ultrasonics Sonochemistry*, **21**(4), 1358-1365.

El-Temsah, Y.S., Sevcu, A., Bobcikova, K., Cernik, M., Joner, E.J. 2016. DDT degradation efficiency and ecotoxicological effects of two types of nano-sized zero-valent iron (nZVI) in water and soil. *Chemosphere*, **144**, 2221-2228.

Elwakeel, K.Z., Guibal, E. 2015. Arsenic(V) sorption using chitosan/$Cu(OH)_2$ and chitosan/CuO composite sorbents. *Carbohydrate Polymers*, **134**, 190-204.

Esmaeili, A., Khoshnevisan, N. 2016. Optimization of process parameters for removal of heavy metals by biomass of Cu and Co-doped alginate-coated chitosan nanoparticles. *Bioresource Technology*, **218**, 650-658.

Fang, F., Kong, L., Huang, J., Wu, S., Zhang, K., Wang, X., Sun, B., Jin, Z., Wang, J., Huang, X.-J., Liu, J. 2014. Removal of cobalt ions from aqueous solution by an amination graphene oxide nanocomposite. *Journal of Hazardous Materials*, **270**, 1-10.

Fei, X., Li, F., Cao, L., Jia, G., Zhang, M. 2015. Adsorption and photocatalytic performance of cuprous oxide/titania composite in the degradation of acid red B. *Materials Science in Semiconductor Processing*, **33**, 9-15.

Feng, L., Cao, M., Ma, X., Zhu, Y., Hu, C. 2012. Superparamagnetic high-surface-area Fe_3O_4 nanoparticles as adsorbents for arsenic removal. *Journal of Hazardous Materials*, **217-218**, 439-446.

Gomes, H.I., Dias-Ferreira, C., Ottosen, L.M., Ribeiro, A.B. 2015. Electroremediation of PCB contaminated soil combined with iron nanoparticles: Effect of the soil type. *Chemosphere*, **131**, 157-163.

Gonçalves, J.O., da Silva, K.A., Rios, E.C., Crispim, M.M., Dotto, G.L., de Almeida Pinto, L.A. 2020. Chitosan hydrogel scaffold modified with carbon nanotubes and its application for food dyes removal in single and binary aqueous systems. *International Journal of Biological Macromolecules*, **142**, 85-93.

Gopal, G., Sankar, H., Natarajan, C., Mukherjee, A. 2020. Tetracycline removal using green synthesized bimetallic nZVI-Cu and bentonite supported green nZVI-Cu nanocomposite: A comparative study. *Journal of Environmental Management*, **254**, 109812.

Gu, W., Li, X., Xing, M., Fang, W., Wu, D. 2018. Removal of phosphate from water by amine-functionalized copper ferrite chelated with La(III). *Science of The Total Environment*, **619-620**, 42-48.

Gupta, A., Vidyarthi, S.R., Sankararamakrishnan, N. 2014. Enhanced sorption of mercury from compact fluorescent bulbs and contaminated water streams using functionalized multiwalled carbon nanotubes. *Journal of Hazardous Materials*, **274**, 132-144.

Gupta, V.K., Agarwal, S., Saleh, T.A. 2011. Chromium removal by combining the magnetic properties of iron oxide with adsorption properties of carbon nanotubes. *Water Research*, **45**(6), 2207-2212.

Gupta, V.K., Chandra, R., Tyagi, I., Verma, M. 2016. Removal of hexavalent chromium ions using CuO nanoparticles for water purification applications. *Journal of Colloid and Interface Science*, **478**, 54-62.

Hu, H., Sun, L., Jiang, B., Wu, H., Huang, Q., Chen, X. 2018. Low concentration Re(VII) recovery from acidic solution by Cu-biochar composite prepared from bamboo (*Acidosasa longiligula*) shoot shell. *Minerals Engineering*, **124**, 123-136.

Hua, Y., Wang, W., Huang, X., Gu, T., Ding, D., Ling, L., Zhang, W.-x. 2018. Effect of bicarbonate on aging and reactivity of nanoscale zerovalent iron (nZVI) toward uranium removal. *Chemosphere*, **201**, 603-611.

Huang, C.-C., Lo, S.-L., Lien, H.-L. 2012. Zero-valent copper nanoparticles for effective dechlorination of dichloromethane using sodium borohydride as a reductant. *Chemical Engineering Journal*, **203**, 95-100.

Huang, J., Cao, Y., Qin, B., Zhong, G., Zhang, J., Yu, H., Wang, H., Peng, F. 2019. Highly efficient and acid-corrosion resistant nitrogen doped magnetic carbon nanotubes for the hexavalent chromium removal with subsequent reutilization. *Chemical Engineering Journal*, **361**, 547-558.

Huong, P.T.L., Huy, L.T., Phan, V.N., Huy, T.Q., Nam, M.H., Lam, V.D., Le, A.-T. 2016. Application of graphene oxide-$MnFe_2O_4$ magnetic nanohybrids as magnetically separable adsorbent for highly efficient removal of arsenic from water. *Journal of Electronic Materials*, **45**(5), 2372-2380.

Husein, D.Z., Hassanien, R., Al-Hakkani, M.F. 2019. Green-synthesized copper nano-adsorbent for the removal of pharmaceutical pollutants from real wastewater samples. *Heliyon*, **5**(8), e02339.

Jung, C., Son, A., Her, N., Zoh, K.-D., Cho, J., Yoon, Y. 2015. Removal of endocrine disrupting compounds, pharmaceuticals, and personal care products in water using carbon nanotubes: A review. *Journal of Industrial and Engineering Chemistry*, **27**, 1-11.

Khamirchi, R., Hosseini-Bandegharaei, A., Alahabadi, A., Sivamani, S., Rahmani-Sani, A., Shahryari, T., Anastopoulos, I., Miri, M., Tran, H.N. 2018. Adsorption property of Br-PADAP-impregnated multiwall carbon nanotubes towards uranium and its performance in the selective separation and determination of uranium in different environmental samples. *Ecotoxicology and Environmental Safety*, **150**, 136-143.

Lan, J., Cheng, Y., Zhao, Z. 2014. Effective organochlorine pesticides removal from aqueous systems by magnetic nanospheres coated with polystyrene. *Journal of Wuhan University of Technology-Mater. Sci. Ed.*, **29**(1), 168-173.

Leng, Y., Guo, W., Su, S., Yi, C., Xing, L. 2012. Removal of antimony(III) from aqueous solution by graphene as an adsorbent. *Chemical Engineering Journal*, **211-212**, 406-411.

Li, M., Wang, B., Yang, M., Li, Q., Calatayud, D.G., Zhang, S., Wang, H., Wang, L., Mao, B. 2020. Promoting mercury removal from desulfurization slurry via S-doped carbon nitride/graphene oxide 3D hierarchical framework. *Separation and Purification Technology*, **239**, 116515.

Liang, J., Liu, J., Yuan, X., Dong, H., Zeng, G., Wu, H., Wang, H., Liu, J., Hua, S., Zhang, S., Yu, Z., He, X., He, Y. 2015. Facile synthesis of alumina-decorated multi-walled carbon nanotubes for simultaneous adsorption of cadmium ion and trichloroethylene. *Chemical Engineering Journal*, **273**, 101-110.

Lin, J.-H., Wu, S.-W., Kuo, C.-Y. 2014. Degradation of gaseous 1,2-dichloroethane using a hybrid cuprous oxide catalyst. *Process Safety and Environmental Protection*, **92**(5), 442-446.

Lin, K.-S., Mdlovu, N.V., Chen, C.-Y., Chiang, C.-L., Dehvari, K. 2018. Degradation of TCE, PCE, and 1,2–DCE DNAPLs in contaminated groundwater using polyethylenimine-modified zero-valent iron nanoparticles. *Journal of Cleaner Production*, **175**, 456-466.

Liu, Z., Ding, C., Gao, P., Xu, Y., Sun, Y., Wen, X., Dai, J., Fei, Z. 2020. Enhanced dechlorination of 2,6-dichlorophenol by carbon nanotubes supported Fe/Ni nanoparticles: Characterization, influencing factors, and kinetics. *Colloids and Surfaces A: Physicochemical and Engineering Aspects*, **585**, 124089.

Lu, C., Chiu, H., Liu, C. 2006. Removal of zinc(II) from aqueous solution by purified carbon nanotubes: kinetics and equilibrium studies. *Industrial & Engineering Chemistry Research*, **45**(8), 2850-2855.

Luan, H., Teychene, B., Huang, H. 2019. Efficient removal of As(III) by Cu nanoparticles intercalated in carbon nanotube membranes for drinking water treatment. *Chemical Engineering Journal*, **355**, 341-350.

Luo, X., Guo, X., Xia, X., Zhang, X., Ma, N., Leng, S., Ullah, S., Ayalew, Z.M. 2020. Rapid and long-effective removal of phosphate from water by zero-valent iron in combination with hypochlorite (ZVI/NaClO). *Chemical Engineering Journal*, **382**, 122835.

Lyu, H., Zhao, H., Tang, J., Gong, Y., Huang, Y., Wu, Q., Gao, B. 2018. Immobilization of hexavalent chromium in contaminated soils using biochar supported nanoscale iron sulfide composite. *Chemosphere*, **194**, 360-369.

Machado, S., Stawiński, W., Slonina, P., Pinto, A.R., Grosso, J.P., Nouws, H.P.A., Albergaria, J.T., Delerue-Matos, C. 2013. Application of green zero-valent iron nanoparticles to the remediation of soils contaminated with ibuprofen. *Science of The Total Environment*, **461-462**, 323-329.

Mahanty, S., Bakshi, M., Ghosh, S., Gaine, T., Chatterjee, S., Bhattacharyya, S., Das, S., Das, P., Chaudhuri, P. 2019. Mycosynthesis of iron oxide nanoparticles using manglicolous fungi isolated from Indian sundarbans and its application for the treatment of chromium containing solution: Synthesis, adsorption isotherm, kinetics and thermodynamics study. *Environmental Nanotechnology, Monitoring & Management*, **12**, 100276.

Mahmoodian, H., Moradi, O., Shariatzadeha, B., Salehf, T.A., Tyagi, I., Maity, A., Asif, M., Gupta, V.K. 2015. Enhanced removal of methyl orange from aqueous solutions by poly HEMA–chitosan-MWCNT nano-composite. *Journal of Molecular Liquids*, **202**, 189-198.

Manilo, M.V., Choma, Z.Z., Barany, S. 2017. Comparative study of Cr(III) adsorption by carbon nanotubes and active carbons. *Colloid Journal*, **79**(2), 212-218.

Mansouriieh, N., Sohrabi, M.R., Khosravi, M. 2019. Optimization of profenofos organophosphorus pesticide degradation by zero-valent bimetallic nanoparticles using response surface methodology. *Arabian Journal of Chemistry*, **12**(8), 2524-2532.

Mao, Q., Zhou, Y., Yang, Y., Zhang, J., Liang, L., Wang, H., Luo, S., Luo, L., Jeyakumar, P., Ok, Y.S., Rizwan, M. 2019. Experimental and theoretical aspects of biochar-supported nanoscale zero-valent iron activating H_2O_2 for ciprofloxacin removal from aqueous solution. *Journal of Hazardous Materials*, **380**, 120848.

Mao, Y., Xi, Z., Wang, W., Ma, C., Yue, Q. 2015. Kinetics of Solvent Blue and Reactive Yellow removal using microwave radiation in combination with nanoscale zero-valent iron. *Journal of Environmental Sciences*, **30**, 164-172.

Masunga, N., Mmelesi, O.K., Kefeni, K.K., Mamba, B.B. 2019. Recent advances in copper ferrite nanoparticles and nanocomposites synthesis, magnetic properties and application in water treatment: Review. *Journal of Environmental Chemical Engineering*, **7**(3), 103179.

Mdlovu, N.V., Lin, K.-S., Chen, Z.-W., Liu, Y.-J., Mdlovu, N.B. 2020. Treatment of simulated chromium-contaminated wastewater using polyethylenimine-modified zero-valent iron nanoparticles. *Journal of the Taiwan Institute of Chemical Engineers*, **108**, 92-101.

Mishra, A.K., Ramaprabhu, S. 2010. Magnetite decorated multiwalled carbon nanotube based supercapacitor for arsenic removal and desalination of seawater. *The Journal of Physical Chemistry C*, **114**(6), 2583-2590.

Modi, A., Bellare, J. 2020. Efficient removal of 2,4-dichlorophenol from contaminated water and alleviation of membrane fouling by high flux polysulfone-iron oxide/graphene oxide composite hollow fiber membranes. *Journal of Water Process Engineering*, **33**, 101113.

Mofradnia, S.R., Ashouri, R., Tavakoli, Z., Shahmoradi, F., Rashedi, H., Yazdian, F., Tavakoli, J. 2019. Effect of zero-valent iron/starch nanoparticle on nitrate removal using MD simulation. *International Journal of Biological Macromolecules*, **121**, 727-733.

Morillo, D., Pérez, G., Valiente, M. 2015. Efficient arsenic(V) and arsenic(III) removal from acidic solutions with Novel Forager Sponge-loaded superparamagnetic iron oxide nanoparticles. *Journal of Colloid and Interface Science*, **453**, 132-141.

Mortazavian, S., Jones-Lepp, T., Bae, J.-H., Chun, D., Bandala, E.R., Moon, J. 2019. Heat-treated biochar impregnated with zero-valent iron nanoparticles for organic contaminants removal from aqueous phase: Material characterizations and kinetic studies. *Journal of Industrial and Engineering Chemistry*, **76**, 197-214.

Nairat, M., Shahwan, T., Eroğlu, A.E., Fuchs, H. 2015. Incorporation of iron nanoparticles into clinoptilolite and its application for the removal of cationic and anionic dyes. *Journal of Industrial and Engineering Chemistry*, **21**, 1143-1151.

Nekouei, F., Nekouei, S., Tyagi, I., Gupta, V.K. 2015. Kinetic, thermodynamic and isotherm studies for acid blue 129 removal from liquids using copper oxide nanoparticle-modified activated carbon as a novel adsorbent. *Journal of Molecular Liquids*, **201**, 124-133.

Nwanya, A.C., Razanamahandry, L.C., Bashir, A.K.H., Ikpo, C.O., Nwanya, S.C., Botha, S., Ntwampe, S.K.O., Ezema, F.I., Iwuoha, E.I., Maaza, M. 2019. Industrial textile effluent treatment and antibacterial effectiveness of *Zea mays* L. Dry husk mediated bio-synthesized copper oxide nanoparticles. *Journal of Hazardous Materials*, **375**, 281-289.

Nyairo, W.N., Eker, Y.R., Kowenje, C., Akin, I., Bingol, H., Tor, A., Ongeri, D.M. 2018. Efficient adsorption of lead (II) and copper (II) from aqueous phase using oxidized multiwalled carbon nanotubes/polypyrrole composite. *Separation Science and Technology*, **53**(10), 1498-1510.

Oleszczuk, P., Kołtowski, M. 2017. Effect of co-application of nano-zero valent iron and biochar on the total and freely dissolved polycyclic aromatic hydrocarbons removal and toxicity of contaminated soils. *Chemosphere*, **168**, 1467-1476.

Pang, Y., Zhou, Y., Luo, K., Zhang, Z., Yue, R., Li, X., Lei, M. 2020. Activation of persulfate by stability-enhanced magnetic graphene oxide for the removal of 2,4-dichlorophenol. *Science of The Total Environment*, **707**, 135656.

Park, C.M., Kim, Y.M., Kim, K.-H., Wang, D., Su, C., Yoon, Y. 2019. Potential utility of graphene-based nano spinel ferrites as adsorbent and photocatalyst for removing organic/inorganic contaminants from aqueous solutions: A mini review. *Chemosphere*, **221**, 392-402.

Peeters, K., Lespes, G., Milačič, R., Ščančar, J. 2015. Adsorption and degradation processes of tributyltin and trimethyltin in landfill leachates treated with iron nanoparticles. *Environmental Research*, **142**, 511-521.

Pei, Z., Li, L., Sun, L., Zhang, S., Shan, X.-q., Yang, S., Wen, B. 2013. Adsorption characteristics of 1,2,4-trichlorobenzene, 2,4,6-trichlorophenol, 2-naphthol and naphthalene on graphene and graphene oxide. *Carbon*, **51**, 156-163.

Peng, D., Wu, B., Tan, H., Hou, S., Liu, M., Tang, H., Yu, J., Xu, H. 2019. Effect of multiple iron-based nanoparticles on availability of lead and iron, and micro-ecology in lead contaminated soil. *Chemosphere*, **228**, 44-53.

Prasad, K.S., Gandhi, P., Selvaraj, K. 2014. Synthesis of green nano iron particles (GnIP) and their application in adsorptive removal of As(III) and As(V) from aqueous solution. *Applied Surface Science*, **317**, 1052-1059.

Qiao, J.-t., Liu, T.-x., Wang, X.-q., Li, F.-b., Lv, Y.-h., Cui, J.-h., Zeng, X.-d., Yuan, Y.-z., Liu, C.-p. 2018. Simultaneous alleviation of cadmium and arsenic accumulation in rice by applying zero-valent iron and biochar to contaminated paddy soils. *Chemosphere*, **195**, 260-271.

Rajesh, R., Iyer, S.S., Ezhilan, J., Kumar, S.S., Venkatesan, R. 2016. Graphene oxide supported copper oxide nanoneedles: An efficient hybrid material for removal of toxic azo dyes. *Spectrochimica Acta Part A: Molecular and Biomolecular Spectroscopy*, **166**, 49-55.

Ramesha, G.K., Vijaya Kumara, A., Muralidhara, H.B., Sampath, S. 2011. Graphene and graphene oxide as effective adsorbents toward anionic and cationic dyes. *Journal of Colloid and Interface Science*, **361**(1), 270-277.

Raut, S.S., Kamble, S.P., Kulkarni, P.S. 2016. Efficacy of zero-valent copper (Cu^0) nanoparticles and reducing agents for dechlorination of mono chloroaromatics. *Chemosphere*, **159**, 359-366.

Sadegh, H., Zare, K., Maazinejad, B., Shahryari-ghoshekandi, R., Tyagi, I., Agarwal, S., Gupta, V.K. 2016. Synthesis of MWCNT-COOH-Cysteamine composite and its application for dye removal. *Journal of Molecular Liquids*, **215**, 221-228.

Salam, M.A. 2017. Preparation and characterization of chitin/magnetite/multiwalled carbon nanotubes magnetic nanocomposite for toxic hexavalent chromium removal from solution. *Journal of Molecular Liquids*, **233**, 197-202.

Saleh, T.A., Sarı, A., Tuzen, M. 2019. Carbon nanotubes grafted with poly(trimesoyl, m-phenylenediamine) for enhanced removal of phenol. *Journal of Environmental Management*, **252**, 109660.

Senthil Kumar, P., Selvakumar, M., Babu, S.G., Jaganathan, S.K., Karuthapandian, S., Chattopadhyay, S. 2015. Novel CuO/chitosan nanocomposite thin film: facile hand-picking recoverable, efficient and reusable heterogeneous photocatalyst. *RSC Advances*, **5**(71), 57493-57501.

Shao, Y., Gao, Y., Yue, Q., Kong, W., Gao, B., Wang, W., Jiang, W. 2020. Degradation of chlortetracycline with simultaneous removal of copper (II) from aqueous solution using wheat straw-supported nanoscale zero-valent iron. *Chemical Engineering Journal*, **379**, 122384.

Simamora, A.J., Hsiung, T.L., Chang, F.C., Yang, T.C., Liao, C.Y., Wang, H.P. 2012. Photocatalytic splitting of seawater and degradation of methylene blue on CuO/nano TiO_2. *International Journal of Hydrogen Energy*, **37**(18), 13855-13858.

Singha Deb, A.K., Dwivedi, V., Dasgupta, K., Musharaf Ali, S., Shenoy, K.T. 2017. Novel amidoamine functionalized multi-walled carbon nanotubes for removal of mercury(II) ions from wastewater: Combined experimental and density functional theoretical approach. *Chemical Engineering Journal*, **313**, 899-911.

Sohrabi, S., Akhlaghian, F. 2016. Modeling and optimization of phenol degradation over copper-doped titanium dioxide photocatalyst using response surface methodology. *Process Safety and Environmental Protection*, **99**, 120-128.

Sotelo, J.L., Rodríguez, A.R., Mateos, M.M., Hernández, S.D., Torrellas, S.A., Rodríguez, J.G. 2012. Adsorption of pharmaceutical compounds and an endocrine disruptor from aqueous solutions by carbon materials. *Journal of Environmental Science and Health, Part B*, **47**(7), 640-652.

Stevenson, L.M., Adeleye, A.S., Su, Y., Zhang, Y., Keller, A.A., Nisbet, R.M. 2017. Remediation of cadmium toxicity by sulfidized nano-iron: the importance of organic material. *ACS Nano*, **11**(10), 10558-10567.

Su, B., Lin, J., Owens, G., Chen, Z. 2020. Impact of green synthesized iron oxide nanoparticles on the distribution and transformation of As species in contaminated soil. *Environmental Pollution*, **258**, 113668.

Sun, T., Zhao, Z., Liang, Z., Liu, J., Shi, W., Cui, F. 2017. Efficient As(III) removal by magnetic CuO-Fe_3O_4 nanoparticles through photo-oxidation and adsorption under light irradiation. *Journal of Colloid and Interface Science*, **495**, 168-177.

Sun, Y., Wang, Q., Chen, C., Tan, X., Wang, X. 2012. Interaction between Eu(III) and graphene oxide nanosheets investigated by batch and extended X-ray absorption fine structure spectroscopy and by modeling techniques. *Environmental Science & Technology*, **46**(11), 6020-6027.

Tan, P., Sun, J., Hu, Y., Fang, Z., Bi, Q., Chen, Y., Cheng, J. 2015. Adsorption of Cu^{2+}, Cd^{2+} and Ni^{2+} from aqueous single metal solutions on graphene oxide membranes. *Journal of Hazardous Materials*, **297**, 251-260.

Tofighy, M.A., Mohammadi, T. 2011. Adsorption of divalent heavy metal ions from water using carbon nanotube sheets. *Journal of Hazardous Materials*, **185**(1), 140-147.

Tomašević, A., Kiss, E., Petrović, S., Mijin, D. 2010. Study on the photocatalytic degradation of insecticide methomyl in water. *Desalination*, **262**(1), 228-234.

Usman, M., Ahmed, A., Yu, B., Peng, Q., Shen, Y., Cong, H. 2019. Photocatalytic potential of bio-engineered copper nanoparticles synthesized from *Ficus carica* extract for the degradation of toxic organic dye from waste water: Growth mechanism and study of parameter affecting the degradation performance. *Materials Research Bulletin*, **120**, 110583.

Üzüm, Ç., Shahwan, T., Eroğlu, A.E., Lieberwirth, I., Scott, T.B., Hallam, K.R. 2008. Application of zero-valent iron nanoparticles for the removal of aqueous Co^{2+} ions under various experimental conditions. *Chemical Engineering Journal*, **144**(2), 213-220.

Verma, B., Balomajumder, C. 2020. Surface modification of one-dimensional carbon nanotubes: a review for the management of heavy metals in wastewater. *Environmental Technology & Innovation*, **17**, 100596.

Vilardi, G., Mpouras, T., Dermatas, D., Verdone, N., Polydera, A., Di Palma, L. 2018. Nanomaterials application for heavy metals recovery from polluted water: The combination of nano zero-valent iron and carbon nanotubes. Competitive adsorption non-linear modeling. *Chemosphere*, **201**, 716-729.

Vuković, G.D., Marinković, A.D., Čolić, M., Ristić, M.Đ., Aleksić, R., Perić-Grujić, A.A., Uskoković, P.S. 2010. Removal of cadmium from aqueous solutions by oxidized and ethylenediamine-functionalized multi-walled carbon nanotubes. *Chemical Engineering Journal*, **157**(1), 238-248.

Wang, B., Dong, H., Li, L., Wang, Y., Ning, Q., Tang, L., Zeng, G. 2020. Influence of different co-contaminants on trichloroethylene removal by sulfide-modified nanoscale zero-valent iron. *Chemical Engineering Journal*, **381**, 122773.

Wang, G., Zhang, S., Xu, X., Li, T., Li, Y., Deng, O., Gong, G. 2014. Efficiency of nanoscale zero-valent iron on the enhanced low molecular weight organic acid removal Pb from contaminated soil. *Chemosphere*, **117**, 617-624.

Wang, H., Yuan, X., Wu, Y., Huang, H., Zeng, G., Liu, Y., Wang, X., Lin, N., Qi, Y. 2013. Adsorption characteristics and behaviors of graphene oxide for Zn(II) removal from aqueous solution. *Applied Surface Science*, **279**, 432-440.

Wang, S., Ma, X., Zheng, P. 2019. Sulfo-functional 3D porous cellulose/graphene oxide composites for highly efficient removal of methylene blue and tetracycline from water. *International Journal of Biological Macromolecules*, **140**, 119-128.

Wang, T., Liu, Y., Wang, J., Wang, X., Liu, B., Wang, Y. 2019. In-situ remediation of hexavalent chromium contaminated groundwater and saturated soil using stabilized iron sulfide nanoparticles. *Journal of Environmental Management*, **231**, 679-686.

Wu, L.-K., Wu, H., Zhang, H.-B., Cao, H.-Z., Hou, G.-Y., Tang, Y.-P., Zheng, G.-Q. 2018. Graphene oxide/$CuFe_2O_4$ foam as an efficient absorbent for arsenic removal from water. *Chemical Engineering Journal*, **334**, 1808-1819.

Xiao, X., Wang, Q., Owens, G., Chiellini, F., Chen, Z. 2019. Reduced graphene oxide/iron nanoparticles used for the removal of Pb (II) by one step green synthesis. *Journal of Colloid and Interface Science*, **557**, 598-607.

Xie, Y., Cheng, W., Tsang, P.E., Fang, Z. 2016. Remediation and phytotoxicity of decabromodiphenyl ether contaminated soil by zero valent iron nanoparticles immobilized in mesoporous silica microspheres. *Journal of Environmental Management*, **166**, 478-483.

Xie, Y., Fang, Z., Cheng, W., Tsang, P.E., Zhao, D. 2014. Remediation of polybrominated diphenyl ethers in soil using Ni/Fe bimetallic nanoparticles: Influencing factors, kinetics and mechanism. *Science of The Total Environment*, **485-486**, 363-370.

Xingu-Contreras, E., García-Rosales, G., García-Sosa, I., Cabral-Prieto, A. 2020. Degradation of methyl orange using iron nanoparticles with/without support at different conditions. *Microporous and Mesoporous Materials*, **292**, 109782.

Xiong, T., Yuan, X., Wang, H., Leng, L., Li, H., Wu, Z., Jiang, L., Xu, R., Zeng, G. 2018. Implication of graphene oxide in Cd-contaminated soil: A case study of bacterial communities. *Journal of Environmental Management*, **205**, 99-106.

Xu, L., Yang, Y., Li, W., Tao, Y., Sui, Z., Song, S., Yang, J. 2019. Three-dimensional macroporous graphene-wrapped zero-valent copper nanoparticles as efficient micro-electrolysis-promoted Fenton-like catalysts for metronidazole removal. *Science of The Total Environment*, **658**, 219-233.

Xu, Q., Li, W., Ma, L., Cao, D., Owens, G., Chen, Z. 2020. Simultaneous removal of ammonia and phosphate using green synthesized iron oxide nanoparticles dispersed onto zeolite. *Science of The Total Environment*, **703**, 135002.

Yang, B., Zhou, P., Cheng, X., Li, H., Huo, X., Zhang, Y. 2019. Simultaneous removal of methylene blue and total dissolved copper in zero-valent iron/H_2O_2 Fenton system: Kinetics, mechanism and degradation pathway. *Journal of Colloid and Interface Science*, **555**, 383-393.

Yang, S.-T., Chang, Y., Wang, H., Liu, G., Chen, S., Wang, Y., Liu, Y., Cao, A. 2010. Folding/aggregation of graphene oxide and its application in Cu^{2+} removal. *Journal of Colloid and Interface Science*, **351**(1), 122-127.

Yap, P.L., Tung, T.T., Kabiri, S., Matulick, N., Tran, D.N.H., Losic, D. 2020. Polyamine-modified reduced graphene oxide: A new and cost-effective adsorbent for efficient removal of mercury in waters. *Separation and Purification Technology*, **238**, 116441.

Zambianchi, M., Durso, M., Liscio, A., Treossi, E., Bettini, C., Capobianco, M.L., Aluigi, A., Kovtun, A., Ruani, G., Corticelli, F., Brucale, M., Palermo, V., Navacchia, M.L., Melucci, M. 2017. Graphene oxide doped polysulfone membrane adsorbers for the removal of organic contaminants from water. *Chemical Engineering Journal*, **326**, 130-140.

Zghal, S., Jedidi, I., Cretin, M., Cerneaux, S., Abdelmouleh, M. 2020. One-step synthesis of highly porous carbon graphite/carbon nanotubes composite by in-situ growth of carbon nanotubes for the removal of humic acid and copper (II) from wastewater. *Diamond and Related Materials*, **101**, 107557.

Zhang, M., Wang, Y., Zhao, D., Pan, G. 2010. Immobilization of arsenic in soils by stabilized nanoscale zero-valent iron, iron sulfide (FeS), and magnetite (Fe_3O_4) particles. *Chinese Science Bulletin*, **55**(4), 365-372.

Zhang, Z., Chen, H., Wu, W., Pang, W., Yan, G. 2019. Efficient removal of Alizarin Red S from aqueous solution by polyethyleneimine functionalized magnetic carbon nanotubes. *Bioresource Technology*, **293**, 122100.

Zhao, G., Ren, X., Gao, X., Tan, X., Li, J., Chen, C., Huang, Y., Wang, X. 2011. Removal of Pb(ii) ions from aqueous solutions on few-layered graphene oxide nanosheets. *Dalton Transactions*, **40**(41), 10945-10952.

Zhao, X., Jia, Q., Song, N., Zhou, W., Li, Y. 2010. Adsorption of Pb(II) from an aqueous solution by titanium dioxide/carbon nanotube nanocomposites: kinetics, thermodynamics, and isotherms. *Journal of Chemical & Engineering Data*, **55**(10), 4428-4433.

Zhu, F., Li, L., Ma, S., Shang, Z. 2016. Effect factors, kinetics and thermodynamics of remediation in the chromium contaminated soils by nanoscale zero valent Fe/Cu bimetallic particles. *Chemical Engineering Journal*, **302**, 663-669.

Zou, H., Hu, E., Yang, S., Gong, L., He, F. 2019. Chromium(VI) removal by mechanochemically sulfidated zero valent iron and its effect on dechlorination of trichloroethene as a co-contaminant. *Science of The Total Environment*, **650**, 419-426.